Functional analysis of the *Drosophila* microtubule regulator Mini spindles

Amy Brittle

PRESENTED FOR THE DEGREE OF DOCTOR OF PHILOSOPHY

UNIVERSITY OF EDINBURGH

JANUARY 2005

Contents

Acknowledgements		xiv
Abstract		xv
Abbreviations		xvi
Chapter 1	**Introduction**	Page
1.1	Functions of the microtubule network	1
1.1.1	Cell division	1
1.1.2	Interphase	2
1.2	Microtubule structure and dynamic behaviour.	3
1.2.1	Structure of the polymer	3
1.2.2	Microtubule dynamics *in vitro.*	4
1.2.3	The stabilising end structure	5
1.2.4	Microtubule dynamics *in vivo.*	7
1.2.5	Functions of dynamic instability *in vivo.*	8
1.3	Microtubule regulators	8
1.3.1	Nucleation	9
1.3.2	Regulators of microtubule dynamics	11
1.3.2.1	Stabilisers	11
1.3.2.2	Destabilisers	13
1.3.3	Motor proteins	16
1.3.4	Mechanisms for microtubule organisation	17
1.3.4.1	Minus ends capture	17
1.3.4.2	Capture of plus ends	18
1.3.4.3	Microtubule bundling	20

1.4	*Drosophila* as a model organism for studying microtubule regulation	21
1.5	Mini spindles and the Dis1/TOG family of MAPs.	23
1.5.1	Protein Structure	23
1.5.2	Functions of the Dis1/TOG family of proteins.	25
1.5.2.1	Regulation of plus end dynamics.	25
1.5.2.2	Role of Dis1/TOG proteins at the kinetochores.	28
1.5.2.3	Roles at the centrosomes/SPB	30
1.5.2.4	Interphase roles	32
1.5.3	Protein interactions and regulation	34
1.5.3.1	Regulation of centrosome localisation	35
1.6	Aims of this study	36
Chapter 2	**Materials and methods**	**43**
2.1	Commonly used buffers and reagents	43
2.2	DNA Manipulations	44
2.2.1	Dissolving and storage	44
2.2.2	Ethanol precipitation	44
2.2.3	Molecular Analysis of DNA	44
2.2.4	DNA modifying enzymes	45
2.2.5	Agarose gel electroporesis	45
2.2.6	Gel purification	45
2.2.7	DNA sequencing	46
2.2.8	Site directed mutagenesis	46

2.3	Analysis of Proteins	47
2.3.1	SDS polyacrylamide gel electrophoresis (SDS-PAGE)	47
2.3.2	Western blotting	48
2.3.3	Antibody purification	49
2.4	*Escherichia coli* Manipulations	*50*
2.4.1	*E.coli* strain used in this study	*50*
2.4.2	Media and growth conditions	50
2.4.3	Selective antibiotics	51
2.4.4	Transformation of *E.coli*	51
2.4.5	Isolation of plasmid DNA from *E.coli*.	52
2.5	Fly methods	52
2.5.1	Fly maintenance	52
2.5.2	Genetic analysis	52
2.5.2.1	Fly crosses	52
2.5.2.2	Rescues and recombination	53
2.5.2.3	Determining lethal phase of mutants	53
2.5.2.4	Female sterility tests	54
2.5.3	EMS mutagenesis	54
2.5.4	Sequencing from genomic fly/larvae DNA	55
2.5.5	Preparing fly protein samples for SDS-PAGE	57
2.5.6	Cytological analysis	57
2.5.6.1	Immunostaining larval brains	57
2.5.6.2	Brain squashes	58
2.5.6.3	Dissection and immunostaining of oocytes	58
2.5.6.4	Immunostaining of syncytial embryos	59
2.5.6.5	Cytological analysis of fly blood cells	60
2.5.6.6	Antibodies used for Immunostaining	60

2.5.7	Co-immunoprecipitations from larval extract.	61
2.5.8	Microtubule binding assay	62
2.6	Tissue culture methods	62
2.6.1	Maintaining S2 cell cultures	63
2.6.2	Immunofluorescence in S2 cells	63
2.6.3	RNA interference in S2 cells	65
2.6.4	Transfection of S2 cells	67
2.6.5	Drug treatment	67
2.6.6	Microtubule dynamics in live S2 cells.	68
2.6.7	FRAP	69
Chapter 3	**Isolation of new *msps*, *d-tacc* and *ncd* alleles**	**82**
3.1	Background	82
3.2	Obtaining new *msps*, *dtacc* and *ncd* alleles	83
3.3	Determining lethal phase / sterility of new mutants	85
3.4	Recombination of new mutants to remove extra chromosomal mutations	86
3.5	Genetic analysis of new alleles.	87
3.6	Determining DNA mutations of *msps* and *d-tacc* alleles.	88

Chapter 4	**Protein and cytological analysis of new *msps* and *d-tacc* alleles**	99
4.1	Background	99
4.2	Presence and level of mutant Msps protein.	99
4.3	Cytological defects of *msps* alleles and mutant protein localisation.	102
4..3.1	*msps*^{51} cytological analysis	102
4.3.2	*msps*^{146} cytological analysis	103
4.3.3	Msps^{S10} cytological analysis	104
4.3.3.1	Msps^{S10} localises to the centrosomes in somatic mitosis	104
4.3.3.2	Female meiotic defects in msps^{S10} oocytes	104
4.3.3.3	Embryonic mitotic defect in *msps*^{S10} embryos	105
4.4	Mutant Msps protein binding to D-TACC.	106
4.5	Microtubule binding.	107
4.6	Characterisation of the new d-tacc^{S3} allele.	108
Chapter 5	**The role of Msps in interphase microtubule regulation**	119
5.1	Background	119
5.2	Msps localisation in *Drosophila* S2 culture cells.	120

5.3	RNAi depletion of Msps protein from S2 cells.	121
5.4	Mitotic phenotype in Msps depleted cells.	122
5.5	Interphase microtubule defects in Msps depleted cells.	123
5.6	Cell shape and actin localisation in Msps depleted cells.	125
5.7	Co-depletion of Kinl microtubule destabilisers with Msps.	125
5.8	D-TACC depletion does not result in interphase microtubule defects.	127
5.9	Expression of the N-terminal region of Msps partially rescues Msps depletion	128
5.9.1	Construction of Msps C-terminal deletion construct and mutation at a conserved residue	128
5.9.2	Expression of Msps N-terminal constructs in Msps depleted cells	129
5.10	Microtubule dynamics in Msps depleted cells.	130
5.11	Microtubule bundles induced by Msps depletion are very stable.	132
5.12	Defective organisation of interphase microtubules in blood cells from *msps* mutant larvae.	133

Chapter 6	**Genetic interaction of a new meiotic spindle mutant, with *msps, d-tacc* and *ncd.***	154
6.1	Background	154
6.2	Genetic interactions between *triplet* and previously identified meiotic spindle mutants.	155
6.2.1	Creation of double mutants	155
6.2.2	Cytological analysis indicates that *trp* genetically interacts with *msps* and *d-tacc* but not *ncd*.	156
6.3	Analysis of Triplet function in S2 cells.	158
Chapter 7	**Discussion**	165
7.1	Insights into Msps and D-TACC function provided by screening and analysis of new alleles	165
7.1.1	Alleles isolated in the screen	165
7.1.2	Mutant protein stability	167
7.1.3	The C-terminus of Msps is involved in D-TACC interaction	167
7.1.4	Microtubule binding	169
7.1.5	Mitotic spindle function	170
7.1.6	Meiotic spindle function	171
7.1.7	Summary of screening and mutant analysis	172
7.2	Msps function in interphase microtubule regulation	173

7.2.1	Msps has a role in interphase microtubule organisation	173
7.2.2	A role for the Msps N-terminal domain in interphase function	174
7.2.3	Msps acts independently from the Kin I destabilising proteins in interphase microtubule regulation	175
7.2.4	Msps acts independently of D-TACC in interphase	176
7.2.5	Msps acts as an anti-pause factor in *Drosophila* cells	177
7.3	Characterisation of new meiotic spindle mutant, *triplet*	178
7.3.1	Role in spindle unification	178
7.3.2	*trip* has an epistatic relationship with *msps* and *d-tacc*	179
7.3.3	Summary and future directions	180
Appendix I		182
References		183

Figures and tables

Chapter 1	**Introduction**	Page
Figure 1.1	Microtubule organisation changes during the cell cycle and though development.	38
Figure 1.2	Microtubule structure	39
Figure 1.3	Microtubule dynamic instability and end structure	40
Figure 1.4	Protein structure of the Dis1/TOG family of MAPs	41
Figure 1.5	The function of the Dis1/TOG family in microtubule regulation.	42

Chapter 2	**Materials and Methods**	
Table 2.1	Antibodies used in Western blotting	71
Table 2.2	Fly stocks used in this study	72
Figure 2.1	Recombination crossing strategy	74
Figure 2.2	Rescue of mutant *msps* alleles	75
Table 2.3	Primers used to amplify and sequence *msps* genomic DNA	76
Table 2.4	Primers used to amplify and sequence d-tacc genomic DNA	77
Table 2.5	Primers used to create dsRNA for RNA interference experiments	78
Figure 2.3	Preparation of DNA template for the transcription of dsRNA	81

Chapter 3 Isolation of new *msps*, *d-tacc* and *ncd* alleles

Figure 3.1 The crossing scheme used to isolate new *msps, ncd* and *d-tacc* alleles. 90
Table 3.1 Mutants identified in EMS screen 91
Table 3.2 Lethality/viability of newly isolated alleles in combination with single $msps^{P}$, $d\text{-}tacc^{stella}$ and ncd^{1} alleles. 92
Figure 3.2 Recombination strategy for *msps* and *d-tacc* mutants to remove unwanted mutations 93
Table 3.3 Lethal phase and rescue of recombinants created to clean up chromosomes of new mutant alleles 94
Table 3.4 Viability and female sterility of combinations of *msps* mutant alleles. 95
Figure 3.3 Strategy for sequencing the new *msps and d-tacc* alleles. 96
Table 3.5 DNA mutations and resulting amino acid changes in new *msps* and *d-tacc* alleles. 97
Figure 3.4 Predicated mutant Msps proteins produced by new *msps* alleles. 98

Chapter 4 Protein and cytological analysis of new *msps* and *d-tacc* alleles

Figure 4.1 Msps protein levels in wild-type and *msps* mutant larvae. 110
Figure 4.2 $msps^{51}$ larval neuroblasts contain mitotic spindle defects. 111
Figure 4.3 Msps51 protein does not localise to centrosomes larval neuroblasts. 112
Figure 4.4 $msps^{S10}$ female meiotic phenotype and protein localisation. 113
Figure 4.5 $msps^{S10}$ protein localises to spindle microtubules and 114

centrosomes in embryonic mitosis.
Figure 4.6 D-TACC protein levels are not severely affected in *msps* mutants. 115
Figure 4.7 Truncation of the C-terminal 588 amino acids of Msps protein abolishes D-TACC binding. 116
Figure 4.8 $Msps^{51}$ protein is pulled down with tubulin in a microtubule binding assay. 117
Figure 4.9 $dtacc^{S3}$ mutant flies contain a truncated D-TACC protein 118

Chapter 5 The role of Msps in interphase microtubule regulation.

Figure 5.1 Msps microtubule localisation in S2 cells. 134
Figure 5.2 D-TACC and Msps protein levels decrease in cells treated with *msps* dsRNA. 135
Figure 5.3 Msps depletion results in mitotic spindle defects 136
Figure 5.4 Time course of Mitotic spindle phenotype in control and *msps* RNAi cells 137
Figure 5.5 Interphase microtubule organisation is altered after Msps depletion. 138
Figure 5.6 Interphase microtubule phenotype is not affected by growing *msps* RNAi cells continuously on con A. 139
Figure 5.7 No difference in the actin staining pattern is observed in control and *msps* RNAi treated cells. 140
Figure 5.8 Co-depletion of Kinl proteins with Msps does not restore a normal array of microtubules. 141
Figure 5.9 D-TACC but not Msps protein is depleted by addition of D-TACC dsRNA to S2 cells 142
Figure D-TACC depletion does not effect mitotic spindle 143

5.10	formation or Msps localisation to the spindle and centrosomes.	
Figure 5.11	D-TACC depletion does not alter interphase microtubule organisation or Msps localisation	144
Figure 5.12	Construction of plasmids expressing MspsN and MspsN-E190K.	145
Figure 5.13	Point mutation in conserved residue of Msps.	146
Figure 5.14	N-terminal region of Msps partially rescues depletion of endogenous Msps.	147
Figure 5.15	Truncated Msps proteins, MspsN and MspsN-E190K, do not localise to microtubules in S2 cells.	148
Figure 5.16	Extensive microtubule pausing results from Msps depletion.	149
Figure 5.17	Pausing increases in Msps depleted cells but growth rate is unaffected.	150
Figure 5.18	Microtubules in Msps depleted cells are stable against the activity of a depolymerising drug.	151
Figure 5.19	Msps depletion results in reduced microtubule dynamicity.	152
Figure 5.20	Abnormal interphase microtubule organisation in haemocytes from *msps* mutants	153

Chapter 6	**Genetic interaction of a new meiotic spindle mutant with *msps, d-tacc* and *ncd.***	
Figure 6.1	Creation of trp^{GT28} and $msps^{208}$ double mutants by recombination.	160
Figure 6.2	Creation of trp^{GT28} and ncd^{1} double mutants by	161

recombination.

Figure 6.3 Individual spindles form around chromosomes in trp^{GT28}, $d\text{-}tacc^{stella}$ trp^{GT28} and $msps^{208}$ trp^{GT28} oocytes. 162

Figure 6.4 trp^{GT28} ncd^{1} oocytes display a the *triplet* and *ncd* spindle phenotypes. 163

Figure 6.5 Trp depletion from S2 cells causes an increase in mitotic index. 164

Acknowledgements

Firstly, I would like to thank Hiro for all his help and patient supervision during my time in his lab. Thanks to all the members of the Ohkura lab, past and present, for supplying me with endless help, support and regular tea breaks. Thanks must also go to honours and summer students, Marissa Brown, Duncan Sproul and Fiona Murray-Zmyewski for help with various aspects of the mutant screening, analysis and antibody production. I must also thank the Edinburgh fly community for advice over the years.

Thanks to friends in Edinburgh who have made my time here fantastic fun, and have not laughed at me too much when I complain about my mutant flies.

And finally, thanks to my parents and to Michael.

Abstract

Functional analysis of the *Drosophila* microtubule regulator Mini spindles

The Drosophila gene, *mini spindles* (*msps*), is a member of a family of proteins involved in microtubule regulation. Previous studies have demonstrated that Msps protein is essential for bipolar spindle formation in both mitosis and female meiosis. The aim of this study was to uncover novel roles for the protein and define regions of the protein important for specific functions.

In this study, the functions of different regions of the protein were examined by the creation and analysis of new *msps* alleles. Analysis of one allele, $msps^{51}$, indicated that the C-terminal region is essential for centrosome localisation and for the protein to bind to the centrosome associated protein, D-TACC. Furthermore, an interaction between *msps* and *d-tacc* with a novel meiotic spindle mutant, was uncovered by genetic analysis.

Msps depletion from Drosophila culture cells (S2 cells) revealed a dramatic role for Msps in interphase microtubule organisation. In the depleted cells, microtubules could no longer extend to the cell cortex and frequently bundled microtubules were seen. This phenotype was investigated by the analysis of microtubule dynamics in live cells. Msps was found to increase the dynamicity of the microtubules by preventing pausing. Msps function in interphase microtubule regulation was demonstrated to be independent of known Msps interactors, D-TACC and the KinI destabilising kinesins.

This study demonstrated that Msps plays an essential role interphase microtubule organisation, in addition to maintaining the bipolar spindle. Furthermore, Msps regulates microtubule organisation by acting as an anti-pause factor.

Abbreviations

5'-UTR	5 prime untranslated region
Con A	concanavilin A
DAPI	4,6-Diamidino-2-phenylindole
DNA	deoxyribonucleic acid
EDTA	ethylenediamine tetra acetic acid
EGTA	ethyleneglycol tetra acetic acid
EMS	ethylmethane sulfonate
FCS	foetal calf serum
FRAP	fluorescence recovery after photobleaching
GDP	guanosine diphosphate
GST	glutathione *S*-transferase
GTP	guanosine triphosphate
GFP	green fluorescent protein
MBP	maltose binding protein
MT	microtubule
MTOC	Microtubule organising centre
PBS	phosphate buffered saline
PCR	polymerase chain reaction
PMSF	phenylmethylsulfonyl fluoride
RNA	ribonucleic acid
SDS	sodium dodecylsulphate
SDS-PAGE	SDS-polyacrylamide gel electrophoresis
SPB	spindle pole body
Tris	2-amino-2-(hydroxymethyl)-1,3-propanediol
w/v	weight/volume

Chapter 1 Introduction

1.1 Functions of the microtubule network

Microtubules are found in all dividing eukaryotic cells and in most differentiated cell types. In dividing cells, microtubules form a very dynamic structure, known as the spindle, which physically segregates the chromosomes and orientates the plane of cell cleavage. In non-dividing cells, microtubules are involved in a diverse range of activities including cell morphogenesis, cell migration and intracellular transport of vesicles and organelles.

In order for microtubules to fulfil their many functions during the cell cycle and through development, they must be remodelled into a variety of different structures. A microtubule is a polymer of tubulin and has intrinsic properties that allow it to be restructured very rapidly (Amos and Klug, 1974; Mitchison and Kirschner, 1984). In addition, many layers and types of regulation act on the microtubule polymers to create the desired structures for a vast array of functions.

1.1.1 Cell division

Correct segregation of replicated DNA is an essential process that must occur efficiently in all cells. Eukaryotes have developed two types of chromosome segregation. In mitosis, the division of the somatic cells of the organism, DNA is replicated and divided equally, producing daughter cells with the same number of chromosomes as the mother cell. Meiosis, the division from which gametes arise, leads to daughter cells with half the number of chromosomes as the mother cell.

Despite the different outcomes, microtubules are organised into a spindle with a common structure in both types of division (figure 1.1.A and B). There must be two

spindle poles from which dynamic microtubules of uniform polarity (with minus ends at the poles and plus ends at the spindle equator) emanate. The plus ends of the microtubules will capture the chromosomes, at sites known as kinetochores, and align the chromosomes at the equator of the spindle. Chromosomes can then be pulled in opposite directions so that the DNA is segregated equally (reviewed Wittmann et al, 2001).

Following chromosome segregation the cell is cleaved into two daughter cells, by the ingression of the cleavage furrow (reviewed (Glotzer, 2001). The mechanical force for the cleavage is provided by the actin-based contractile ring. Spindle microtubules are essential for positioning and initiating furrow formation (Glotzer, 2004). If microtubules are depolymerised during metaphase or very early anaphase cleavage furrow formation is inhibited, indicating that microtubules are essential for this process. Both the astral microtubules and the central spindle, which forms from bundling of spindle microtubules following the start of anaphase, have been implicated in inducing furrow formation.

1.1.2. Interphase

In many interphase cells, the microtubule network is organised into a radial array with the minus ends centrally placed and the plus ends freely exploring the cytoplasm (figure 1.1.C). Radial microtubule arrays direct intracellular traffic, maintain cell polarity and position organelles within the cell.

The most fundamental and common function of the microtubule network is to provide polarity. Microtubules themselves are polarised, with a minus and plus end, and this polarity is utilised by the cell in a number of ways. For example, microtubules are used as tracks along which motor proteins travel (reviewed Vale, 1987; Goldstein, 2001; Mallik and Gross, 2004). Different motors can move towards either the plus or

minus end, and by using polarity in this way, can carry a variety of cargos to specific locations in the cell, determined by the orientation of the microtubules.

Although many interphase animal cells have radial distributions of microtubules, non-radial arrays are frequently generated in many differentiated cells to expand the functional capacity of the microtubule cytoskeleton. For example, in polarised epithelial cells, microtubules form an apico-basal array with their minus ends concentrated near the apical surface (figure 1.1.D) (reviewed Mogensen, 1999). This array directs the vesicle trafficking that is central to the function of epithelia. Another specialised cell type, the neuronal cell, contains bundles of microtubules that are essential for neuronal process formation and maintenance (figure 1.1.E) (reviewed Kobayashi and Mundel, 1998).

A microtubule cytoskeleton is present in the vast majority of cells and contributes too many cellular functions. This diversity comes from the ability of microtubules to form a variety of structures that reflect the requirement of the specific cell type. The ability to be quickly rearranged comes partially from the dynamic properties of the tubulin polymer. In the following sections I will discuss the nature of the polymer and how it is regulated in the cell.

1.2. Microtubule structure and dynamic behaviour

1.2.1 Structure of the polymer

Microtubules are polymers consisting of tubulin, which itself consists of a heterodimer composed of alpha- and beta-tubulin monomers (Amos and Klug, 1974). During polymerisation, the head to tail association of alpha/beta-tubulin results in linear protofilaments that associate laterally to form 25nm wide hollow cylindrical polymers (Evans *et al.*, 1985) (figure 1.2). *In vitro* microtubules polymerised from

mammalian brain tubulin have between 10 and 15 protofilaments per microtubule. Microtubules *in vivo* and microtubules nucleated *in vitro* from centrosomes have predominantly 13 protofilaments (Evans *et al.*, 1985).

During polymerisation, GTP bound to beta-tubulin, at the exchangeable or E-site, is hydrolyzed to GDP (David-Pfeuty *et al.*, 1977; MacNeal and Purich, 1978). The GDP remains in the E-site while the beta-tubulin remains as a polymer and is only exchanged for GTP when the tubulin is released. The beta-tubulin can then undergo another round of polymerisation. alpha-tubulin also binds GTP but it is not exchanged and is not hydrolyzed during polymerisation (Spiegelman *et al.*, 1977).

The head to tail association of alpha and beta-tubulin subunits gives the microtubule polarity, and consequentially, the two ends have different polymerisation and depolymerisation rates; the slower growing end is the minus end and the faster growing end is the plus end (Allen and Borisy, 1974). Polarity plays a crucial role in the function of the microtubule polymer in the cell.

1.2.2 Microtubule dynamics *in vitro*

In 1984, a novel mechanism, termed dynamic instability, was proposed for microtubule dynamics based on analysis of the length distributions of fixed microtubules (Mitchison and Kirschner, 1984). The model described that a population of microtubules can display an overall steady state whilst single microtubules never reach a steady state. Microtubules remain for prolonged periods in a state of polymerisation or depolymerisation with infrequent changes between the two states. The existence of such behaviour was confirmed by real time analysis of single microtubule dynamics *in vitro* using dark field or DIC videomicroscopy (Horio and Hotani, 1986; Walker *et al.*, 1988).

Observations of microtubules assembled *in vitro* from purified tubulin led to the description of dynamic instability by four parameters: the rates of polymerisation and

depolymerisation, the frequency of catastrophe (the transition from polymerisation to depolymerisation) and the frequency of rescue (the transition from depolymerisation to polymerisation (figure 1.3) (Walker *et al.*, 1988).

Studies using nonhydrolysable GTP analogues have lead to important conclusions about the thermodynamics of microtubule polymerisation. Studies with different GTP analogues, including GMPCPP, revealed that microtubules can polymerise without hydrolysing GTP and that the microtubule lattice is more stable with a GTP analogue bound to beta-tubulin than with GDP (reviewed Desai and Mitchison, 1997). The function of GTP hydrolysis appears to be to destabilise the microtubule lattice by the inclusion of GDP subunits. This theory was confirmed by the discovery of conditions that will trigger the hydrolysis of GMPCPP; hydrolysis destabilises the lattice and results in rapid depolymerisation (Caplow *et al.*, 1994).

1.2.3 The stabilising end structure

Thermodynamic analysis revealed that GTP hydrolysis weakens the microtubule lattice but it does not explain how a microtubule can remain in a polymerising or depolymerising state, or how a switch is made between the two states. The idea of a stabilising structure at the end of a microtubule was developed to explain how prolonged growth is sustained. The presence of a stabilising cap is supported by the effect seen when a microtubule is severed with UV or a glass needle (Tran *et al.*, 1997b; Walker *et al.*, 1989). The newly exposed microtubule plus end rapidly depolymerised, as if a stabilising structure has been removed. Minus ends behaved differently after severing and either grow or undergo brief shrinkage events followed by rescue, (Tran *et al.*, 1997b; Walker *et al.*, 1989) indicating that a stabilising structure is not required or rescue is very frequent at the minus end.

The stabilising structure was originally proposed to be a cap of GTP-tubulin subunits at the end of the microtubule, protecting the unstable GDP-tubulin lattice

from depolymerising (Mitchison and Kirschner, 1984). Since the initial idea was proposed many attempts have been made to determine the nature of such a GTP cap, but debate still rages concerning its composition and even its very existence (Panda *et al.*, 2002; Caplow and Shanks, 1996; Caplow and Fee, 2003). The GTP-tubulin, if present, can not be large as GTP hydrolysis is equal to tubulin addition (Vandecandelaere *et al.*, 1999). Experiments to estimate the number of GMPCPP-tubulin subunits required to stabilise GDP microtubules against depolymerisation, indicate that 1-3 layers of GTP-tubulin subunits would be sufficient to stabilise a microtubule end (Caplow and Shanks, 1996; Drechsel and Kirschner, 1994). Nevertheless, conclusive evidence in support of a GTP-cap remains elusive and its existence and nature remains controversial.

Structural approaches using electron microscope (EM) analysis of pure tubulin polymerisation have demonstrated that the regulation of microtubule assembly and dynamics involves changes in their end structure (Mandelkow *et al.*, 1991; Chretien *et al.*, 1995; Hyman *et al.*, 1995; Muller-Reichert *et al.*, 1998; Tran *et al.*, 1997a; Vandecandelaere *et al.*, 1999). At the ends of growing microtubules, sheets of tubulin are observed, whereas shrinking microtubules display curved protofilaments peeling outwards from the ends (figure 1.3). Such observations and the flexible nature of tubulin polymer (Janosi *et al.*, 1998) has led to the hypothesis that the tubulin sheet acts as a structural cap to stabilise the growing end. Complete closure of this sheet into a tube (blunt end) may induce shrinkage events, as the intrinsically curved protofilaments desire to be released from this structure (Hyman *et al.*, 1995; Tran *et al.*, 1997a; Muller-Reichert *et al.*, 1998).

In a population of microtubules undergoing dynamic instability in *Xenopus* egg extracts, microtubule growth correlates with the presence of tubulin sheets (Arnal *et al.*, 2000). Increased catastrophe frequency (through the addition of a catastrophe promoting protein) correlates with an increase in frayed ends. An increase in blunt ends was also seen on the addition of low amounts of a catastrophe promoter. The blunt end was, therefore, proposed to represent an intermediate between the sheet and

frayed conformation (Arnal *et al.*, 2000; Tran *et al.*, 1997b). Structural changes in the ends of microtubules are related to the dynamic state.

1.2.4 Microtubule dynamics *in vivo*

In vitro studies have revealed much about the nature of microtubule dynamics, however, how does the situation *in vivo* compare? Microscopy techniques to examine single microtubule dynamics in live cells have been developed and reveal that *in vivo* microtubules have higher polymerisation rates and higher transition frequencies than their *in vitro* counterparts (reviewed Cassimeris, 1993). Using the relationship between polymerisation rate and catastrophe frequency for pure tubulin as a reference, at such high rates of polymerisation seen *in vivo,* very low levels of catastrophe would be expected. This is not the case, suggesting mechanisms exist to increase polymerisation and promote catastrophes *in vivo*. An additional difference is the higher frequency of pausing, where microtubules neither polymerise nor depolymerise, witnessed *in vivo* than *in vitro* (Walker *et al.*, 1988; Shelden and Wadsworth, 1993). The nature of the paused state is poorly understood, although it has been proposed as an intermediate between growth and shrinkage and to correspond to the blunt ended structure seen by EM (Arnal *et al.*, 2000; Tran *et al.*, 1997b).

In vivo studies indicate that away from the cortex, microtubules consistently grow with few catastrophes and a high rescue frequency (Komarova *et al.*, 2002b). Once at the cortex, microtubules display fluctuating behaviour with higher frequencies of catastrophe and rescue, which ensure that the microtubules stay associated with the cortical region. Microtubules become more stable at the cortex and molecules involved in selectively stabilising plus ends at the cortex have been uncovered (Fukata *et al.*, 2003).

The discrepancies between microtubule dynamics *in vitro* and *in vivo*, and the variations in dynamics seen spatially and temporally within the cell, signify that mechanisms must exist within the cell to regulate microtubule behaviour. The

discovery of factors involved in regulating microtubule dynamics is crucial to understanding microtubule dynamics *in vivo*.

1.2.5 Functions of dynamic instability *in vivo*

What is the biological relevance of dynamic instability? In the cell, the polymer forms an array of different structures allowing the microtubule network to fulfil many different functions. Polymerisation dynamics allow the microtubule cytoskeleton to be rapidly reorganised within the cell.

In 1986 Mitchison and Kirschner proposed the "search and capture" model for microtubule attachment to kinetochores (Kirschner and Mitchison, 1986; Mitchison and Kirschner, 1984). The basic idea for this model is that through dynamic instability plus ends of the microtubule can probe the 3D space until it is captured by a kinetochore and stabilised. Dynamic instability allows microtubules to search the three dimensional space of the cell more effectively than equilibrium polymerisation, enabling microtubules to find specific targets in the cell (Holy and Leibler, 1994). Such behaviour is essential to functions such as kinetochore capture in the bipolar spindle and microtubule interactions with the cell cortex.

1.3. Microtubule regulators

Microtubules have the intrinsic property of dynamic instability which enables them to be remodelled rapidly into new structures and shapes. Nevertheless, various systems must be in place to organise the microtubules temporally and spatially within the cell. Here I will discuss some of the major mechanisms and proteins involved in microtubule regulation. I have broadly placed these mechanisms in the following categories: nucleation, regulation of microtubule dynamics, microtubule motor proteins and linking or bundling mechanisms that influence microtubule distribution

and interactions. In the following sections I will discuss these categories of regulators and some of the key mechanisms and proteins that have been uncovered.

1.3.1 Nucleation

The principle microtubule nucleation sites within the cell are described as microtubule organising centres (MTOCs). The primary MTOC is the spindle pole body (SPB) in yeast, and centrosome in higher eukaryotes. In interphase cells one centrosome or SPB is found within the cell but on entry into mitosis the structure duplicates and acts as the key nucleator of microtubules during spindle formation.

Centrosomes primarily consist of a pair of centriolar cylinders, consisting of 9 sets of triplet microtubules, surrounded by a cloud of pericentriolar material (PCM) (Bornens, 2002). There are two centrioles, the mother and daughter, lying at right angles to one another in close proximately. The PCM is the source of microtubule nucleation due to the presence of gamma-tubulin containing ring complexes (gamma-TURCs) that can nucleate microtubules *in vitro* and that appear to be anchored within the PCM when visualised by electron microscopy (Moritz *et al.*, 1995; Zheng *et al.*, 1995). Early in mitosis, recruitment of gamma-tubulin to the centrosome is increased 5 fold to stimulate the increased microtubule nucleation that is needed at this time to build the mitotic spindle (Khodjakov and Rieder, 1999). In many interphase cells the centrosome is also responsible for the nucleation of microtubules, but in some specialised cell types of multicellular organisms and also in some unicellular eukaryotes, additional nucleation sites have been identified (Sawin *et al.*, 2004; Mogensen and Tucker, 1987).

Female meiotic cells and plant cells do not have a conventional centrosome, indicating that centrosomes are not essential for the microtubule nucleation needed to form a spindle. Therefore, mechanisms must exist in the absence of centrosomal MTOCs to nucleate and organise the bipolar spindle array. Insights into this mechanism were provided by observations in *Drosophila* oocytes. A mass of

microtubules were seen to assemble on the meiotic chromosomes and then be bundled into a tapered bipolar spindle (Theurkauf and Hawley, 1992). Further experiments in metaphase-arrested *Xenopus* egg extracts found a similar method of spindle formation in the absence of centrosomes (Heald *et al.*, 1996). Clearly chromosomes have the ability to assemble microtubules in the absence of centrosomes.

The mechanism of chromosome induced microtubule polymerisation is initiated by the small GTPase Ran, a factor essential for nuclear import in interphase (Kalab *et al.*, 1999; Wilde and Zheng, 1999). A high concentration of GTP-Ran accumulates near to chromosomes in mitosis as its exchange factor, RCC1, localises to chromatin. Active Ran-GTP promotes spindle assembly by releasing spindle assembly factors and molecular motors from inhibition by importin alpha and beta (Ems-McClung *et al.*, 2004; Gruss *et al.*, 2001; Wiese *et al.*, 2001). One such factor, TPX2 (targeting protein for Xklp2) is a microtubule associated protein, and when released from importin inhibition, promotes microtubule assembly around the chromosomes (Gruss *et al.*, 2001). The mechanism by which TPX2 promotes this assembly is not understood but it does not act like a conventional microtubule stabiliser (Schatz *et al.*, 2003). In addition, the Ran-GTP system is involved in later stages of acentrosomal spindle formation and evidence now indicates that the system plays a number of important roles in centrosomal spindle assembly (Arnaoutov and Dasso, 2003; Li and Zheng, 2004; Moore *et al.*, 2002; Nachury *et al.*, 2001).

Directing microtubule nucleation at specific locations in the cell through the presence of MTOCs is the first step in microtubule organisation. By recruiting microtubule nucleators at specific times during the cell cycle and development microtubules can be organised over time as well as space.

1.3.2 Regulators of microtubule dynamics

Microtubules are more dynamic *in vivo* than those made of purified tubulin in vitro, suggesting that cellular factors regulate microtubule turnover *in vivo*. Furthermore, mitotic microtubules turn over 5- to 10- fold faster than interphase microtubules in mammalian epithelial cells, indicating that these cellular factors are regulated during the cell cycle (Saxton *et al.*, 1984). Variations of dynamics have also been recorded in different cell types and spatially within the cell (Shelden and Wadsworth, 1993; Komarova *et al.*, 2002b).

Analysis of microtubule asters in *Xenopus* egg extracts has demonstrated that one mechanism to increase microtubule turnover would be to increase catastrophe rate at plus ends. Similar studies in sea urchin egg extracts show that suppression of MT rescue can bring about similar increases in turnover rate (Desai and Mitchison, 1997). Analysis in intact cells, demonstrates that the transition from interphase to mitosis correlates with an increase in catastrophe and a decrease in rescue frequency (Rusan *et al.*, 2001). Altering the parameters of microtubule behaviour appears to be a key mechanism for the rapid reorganisation of the interphase array into a mitotic spindle.

The striking variation in microtubules dynamics, suggests that there is a complex network of microtubule regulators at work in the cell. A number of proteins that influence dynamic parameters have been uncovered and are traditionally categorised as either stabilisers or destabilisers.

1.3.2.1 Stabilisers

The first group of microtubule stabilising proteins to be identified came from studies of neuronal cells. With the purification of microtubules from bovine and porcine brains, microtubule associated proteins (MAPs) that bind to and stabilise microtubules were co-purified (reviewed Desai and Mitchison, 1997). All of these proteins stabilise microtubules and promote assembly. Neuronal MAPs, MAP1, MAP2

and Tau, affect microtubule dynamics by slightly increasing the polymerisation rate, vastly reducing the catastrophe rate and increasing the rescue rate. This results in an increase in the amount of polymerised tubulin and reduces the turn over rate. The stable microtubules produced by these MAPs are required for neurite formation.

Strong evidence indicates that the MAPs comprise a redundant system compensating for each others functions (Takei *et al.*, 2000). Mice with single knock outs of *tau* or *map1b* have only mild abnormalities, whereas, much more severe neuronal defects are seen in double knock out mice.

The MAP4 is related to the neuronal MAPs but is ubiquitously distributed. *In vitro* MAP4 specifically increases rescue frequency whilst other parameters remain unaffected (Ookata *et al.*, 1995). Depletion results in no obvious microtubule defects in interphase or mitosis (Wang *et al.*, 1996). However, polymer level is reduced in interphase in HeLa cells depleted of the protein (Nguyen *et al.*, 1999).

The conventional MAPs stabilise microtubules primarily through the suppression of catastrophe rate but XMAP215, discovered in *Xenopus* egg extracts, affects dynamics in a different way (Gard and Kirschner, 1987). XMAP215 was the first member of a family of highly conserved proteins, the Dis1/TOG family, to be discovered. The *Drosophila* member of this family, Mini spindles (Msps), is the focus of this study and will be discussed in detail, along with the other members of the family, in later sections.

An expanding group of proteins known as the plus-end tracking proteins (+TIPs) have been identified and appear to play roles in the regulation of plus end microtubule dynamics (Carvalho *et al.*, 2003). CLIP170 the founding member of this family was originally identified as a protein that binds endocytic vesicles to microtubules (Pierre *et al.*, 1992; Rickard and Kreis, 1990). It was later shown to bind specifically to growing plus ends, a distinguishing feature of the +TIP proteins (Perez *et al.*, 1999). CLIP170 promotes the rescue of microtubules at the cell cortex in human cells to ensure they remain at the cell periphery (Komarova *et al.*, 2002a). The role of the protein is conserved in the fission yeast homologue Tip1 which is required for the

targeting of microtubules to the ends of the cell (Brunner and Nurse, 2000) but, rather than promoting rescue, the protein appears to suppress catastrophe in fission yeast. Whether CLIP proteins alter microtubule dynamics directly or through interaction with another protein is not known.

The CLIP-associated proteins (CLASPs) bind to CLIP protein and also localises to the plus ends of microtubules (Akhmanova *et al.*, 2001). A role for these proteins in the stabilisation of microtubules at the leading edge of motile fibroblasts and regulation of kinetochore microtubule dynamics has been demonstrated (Maiato *et al.*, 2003; Maiato *et al.*, 2002; Akhmanova *et al.*, 2001). Again, it is not known if CLASP directly alters microtubule dynamics or acts through another protein.

Another TIP protein influencing microtubule dynamics is the highly conserved EB1 protein (Tirnauer and Bierer, 2000). When human EB1 protein is added to *Xenopus* extracts, plus end pausing is reduced significantly along with a reduction in catastrophe rate (Tirnauer *et al.*, 2002b). Furthermore perturbing EB1 function in budding yeast and *Drosophila* cells increased pausing (Tirnauer *et al.*, 1999; Rogers *et al.*, 2002; Nakamura *et al.*, 2001), identifying EB1 is the first known anti-pause factor.

There are a growing number of plus end proteins that promote microtubule growth and stability (reviewed Carvalho *et al.*, 2003). Understanding of how these proteins function mechanistically both individually and in a co-ordinated fashion, to promote microtubule stabilisation is lacking and further studies are needed.

1.3.2.2 Destabilisers

The high frequency of catastrophes that are seen *in vivo* compared to pure tubulin suggests the existence of factors that induce catastrophe, acting to reduce net assembly and increase microtubule turnover. A number of factor that promote microtubule destabilisation have been identified.

The OP18/Stathmin protein was first identified as being up-regulated in some tumours. Subsequently, the protein was reported to increase catastrophe frequency three to sixfold *in vitro* (Belmont and Mitchison, 1996; Belmont *et al.*, 1996) and to cause microtubule depolymerisation when overexpressed in cells (Marklund *et al.*, 1996). Op18 has the ability to sequester free tubulin (Jourdain *et al.*, 1997) and to promote catastrophe (Belmont and Mitchison, 1996). The two activities can be separated in the protein and both may contribute to microtubule destabilisation (Howell *et al.*, 1999). Microtubules assembled in the presence of a non-hydrolyzable GTP analogue are resistant to Op18 promoted depolymerisation, suggesting the protein may act by stimulating GTP hydrolysis. The mechanism by which OP18 promotes depolymerisation is still being actively researched.

Another major group of destabilisers are the KinI kinesins. These proteins are a subfamily of the kinesins that constitute a superfamily of microtubule based motor proteins (Desai *et al.*, 1999b). Intriguingly, rather than translocating along microtubules, the KinI family is involved in the regulation of microtubule dynamics at both the plus and minus end. Depletion of the KinI protein, XKCM1, from *Xenopus* extracts results in increased size of the mitotic spindle and measurements of microtubule dynamics reveal a dramatic decrease in catastrophe rate (Walczak *et al.*, 1996). *In vitro* experiments indicate that the Dis1/TOG family of microtubule stabilisers oppose the KinI destabilising activity (Tournebize *et al.*, 2000; Kinoshita *et al.*, 2002). This interaction will be discussed in detail later.

In mitosis the mammalian homologue of XKCM1, MCAK, is localised to the spindle poles and centromeric region (Maney *et al.*, 1998). Depletion of the protein through antibody injection results in spindle formation defects with very long microtubules, consistent with a role as a microtubule destabiliser (Kline-Smith and Walczak, 2002). Specific delocalisation of MCAK from the centromeres results in chromosome congression and kinetochore attachment defects, suggesting a role in destabilising improper kinetochore attachments (Kline-Smith *et al.*, 2004). Evidence

also specifies a role for the KinI proteins in regulating dynamics in interphase (Kline-Smith and Walczak, 2002).

The crystal structure of Kif2C, a mouse KinI, was recently solved and in silico docking experiments suggested mechanisms for KinI-promoted microtubule depolymerisation (Ogawa *et al.*, 2004). The class specific neck was predicted to facilitate binding to the microtubule plus end by interacting with the lumen of the microtubule to prevent lateral interactions between the protofilaments. The molecule may then stabilise the curved protofilament conformation and thus promote catastrophe. Promotion of a curved structure has been suggested by electron microscopy studies (Moores *et al.*, 2002) and preference for plus end binding has also been demonstrated (Hunter *et al.*, 2003). Binding of the protein to the curved filament was proposed to trigger ATP hydrolysis although the exact function of this hydrolysis is not clear. Confirmation of the structural interactions postulated by the in silico docking experiments of Ogawa *et al* (2004) awaits the co-crystallisation of a KinI protein with microtubules.

Another family of kinesins, the Kip3 proteins have also been implicated in microtubule destabilisation. Depletion of Kip3 protein KLP67A from *Drosophila* S2 cells results in elongated spindle microtubules similar to those seen following depletion of the Kin I kinesin KLP10A. Similarly the fission yeast mutant alleles of kip3 kinesins *klp5* and *klp6* have long stable microtubules that are resistant to depolymerising drugs (West *et al.*, 2001).

An additional mechanism for destabilising microtubules is to sever the microtubule polymer. Severing activity was detected in *Xenopus* egg extracts when microtubules were stabilised by taxol. The severing activity is low in interphase and activated during meiosis (Vale, 1991) where it may aid in the rapid reorganisation of the microtubule cytoskeleton that occurs during the transition from interphase to M phase.

Proteins identified as having severing activity include p56, p48(EF -1) and the most well characterised, katanin (Shiina *et al.*, 1995). Katanin is a heterodimer that is

responsible for the majority of M-phase severing activity in *Xenopus* extracts (McNally and Thomas, 1998) and may be involved in microtubule poleward flux at centrosomes (McNally *et al.*, 1996). In addition, the protein has an essential role in neurons, releasing microtubules nucleated at the centrosome for transport into axons and dendrites (Ahmad *et al.*, 1999).

1.3.3. Motor proteins

Microtubule motors are proteins that can bind to and translocate along microtubules, in either direction, in an ATP dependent manner (reviewed Mallik and Gross, 2004). The polarity of microtubules is utilised to provide direction and the distribution of microtubules will influence where motors can travel. Motors can interact with many different cargos, transporting them via microtubules to specific localisations in the cell and thus contributing to asymmetrical distribution of components of the cell. Such asymmetrical distribution is key for many cellular processes. For example, motors are required to direct the localisation of mRNAs important for correct development in oogenesis and early embrogenesisis (reviewed Saxton, 2001).

Microtubule motor proteins play key roles in the formation, maintenance and function of the bipolar spindle (reviewed (Heald, 2000). Motors are involved in sliding microtubules in relation to one another in order to form the spindle shape (Sharp *et al.*, 2000). They remain important in maintaining the forces within the spindle through metaphase and in spindle elongation in anaphase (Sharp *et al.*, 1999).

The two major classes of microtubule motors are the dynein and kinesin families (review Goldstein, 2001). Kinesins are a very large family of proteins in which there is a conserved motor domain and a diverse range of tail regions. These different tail regions allow the proteins to interact with a vast array of intracellular pathways. In this way, kinesins can link to many cargos and cross-link to microtubules

and other cytoskeletal elements. The cytoplasmic dyneins are far less diverse, yet are involved in a similarly vast number of cellular processes. In the case of dynein, multiple functions are supported through the diverse proteins that interact with the motor (reviewed Mallik and Gross, 2004)

1.3.4. Mechanisms for microtubule organisation

In addition to regulators of microtubule dynamics and motors, there are mechanisms in the cell that influence the distribution or pattern of microtubules within the cell by anchoring or linking microtubules. I will discuss some of the key mechanisms and proteins involved in these processes.

1.3.4.1 Minus end capture

Previously, I described the role of the centrosome as the site of microtubule nucleation. In addition, the centrosome plays a key role as the major site of minus end stabilisation and anchorage in the cell. Radial arrays of microtubules, produced by localised nucleation, are reinforced by the anchoring of minus ends to the centrosomes. The gamma-TuRC complex is believed to act as a minus end capping complex in addition to nucleating microtubules (Wiese and Zheng, 2000; Moritz *et al.*, 2000).

In interphase, dynein and its activator dynactin, play a crucial role in maintaining focused arrays of microtubules in interphase, in addition to their roles in mitosis (Quintyne and Schroer, 2002; Quintyne *et al.*, 1999). The centrosomal component ninein is a strong candidate for a role in anchoring, as the protein concentrates around the mother centriole (Bouckson-Castaing *et al.*, 1996) and is also localised to the minus ends of noncentrosomal microtubule bundles associated with apical noncentromsomal sites in epithelial cells (Mogensen *et al.*, 2000).

In the spindle, microtubules are in a constant state of flux with microtubules polymerising at the plus ends and depolymerising at the minus ends. In contrast, the minus ends of astral microtubules remain anchored and do not depolymerise. The mechanisms governing this difference are unknown. In spindle formation, it is clear that dynein together with NuMA are important for focusing the poles of the spindle and crosslinking microtubules at the poles (Merdes *et al.*, 2000). There is also some evidence for the Dis1/TOG family of proteins in maintaining the centrosome array in mitosis (Usui *et al.*, 2003) but whether these proteins simply stabilise microtubule dynamics or physically link microtubules to the centrosome has not been determined.

1.3.4.2 Capture of plus ends.

Anchoring of minus ends at MTOCs allows the more dynamic plus ends of microtubules to freely explore the cytoplasm where they may interact with targets. Such interactions are essential for a number of cellular functions, including the creation of kinetochore attachments and cortical interactions. The success of this method of microtubule attachment comes from dynamic instability of microtubules but nevertheless regulation is needed. Microtubule growth needs to be promoted at the poles, but in the cytoplasm microtubule catastrophe promoters, such as OP18 and the KinI kinesins, are required to produce the highly dynamic plus ends needed for successful search and capture of the kinetochores.

Live imaging in vertebrate cells enabled researchers to visualise the attachment of microtubules to kinetochores (Hayden *et al.*, 1990). Microtubules that make an attachment quickly become stabilised, whereas those that do not, depolymerise. This initial attachment is dependent upon the minus end motor activity of cytoplasmic dynein (Vaisberg *et al.*, 1993) which is highly concentrated at unattached kinetochores (review by (Banks and Heald, 2001). Another motor concentrated at the kinetochore, CENP-E is also implicated in the initial encounters of the kinetochore with microtubules (McEwen *et al.*, 2001; Putkey *et al.*, 2002).

Once an initial attachment is made additional microtubules become attached to from a bundle of microtubules called the kinetochore microtubule fibre. Whilst dynein and CENP-E are involved in initial attachments, they are not essential for kinetochore microtubule formation (McEwen *et al.*, 2001; Vaisberg *et al.*, 1993). Pioneering biochemical and genetic experiments in budding and fission yeast have enabled researchers to build up a picture of the protein hierarchy of the kinetochore and the protein complexes important for microtubule kinetochore attachment (Wigge and Kilmartin, 2001; He *et al.*, 2001; Westermann *et al.*, 2003; De Wulf *et al.*, 2003). Not all of the protein complexes described in yeast are conserved in higher eukaryotes. However, the Ndc80 complex, crucial to the attachment process, is well conserved (DeLuca *et al.*, 2002; Howe *et al.*, 2001; McCleland *et al.*, 2003; Wigge and Kilmartin, 2001).

The Ndc80 complex itself does not directly bind to microtubules. In budding yeast the DASH complex is believed to mediate interaction between the microtubule ends and the kinetochore (De Wulf *et al.*, 2003), but, no animal equivalent of this complex has been found. The search continues to find the factors and understand the mechanisms involved the formation of a stable kinetochore microtubule attachment.

Even as kinetochore microtubules are stabilised, they exhibit highly regulated dynamics associated with chromosome movement as revealed by the use of tagged tubulin subunits and photobleaching experiments. Microtubule depolymerisation at the kinetochore and motor activity combine to create a pulling force on the kinetochore that induces polymerisation at the lagging sister kinetochore. This co-ordinated movement is used to align the chromosomes at the metaphase plate. It has been suggested that microtubule growth promoters, such as CLASPs (Maiato *et al.*, 2003) or EB1 (Tirnauer *et al.*, 2002a), which localise to kinetochores, play a role in regulating this process.

The plus end tracking proteins also play roles in regulating microtubule behaviour at the cell cortex. The Rho-family of GTPases, known to regulate the actin cytoskeleton, have recently been implicated in controlling the reorganisation of the

microtubule network in migrating cells (Fukata *et al.*, 2003; Wittmann *et al.*, 2003). The Rho-GTP regulators appear to act through some +TIP proteins, to capture and selectively stabilise microtubules at cortical sites at the leading edge. For example, the plus end localising protein CLIP-170 interacts with IQGAP, a molecule that binds to the actin cytoskeleton and is an effector of Cdc42 and Rac1, to direct the microtubule array (Fukata *et al.*, 2002). Microtubules also appear to be stabilised through inactivation of the catastrophe promoter OP18/stathmin through the Rac system (Wittmann *et al.*, 2004).

Specific structures in the cell, such as centrosomes and kinetochores, are involved in organising specific microtubule arrangements that are required for cellular functions. These structures regulate and co-ordinate the activities of nucleation, anchoring and regulation of dynamics by recruitment of specific proteins.

1.3.4.3 Microtubule bundling

Microtubule bundling is a common event in many different organisms and cell types. Within the spindle, microtubules are bundled into poles and motor proteins are clearly involved in this process (Heald, 2000). In neurons, parallel bundles of microtubules form in the axon and the presence of these bundles is dependent upon neuronal MAPs such as Tau and MAP1B (Takei *et al.*, 2000).

Bundling activities for MAPs have been frequently reported but in many cases this may be an artefact of protein overexpression (Haren and Merdes, 2002; Raemaekers *et al.*, 2003; Bu and Su, 2001). The presence of two microtubule binding sites through dimerisation with itself or another MAP could easily facilitate microtubule bundling. The formation of small bundles is common in most cells, for example, the interphase microtubules in fission yeast are known to be small bundles of 4-7 microtubules (Sagolla *et al.*, 2003). Even in tissue culture cells with extended microtubule arrays, microtubules will occasionally converge forming small bundles, suggesting microtubules have an affinity for each other. The bundling activity of

microtubules is not well understood and to my knowledge no factors that disrupt interphase bundling have been discovered. There are many redundant process involved in this phenomenon.

1.4 *Drosophila* as a model organism for studying microtubule regulation

The fruit fly, *Drosophila melanogaster*, has been used extensively as an experimental organism. A number of factors have come together to promote *Drosophila* as an important model organism for studying cellular and developmental biology. Firstly, strong genetic understanding of the organism and the many techniques and resources that have been created, allow manipulation of the organism. Secondly, *Drosophila* has a rapid life cycle and can be easily and inexpensively maintained. Finally, *Drosophila* is a multicellular organism enabling the study of a range of different tissues at different developmental stages.

How can *Drosophila* be used to examine microtubule regulation? Genetic screens have been used to identify essential genes involved in cell division, many of which are conserved in other organisms. These include major regulators of cell division and spindle assembly Polo and Aurora, and also MAPs such as Mini-spindles and Mast (Glover *et al.*, 1995; Sunkel and Glover, 1988; Cullen *et al.*, 1999; Lemos *et al.*, 2000).

Microtubules in cell division have been studied extensively in *Drosophila* (Kwon and Scholey, 2004). Mutations in genes essential for cell division can lead to lethality at various stages of fly development (Glover, 1989). In the case of larval lethals, cell division defects and spindle abnormalities can be detected by examining mitotic cells of the larval neuroblast. In addition, the syncytial embryo is also a useful tissue to examine the mitotic spindle. The development of live imaging techniques of these embryos has allowed spindle formation to be followed in real time, allowing

greater understanding of the processes involved (Sharp *et al.*, 2000). Effects of protein inactivation, either through mutation or by antibody injection, can also be followed (Maiato *et al.*, 2002; Sharp *et al.*, 2000). Such analysis has given insights into how different proteins regulate the spindle.

Studies of female meiosis in *Drosophila* have uncovered some of the mechanisms and proteins involved in spindle formation in the absence of centrosomes (Theurkauf and Hawley, 1992). The microtubule motor, Ncd (non-claret disjunctional), first identified as being involved in meiotic spindle formation (Matthies *et al.*, 1996), has subsequently been shown to play a non-essential role in mitotic spindle assembly (Sharp *et al.*, 2000). Male meiosis has also been used to examine the function of proteins in spindle assembly and also in cytokinesis. Advantages of using these cells is that cytokinesis defects can be easily and unambiguously identified and meiotic spindles are large, and thus good for cytology (Giansanti *et al.* 2001). Several mutations that disrupt cytokinesis have been identified that have helped to outline the importance of the central spindle for cytokinesis (Giansanti *et al.*, 2001).

Flies have also been used to study interphase microtubule arrays. EM studies of epidermal wing cells in adult flies have given insight into the structure, capture and nucleation of the microtubule bundles in these cells that are arranged in the absence of centrosomes (Mogensen and Tucker, 1987). Microtubule structure has also been examined in various stages of oogenesis where the microtubule network is required for the transport and anchoring of mRNA and proteins. Correct localisation of these cargos is essential for development of the oocyte and the embryo (reviewed (Saxton, 2001).

Drosophila culture cells are increasingly being used to examine many aspects of cell biology. The S2 cell culture line is particularly amenable to dsRNA interference and has been used in a number of large scale screens including some examining the cytoskeleton (Goshima and Vale, 2003; Rogers *et al.*, 2003; Echard *et al.*, 2004). Until recently the cytology in these cells was poor due to the spherical nature of the cells. However, if grown on a surface coated in the lectin concanavalin A (con A),

cells become a flat disc shape with a raised centre containing the nucleus and organelles (Rogers *et al.*, 2002). As the cell spreads the microtubules extend out to the periphery and in the flat area around the edge of the cell single microtubules can be visualised. This property allows individual microtubule dynamics to be followed in the cell (Rogers *et al.*, 2002).

To conclude, the strong genetic understanding of *Drosophila* is a great advantage to the microtubule researcher, as it allows genetic manipulation. In addition, as a multicellular organism microtubules can be examined in a variety of tissues at different stages of development to gain a fuller understanding of microtubule regulation through time and development.

1.5 Mini spindles and the Dis1/TOG family of MAPs

In this study, the *Drosophila* protein Mini spindles (Msps) will be investigated. Studies of this protein, and other members of the Dis1/TOG family, have been carried out in recent years revealing a broad range of roles in microtubule regulation. Here I will discuss what has been revealed about Msps and its homologues and what remains to be uncovered.

1.5.1 Protein Structure

Members of the Dis1/TOG family were discovered independently by a range of genetic and biochemical approaches but were soon recognised as members of the same family from analysis of protein structure. The most characteristic feature of the family is an N-terminal region consisting of 2-5 TOG domains. The TOG domain (referring to the human colonic, hepatic tumour over-expressed gene (ch-TOG)) is a sequence approximately 200 amino acids long, containing up to 5 HEAT repeat motifs (Neuwald

and Hirano, 2000). HEAT repeats have been found in a number of proteins and the name refers to those proteins in which the repeat was first found (huntingtin, elongation factor 3, the PR65/A subunit of protein phosphatase 2A (PP2A) and the kinase TOR). Structural data indicates that the HEAT repeat consists of two helices, A and B, which form a helical hairpin (Neuwald and Hirano, 2000). Neighbouring hairpins stack against each other forming a super-helix (Andrade *et al.*, 2001; Groves *et al.*, 1999) that forms a surface involved in protein interactions (Andrade *et al.*, 2001; Neuwald and Hirano, 2000).

The human TOGp, frog XMAP215, fly Mini spindles, slime mould DdCP224 and plant Mor1 all contain 5 TOG domains and a conserved C-terminal non-repeat region (figure 1.4) (Ohkura *et al.*, 2001). The *C. elegans* protein, Zyg-9 differs from the above group in that it contains only 3 repeats in the N-terminus. The C-terminal non-repeat region has no significant homology to the conserved region in the other proteins. The three yeast proteins, Dis1, Alp14 and Stu2, which have two repeats in the N-terminal region, share little homology in the C-terminal region but all contain a predicted coiled coil.

Localisation to microtubules, centrosomes and in some cases the kinetochore have been demonstrated for members of the Dis1/TOG family (Ohkura *et al.*, 2001). Dissection of domain structure has indicated that the C-terminal region may be involved in all these localisations. In XMAP215, DdCP224, Dis1 and Stu2, the region is sufficient for centrosome localisation (Popov *et al.*, 2001; Graf *et al.*, 2000; Graf *et al.*, 2003; Nakaseko *et al.*, 1996; Usui *et al.*, 2003). In Dis1, it is also responsible for microtubule binding and localisation to the kinetochore (Nakaseko *et al.*, 1996).

The region responsible for microtubule binding in XMAP215 and TOG is less clear cut. *In vitro* microtubule binding experiments indicate that the C-terminal region of XMAP215 strongly binds microtubules whereas the N-terminal and middle fragments only display weak binding (Popov *et al.*, 2001). The TOG protein was bisected, revealing that the N-terminal (1-925) amino acids could strongly associate with microtubules whilst the C-terminus (delete 14-1229aa) had a weak association

(Charrasse *et al.*, 1998). These differences could be explained by the different ways the proteins were dissected in the two experiments. The XMAP215 C-terminal fragment, while able to bind microtubules efficiently *in vitro* does not localise to microtubules correctly in the cell. Instead a punctate staining was seen along microtubules. The N-terminal fragment was able to localise smoothly along the microtubules, but, the staining was much weaker. Therefore, microtubule binding *in vivo* appears to involve multiple regions of the protein.

The domains responsible for Msps protein localisation and function remain to be identified.

1.5.2 Functions of the Dis1/TOG family of proteins

1.5.2.1 Regulation of plus end dynamics

Regulation of microtubule dynamics is a key mechanism for manipulating microtubule organisation within the cell. The Dis1/TOG family has been uncovered as having unique properties of microtubule regulation. The first member of this family to be characterised was the *Xenopus* homologue, XMAP215 (Gard and Kirschner, 1987). The protein, isolated from *Xenopus* egg extracts, promoted microtubule growth at the plus ends 10 fold when added to purified tubulin. At the minus end, the increase in polymerisation is only two fold. Furthermore, addition of purified XMAP215 to microtubules increased the depolymerisation rate and suppressed the number of rescues (Vasquez *et al.*, 1994). The combined effect is the creation of microtubules that are more dynamic than those in a pure tubulin solution. Similar experiments with the human protein TOGp also demonstrated an increase in polymerisation, but in these experiments the increase in elongation rate was the same for both ends of the microtubule (Charrasse *et al.*, 1998). Other families of stabilising MAPs have a small effect on polymerisation and principally reduce the catastrophe frequency and increase

rescue rate (Desai and Mitchison, 1997). XMAP215 demonstrated that, at least *in vitro,* it is a major promoter of polymerisation and thus unique among MAPs so far identified.

Following the experiments using purified XMAP215, further work on the role of this protein was carried out in *Xenopus* egg extracts. Depletion of XMAP215 from egg extracts was found to increase the catastrophe frequency, as well as affecting polymerisation (Tournebize *et al.* 2000). The catastrophe-suppressing function of XMAP215 was not detected with purified protein, as rather than being an intrinsic activity of XMAP215, the protein antagonises XKCM1, a major catastrophe promoter in the extract (Tournebize *et al.*, 2000). XKCM1 is a member of the KinI family of kinesins which destabilise microtubules by increasing the catastrophe frequency (Desai *et al.*, 1999a).

Addition of purified XMAP215 and XKCM1 to pure microtubules *in vitro* produced microtubule dynamics similar to those seen *in vivo*, leading to the conclusion that XKCM1 and XMAP215 are the two major regulators of microtubule dynamics in the cell (Kinoshita *et al.*, 2001). Indeed, spindle assembly in *Xenopus* extract requires XMAP215. Partial depletion of XMAP215 decreases spindle size and near complete depletion prevents spindle formation (Tournebize *et al.*, 2000). Protein truncation analysis revealed that the N-terminal fragment, containing part of the HEAT repeat domain, but lacking the C-terminal microtubule binding and centrosomes localisation domain can rescue defects caused by XMAP215 depletion and appears to contain the catastrophe suppression activity (Popov *et al.*, 2001). This suggests that it is the N-terminal region that directly or indirectly interacts with XKCM1.

Most work on Dis1/TOG proteins had, until recently, pointed towards a role for the proteins in stabilising microtubules. Two papers recently revealed that *in vitro* both XMAP215 and the yeast homologue, Stu2, can act as microtubule destabilisers. Shirasu-Hira *et al.* (2003) incubated pre-formed microtubules, that had been stabilised by the non-hydrolysable GTP analogue GMPCCP, with cytoplasmic fractions under conditions that do not allow polymerisation. They hoped that the assay would identify

novel microtubule destabilisers, however, the new 'destabiliser' they found was XMAP215. It is unclear how this activity is related to the *in vivo* activity of the protein. Electron microscopy indicated that GMPCPP microtubules have a blunt end structure, and the authors proposed that GMPCPP microtubules could serve as a model for the paused (blunt end) state of microtubules and that XMAP215 could destabilise this state. The problem with this interpretation is that there is no direct evidence that paused microtubules have blunt ends either *in vitro* or *in vivo*. One way to test this hypothesis would be to determine the structure of microtubule ends, in extracts partially depleted or overexpressing XMAP215, to see if there is a correlation between the absence of the protein and the presence of blunt ends.

Both microtubule stabilising and destabilising activities have been reported for the budding yeast Stu2 protein (Kosco *et al.*, 2001; van Breugel *et al.*, 2003). *In vitro* studies by Breugel *et al* (2003) found that purified Stu2 protein acts as a microtubule destabiliser, decreasing the polymerisation rate and inducing catastrophes *in vitro,* under conditions very similar to those in which XMAP215 was found to be a microtubule stabiliser. They went on to deplete Stu2p from intact cells and found that cytoplasmic microtubules were longer than those in wild-type cells, and concluded that Stu2 acts as a microtubule destabiliser *in vivo* as well as *in vitro*. An earlier study, *in vivo* microtubule dynamics in Stu2 depleted cells indicated that Stu2 promotes catastrophe *in vivo* but the length of microtubules was not significantly affected and microtubules did not appear to be destabilised (Kosco *et al.*, 2001). In addition, another study revealed defects in spindle elongation following Stu2 inactivation. Such behaviour would not be expected from a microtubule destabilising protein. Whilst both *in vitro* and *in vivo* Stu2p can promote catastrophe, whether Stu2p is a stabiliser or destabiliser *in vivo* is unclear.

The Dis1/TOG family play a role in the regulation of microtubule dynamics; however, the true nature of the proteins' activity *in vivo* is in question. *In vitro* studies indicate that purified proteins can have different effects on microtubules depending on the conditions. Additionally, the activity of Stu2p *in vitro* and *in vivo* differs from that

of XMAP215 *in vitro*. The disparity may reflect differences between the functions of the two proteins; perhaps the activity of the two proteins has diverged. Alternatively, the activity of the protein may be tightly regulated both spatially and temporally, and consequentially the type and stage of the cell observed will reflect different activities of the proteins. Perhaps the Dis1/TOG proteins can have both destabilising and stabilising activities at different times, depending on the presence of other proteins or regulatory mechanisms.

1.5.2.2 Role of Dis1/TOG proteins at the kinetochores

Microtubules within the spindle are polarised with the minus ends focused at the poles and the plus ends extending towards to the chromosomes in the centre of the spindle. The plus ends interact with the sites of microtubule attachment, the kinetochores, and apply the forces that are required for chromosome alignment and segregation. Studies in *Xenopus* revealed a role for XMAP215 in spindle assembly by the promotion of microtubule plus end dynamics (Tournebize *et al.*, 2000). However, studies from fission yeast indicated that these MAPs may play a more specific role in attachment at the kinetochore. Loss of Dis1 results in failure of chromatid separation but spindle formation and elongation occur (Nakaseko *et al.*, 1996; Ohkura *et al.*, 1988). Real time analysis of chromosome segregation in *dis1* mutants reveals that they lack a period equivalent to metaphase (Nabeshima *et al.*, 1998). Such a phenotype could be due to defects in pole to kinetochore attachment. Live imaging of GFP-tagged Dis1 demonstrated that Dis1 localises to kinetochores in mitosis and moreover chromatin immunoprecipitation experiments (CHIP) demonstrated that it associates with the central core of centromeres (Nakaseko *et al.*, 2001). Consequently, Dis1 is perfectly placed to play a role in kinetochore microtubule attachment.

Fission yeast is the only organism found to have two members of the Dis1/TOG family, Dis1 and Alp14. Singly inactivated, these genes are not lethal but double mutants are lethal indicating that the two genes have overlapping functions

(Nakaseko *et al.*, 2001). The phenotypes of the two mutants are not identical. *alp14* deletion, unlike *dis1* deletion, abolishes bipolar spindle assembly (Garcia *et al.*, 2001); furthermore, cytoplasmic microtubules are also affected (Nakaseko *et al.*, 2001). Alp14 might play a more important role in microtubule assembly than Dis1. In addition to spindle defects, the spindle checkpoint is also compromised in *alp14* mutants. This checkpoint prevents chromosome segregation and mitotic exit until all kinetochores are attached to microtubules, ensuring that chromosomes are segregated accurately. When *alp14* mutants are treated with a depolymerising drug, the cells do not maintain a mitotic arrest, a phenotype shared by proteins involved in the spindle checkpoint. As with Dis1, localisation studies revealed that Alp14 protein localises to the kinetochore periphery and centromeric association was confirmed by CHIP (Nakaseko *et al.*, 2001; Garcia *et al.*, 2001). Budding yeast Stu2 localises to the kinetochore and has been implicated in microtubule-kinetochore attachment (He *et al.*, 2001).

It is not clear whether the kinetochore functions of the Dis1/TOG family are conserved in any organisms other than yeast. Reports in other organisms have demonstrated possible kinetochore localisation (Matthews *et al.*, 1998; Graf *et al.*, 2000). The *C. elegans* homologue, Zyg-9 is reported to localise to chromosome periphery in metaphase and accumulates on the chromosomes when microtubules are depolymerised. In addition, Dictyostelium DdCP224 localises to the kinetochore region in metaphase. Kinetochore localisation of Alp14 was only revealed by live imaging and could not be seen in fixed cells (Garcia *et al.*, 2001). Therefore, kinetochore localisation of other proteins in the family may only be revealed by live imaging of tagged proteins.

The importance of Dis1 and Alp14 at the kinetochore was further revealed by studying their interaction with the fission yeast Kip3 destabilising kinesins (Garcia *et al.*, 2002). Mutants in the Kip3 kinesins in fission yeast, Klp5 and Klp6 are viable but have chromosome alignment defects and a delay before the onset of anaphase that results from mad2-dependent activation of the spindle checkpoint. The mutants are not

able to form proper kinetochore attachments. When double mutants were made between klp5/klp6 and alp14/dis1 all combinations were synthetically lethal.

There are two possible explanations for this synthetic lethality. The first possibility is that these two sets of proteins play an antagonistic role in mitosis, with the lethality resulting from the hyperactivation of Klp5/Klp6 in the absence of Alp14/Dis1. The second possibility is that Alp14/Dis1 and Klp5/Klp6 share an additional function that is essential. This question was addressed by assessing if triple mutants *alp14 klp5 klp6* and *dis1 klp5 klp6* were viable. If hyperactivation of Klp5/Klp6 was the cause of lethality removing them both in combination with Alp14/Dis1 would restore viability. This was not the case as alp14klp5klp6 was still lethal. This result indicates that *klp5* and *klp6* mutants are only viable because either Dis1 or Alp14 are functional. The reverse situation also holds true; *alp14* or *dis1* mutants are viable as long as Klp5 and Klp6 are active. This genetic evidence implies that in fission yeast the KinI homologues and the Dis1 family play a collaborative role, rather than an opposing one.

1.5.2.3 Roles at the centrosomes/SPB

Whilst it is not clear how well kinetochore localisation is conserved in the Dis1/TOG family, the proteins all localise to the centrosome/SPB. (Charrasse *et al.*, 1998, Cullen *et al.* 1999, Garcia *et al.*, 2001, Graef *et al.*, 2000, Matthews *et al.*, 1998, Nabeshima *et al.*, 1995, Tournebize *et al.*, 2000, Wang and Huffaker, 1997). When microtubules are destroyed by depolymerising drugs, the MAPs remain localised to the centrosomes, indicating that localisation is not purely due to binding of microtubules localised to the centrosomes. This is supported by electron microscopy data that shows XMAP215 localising to the pericentriolar material of the centrosomes (Popov *et al.* 2001).

Studies in *Drosophila* revealed that the spindle poles need not contain conventional centrosomes to show localisation of a member of the Dis1/TOG family.

The *Drosophila* Msps protein, and its binding partner D-TACC, were the first proteins found to localise to the acentrosomal poles of the female meiotic spindles (Cullen and Ohkura, 2001). As discussed earlier, female meiotic spindles do not have centrosomes and are assembled by the alternative mechanism of chromosome driven spindle assembly. Dis1/TOG proteins, therefore, seem to play a role at both the centrosomal and acentrosomal poles.

Loss of Msps disrupts the integrity of the spindle in the larval neuroblasts (Cullen *et al.*, 1999). The most common defect was the presence of one or two extra spindles, usually sharing a pole with the larger bipolar spindle. The chromosomes are associated with the spindles and the poles all appear to be focused correctly. Mitotic spindle defects similar to those seen in the *msps* mutant were found in human cells when TOG was depleted using RNA interference (Gergely *et al.*, 2003; Holmfeldt *et al.*, 2004). Meiotic spindles in a female sterile allele of *msps* showed a distinctive tripolar phenotype (Cullen and Ohkura, 2001).

Depletion of 90% of XMAP215 protein from *Xenopus* extract resulted in a failure of microtubule spindle assembly around sperm nuclei, whist with 60% depletion, spindles could form but they were shorter in length and sometimes monopolar (Tournebize *et al.*, 2000). In the $msps^{P}$ mutant, Msps protein is reduced to less than 10% wild-type level, yet spindles are still able to form, suggesting that *in vivo*, Msps has an important role to play in maintaining spindle integrity, rather than simply ensuring microtubule assembly.

The role of Dis1/TOG proteins in microtubule plus end regulation has been demonstrated both *in vitro* and *in vivo*. However, it is not clear how this lack of regulation results in the spindle phenotypes seen in both *Drosophila msps* mutants and TOG depleted human cells. Protein localisation to the centrosomes suggests a role for Dis1/TOG proteins in regulating minus ends. This is possible as an effect on minus end polymerisation has been reported (Gard and Kirschner, 1987). A loss of localised microtubule stabilisation at the centrosomes could lead to spindle pole destabilisation and the multipolar phenotypes observed.

A role for budding yeast Stu2p in anchoring microtubule minus ends at the SPB has been demonstrated. In a mutant in which centrosome localisation was specifically disrupted, microtubules detached from the SPB and floated free in the cytoplasm (Usui *et al.*, 2003). The mechanism for this detachment is unknown, but suggests that Stu2p either anchors microtubules or is involved in stabilising the minus ends, to prevent them from depolymerising and subsequently detaching from the SPB.

Accumulation of the Dis1/TOG proteins at the centrosomes could provide a pool of protein to be loaded onto the plus ends of microtubules, growing out from the centrosome. In this way, the proteins could contribute to the increased dynamics of microtubules plus ends seen during mitosis. To support this idea, live imaging of Msps fused to GFP revealed that the protein could be seen as dots moving to and from the centrosome, as thought attached to microtubule plus ends (Lee *et al.*, 2001).

The relationship between the Dis1/TOG family and KinI kinesins has been examined to see if the antagonistic activity described for these two proteins *in vitro* plays a role in spindle assembly. Holmfeldt *et al.* (2004) found that in human cells, the multipolar phenotype seen with TOG depletion is abolished if MCAK (the XKCM1 homologue) is co-depleted with TOG protein. TOG protein appears to be required to protect spindle poles from MCAK activity. Overexpression of TOG counteracts the spindle defects seen when MCAK is overexpressed, supporting the *in vitro* evidence that the two proteins are acting antagonistically in the spindle.

1.5.2.4 Interphase roles

Spindle formation is not the only role of microtubules in the cell. A diverse array of cells depends on the microtubule cytoskeleton to fulfil a range of functions. Appropriate regulation of microtubules in these cells is also required and it is not surprising that the Dis1/TOG family of proteins have been implicated in such regulation.

In plants, the Dis1/TOG homologue, *mor1*, is essential for cortical microtubule organisation but not for the formation of mitotic or cytokinetic microtubules (Whittington *et al.*, 2001). When two temperature sensitive *mor1* mutants are shifted to the restrictive temperature, cortical microtubules become shorter and disorganised. Normal microtubule organisation is restored after a return to the permissive temperature. Such disruption of microtubules results in changes to organ morphology at all stages of development, indicating a role for Mor1 throughout development.

Fission yeast *alp14* was originally isolated as a cell shape mutant, so is also necessary for normal cell morphology (Radcliffe *et al.*, 1998). In fission yeast, microtubules running from the central region to the tips of the cell are important for the maintenance of cell polarity. Microtubules in *alp14* mutants do not reach the tip of the cell, which results in bent or branching cells (Garcia *et al.*, 2001).

Depletion of TOG and MCAK from human cells had no affect on the total amount of polymerised tubulin in the cells. Furthermore, no changes in the interphase microtubule network were seen by immunofluorescence (Gergely *et al.*, 2003; Holmfeldt *et al.*, 2004). Microtubule dynamics were not measured in these cells. The only study of interphase microtubule dynamics *in vivo* has been carried out in budding yeast *stu2* mutants (Kosco *et al.*, 2001). In *stu2* mutants, interphase microtubule catastrophe and rescue rates were promoted in a similar way to those in mitosis.

Although a role for all the Dis1/TOG proteins in interphase microtubule regulation has not yet been shown, many of the proteins localise to interphase microtubules, consistent with a function in cell morphology (Tournebize *et al.*, 2000; Graf *et al.*, 2000; Nakaseko *et al.*, 2001). In addition, the proteins are expressed in post-mitotic cells, such as the adult brain, suggesting a role in interphase (Gard and Kirschner, 1987; Charrasse *et al.*, 1998; Cullen *et al.*, 1999). In spite of this, the role of the Dis1/TOG family in non-mitotic cells of multicellular organisms is yet to be fully explored.

1.5.3 Protein interactions and regulation

Dis1/TOG protein localisation is regulated during the cell cycle, allowing activity to be directed to the sites where it is needed. The dynamic localisation is best highlighted by real time analysis of GFP-tagged Dis1 and Alp14 proteins. Both proteins localise to interphase microtubules and on entry into mitosis, the protein localises to the SPB and kinetochore (Garcia *et al.*, 2001; Nakaseko *et al.*, 2001). In budding yeast and *Dictyostelium,* the proteins localise to the SPB through out the cell cycle (Wang and Huffaker, 1997; Graf *et al.*, 2000), however, in *Xenopus* and human cells, localisation to the centrosomes is confined to mitosis (Charrasse *et al.*, 1998; Tournebize *et al.*, 2000).

Analysis at different stages of *Drosophila* development has shown that there are also developmental changes in localisation (Cullen *et al.*, 1999). In the syncytial embryo Msps remains at the centrosomes throughout the rapid cell cycles that occur in this tissue. In cellularised embryos and in somatic tissues in the brain, where the speed of the cell cycle is slowed down, Msps is localised to the centrosomes only in mitosis.

Changes in localisation of the Dis1/TOG proteins could be partly due to cell cycle dependent phosphorylation. XMAP215 *in vivo* phosphorylation peaks at both meiotic and mitotic M-phases (Gard and Kirschner, 1987) and it is known that Dis1 is phosphorylated *in vivo* at potential Cdc2 sites (Nabeshima *et al.*, 1995). Similarly, TOG is phosphorylated by Cdc2 *in vitro,* and phosphorylation changes the proteins ability to regulate microtubule dynamics (Vasquez *et al.*, 1999). Whether Cdc2 regulation occurs *in vivo* is yet to be determined and mechanisms of phospho-regulation have not been characterised.

1.5.3.1 Regulation of centrosome localisation

The mechanisms of Msps localisation to the acentrosomal poles has been characterised in detail. It involves at least two other proteins, D-TACC, a centrosome localising protein, and Ncd, a minus end directed motor (Cullen and Ohkura, 2001).

D-TACC localises to the poles, physically interacts with Msps and is required for Msps localisation to the poles (Cullen and Ohkura, 2001; Lee *et al.*, 2001). Furthermore, *d-tacc* mutants have the same meiotic spindle defects as *msps* mutants. Ncd is a kinesin-like motor required for bipolar spindle formation in female meiosis (Matthies *et al.*, 1996; Hatsumi and Endow, 1992). Ncd is required to efficiently localise Msps to the poles but D-TACC can localise independently of Ncd. It was therefore proposed that Ncd could transport Msps along the microtubules to the poles where D-TACC could anchor it (Cullen and Ohkura, 2001).

D-TACC is also involved in Msps localisation to the centrosomes in embryonic syncytial mitosis (Lee *et al.*, 2001). Overexpression of D-TACC recruits additional Msps to the poles, whilst the amount of Msps protein at the centrosomes is dramatically reduced in *d-tacc* mutants. Furthermore, in *d-tacc* mutants centrosomal microtubules appear to be destabilised (Gergely *et al.*, 2000).

In addition to recruiting Msps, there is some evidence that D-TACC modulates Msps activity (Lee *et al.*, 2001). Overexpression of the TACC domain results in embryos filling with microtubules asters, with Msps localising to the centre. In *msps* mutant embryos such asters failed to form suggesting the TACC domain somehow activates the microtubule stabilising activity of Msps protein.

D-TACC has subsequently been found to be a member of a conserved family of proteins, the TACC family. In human culture cells, TACC3, one of the three D-TACC homologues, will recruit TOG when it is overexpressed (Lee *et al.*, 2001). The physical interaction between D-TACC and Msps is conserved in the C. elegans homologues TAC-1 and Zyg-9 (Bellanger and Gonczy, 2003; Srayko *et al.*, 2003).

In budding and fission yeast, clear TACC homologues have not been found.

However, recently a possible functional TACC homologue was found in fission yeast (Sato *et al.*, 2004). This protein, Alp7, binds to Alp14 and is responsible for Alp14 localisation to the SPB and spindle microtubules. In budding yeast Stu2p binds to the SPB component Spc72 (Chen *et al.*, 1998), and whilst not a homologue of the TACC proteins, Spc72 plays a key role in Stu2 function at the SPB (Usui *et al.*, 2003). Spc72 binds by one domain to Stu2 and by another to gamma-tubulin. These interactions bring Stu2 and gamma-tubulin together and they act to organise the microtubules at the centrosome. Analysis of a SPC72 mutant that fails to bind Stu2 demonstrated that SPB associated Stu2 is required for astral microtubule anchorage and the regulation of plus end dynamics (Usui *et al.*, 2003).

1.6. Aims of this study

The Dis1/TOG family members have a microtubule regulating activity that is vital for the correct organisation of microtubules during cell division and interphase. The proteins have a conserved domain structure and some functions have been assigned to specific domains. *Drosophila* Mini spindles (Msps) protein is known to play a vital role in the formation or maintenance of the bipolar spindle in both mitosis and female meiosis. The aim of this study was to uncover the domains of Msps protein responsible for localisation, functions and protein interactions, through the creation and analysis of new *msps* mutants. A mutagen that creates single point mutations was used with the aim of inactivating specific functional domains.

Whilst the function of Dis1/TOG proteins in spindle formation has been extensively examined, functions in interphase microtubule regulation have featured less prominently. In plants and yeast interphase roles have clearly been described, however the situation in other higher eukaryotes has not been established. In the current study, the role of Msps in interphase was examined using the *Drosophila* S2 cell culture system.

The current controversy over whether the Dis1/TOG proteins act as microtubule destabilising or stabilising proteins needs to be resolved. The effects *in vivo* of the Dis1/TOG proteins on microtubule dynamics has been studied in yeast but not in higher eukaryotes. In the current study, detailed analysis of the regulation of microtubule dynamics was carried out to uncover the *in vivo* effects of a member of the Dis1/TOG family in microtubule regulation.

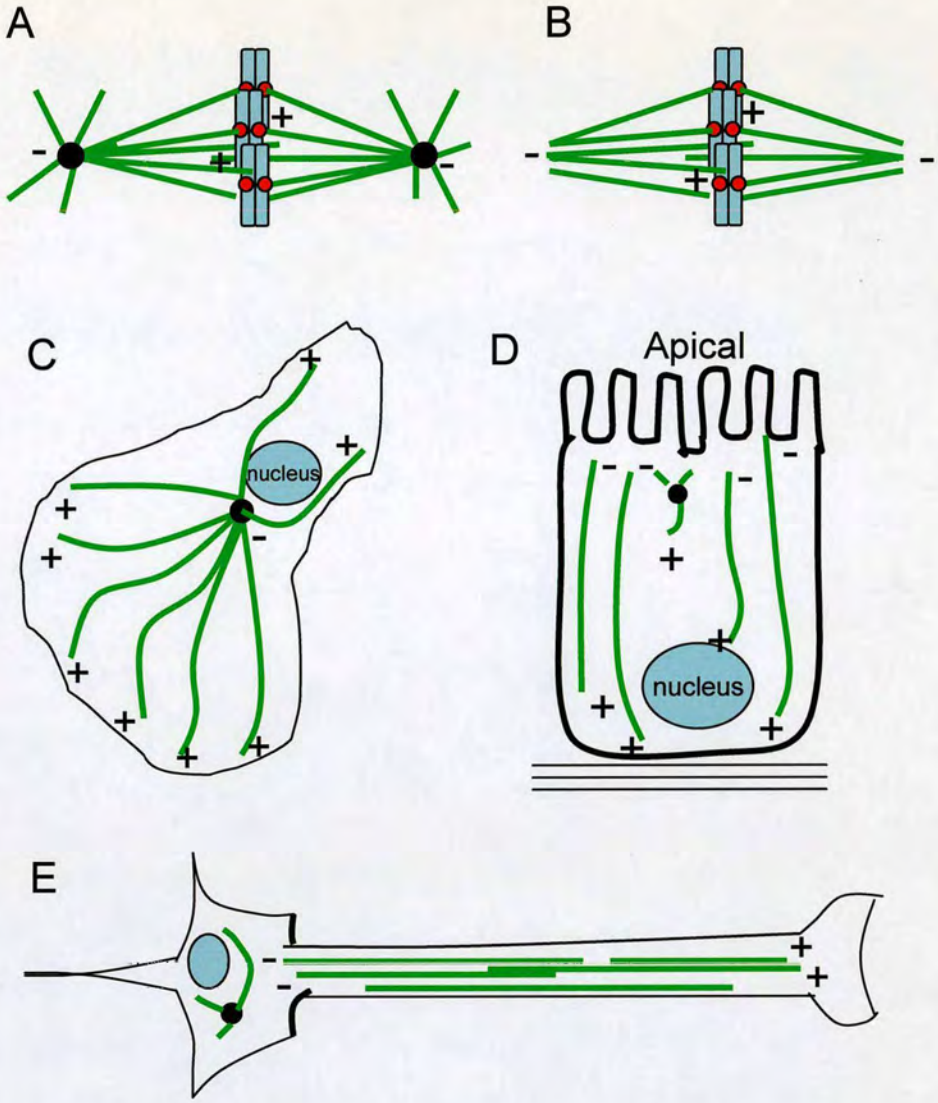

Figure 1.1 Microtubule organisation changes during the cell cycle and through development.

(A) A centrosomal bipolar spindle. Microtubules (green) emanating from the centrosomes (black) attach to the chromosomes (blue) via the kinetochores (red). (B) An acentrosomal bipolar spindle. Female meiotic and mitotic cells in plants lack conventional centrosomes but can still form a bipolar spindle. (C) Radial distribution of microtubules in an interphase cell. The plus ends extend to the cell cortex, while the minus ends remain attached to the centrosome. (D) Epithelial cell in which microtubules orientate with the plus ends towards the basal side and minus ends towards the apical surface. (E) A neuronal cell with axon containing microtubule bundles.
Locations of microtubule plus and minus ends are indicated.

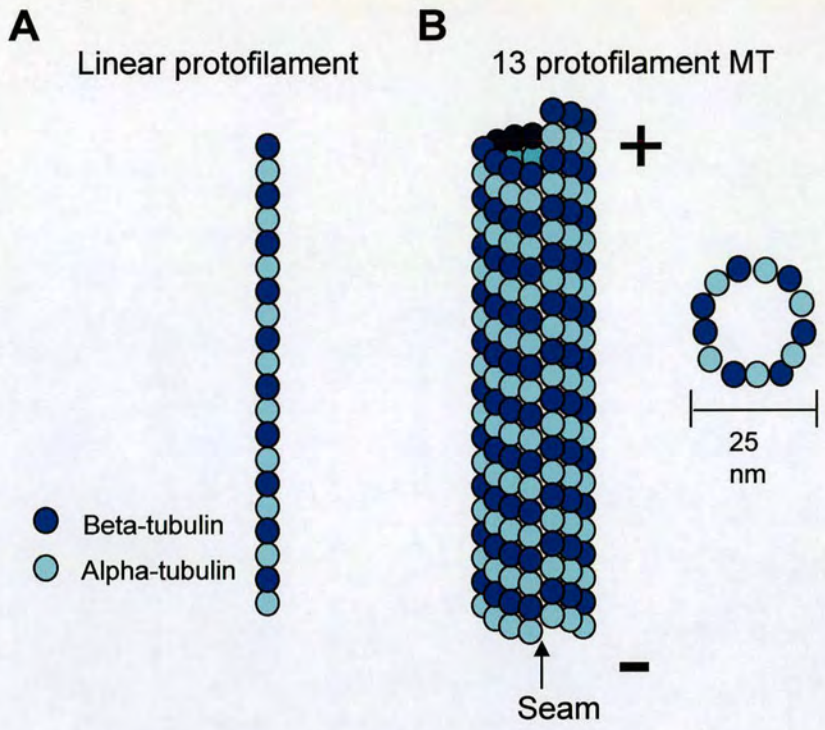

Figure 1.2 Microtubule structure
(A) Head to tail interactions of alpha-beta tubulin dimers form linear protofilaments. (B) 13 linear protofilaments associate laterally to form a 25nm diameter hollow cylindrical polymer (microtubule). Lateral interactions between protofilaments are alpha to alpha and beta to beta except at the seam. Plus and minus signs indicate microtubule polarity.

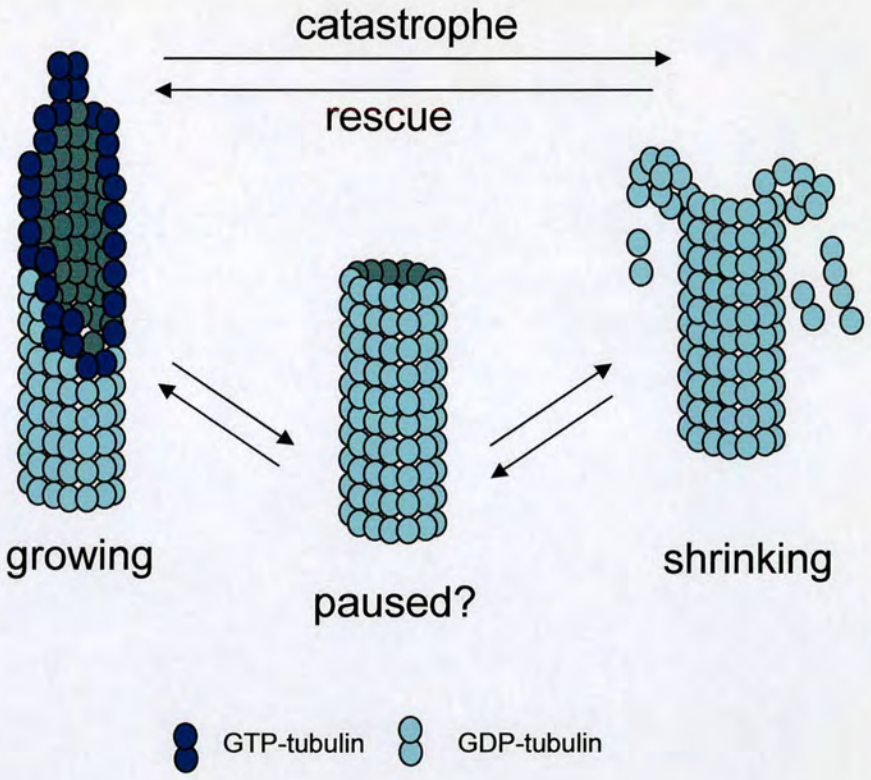

Figure 1.3 Microtubule dynamic instability and end structure

GTP-tubulin is incorporated into polymerising microtubule ends. The bound GTP is hydrolysed during or soon after polymerisation. Therefore, the microtubule lattice is composed primarily of GDP-tubulin. Polymerising microtubules infrequently transit to depolymerisation (catastrophe), either via an intermediate paused state or directly. Similarly, microtubules may switch back to growth (rescue) via the paused intermediate or directly. Growing microtubules are believed to consist of an extended sheet of tubulin, whilst the shrinking microtubule has a curled end structure. The blunt end structure may represent the proposed paused state.

Figure 1.4 Protein structure of the Dis1/TOG family of MAPs
TOG domains (dark blues boxes), HEAT-repeats (pale blue boxes) (Neuwald and Hirano, 2000), conserved C-terminal region (yellow boxes) and coiled-coil regions (purple boxes) are shown in members of the Dis1/TOG family from various organisms.

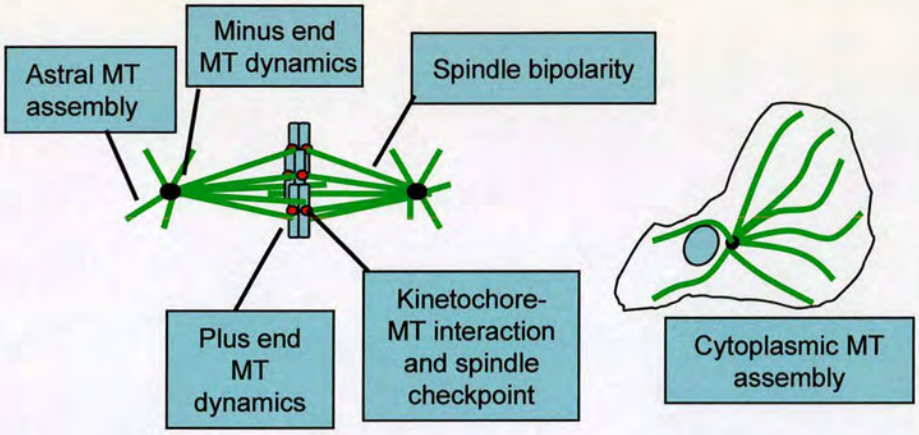

Organism/name	Functions	Interactors
human **TOG**	Promotes MT assembly at both ends. Spindle bipolarity	MT, tubulin dimer, TACC3, Cyclin B
Frog **XMAP215**	Promotes MT assembly at plus ends, counteracts XKCM1 activity, spindle and aster assembly, destabilizes GMPCPP-MTs .	MT, XKCM1*, Cyclin B
Fruit fly **Mini spindles (Msps)**	Spindle bipolarity, cytoplasmic microtubule organization in the oocyte	MT, D-TACC, Ncd*
Nematode **ZYG-9**	Spindle formation, pronuclear migration, rotation of spindle	TAC-1
Fission yeast **Dis1** **Alp14**	Kinetochore-MT interaction Spindle MT assembly, spindle checkpoint, cytoplasmic MT assembly/cell morphogenesis	MT, Klp5/6*
Budding yeast **Stu2**	Kinetochore-MT interaction, spindle elongation, plus end MT dynamics	MT, Spc72, Kip3*
Slime mould **DdCP224**	Centrosome duplication, stabilizing microtubules, cortical interactions of microtubules	
Plant **Mor1**	Cortical MT assembly/cell morphogenesis	

Figure 1.5 The functions of the Dis1/TOG family in microtubule regulation

(A) Protein functions and sites of activity in mitotic and interphase cells. (B) The table summarises the functions and protein interactions described for the Dis1/TOG proteins in various organisms. * indicates that no physical interaction was shown.

Chapter 2 Materials and methods

2.1 Commonly used buffers and reagents

Many of the methods used in this study are based on those described in Molecular Cloning: A Laboratory Manual (Sambrook J et al., 1989).

All chemical used in this study were of analytical grade and were purchased from Sigma, BDH and Fisher Scientific.

TE

10mM TrisHCl, pH7.5
1mM EDTA.

Used as a DNA solvent

Ethidium bromide

10mg/ml stock solution in dH_2O (Sigma)

6X Nucleic acid loading buffer

60% glucose
0.5M EDTA
dH_2O
0.25% Bromophenol Blue

2X SDS protein loading buffer

500mM Tris-Cl pH6.8
10% SDS
20% glycerol
0.2% bromophenol blue
H_2O
10% (v/v) 14.3M β-Mercaptoethanol added at time of use

TAE

50X stock solution. 1X buffer used as electrolyte for agarose gels.
1 litre: 242g Tris base
57.1ml glacial acetic acid
100ml 0.5M EDTA (pH8.0)

2.2 DNA Manipulations

2.2.1 Dissolving and storage

All DNA was dissolved in TE or dH_2O depending on subsequent uses. DNA solutions were stored at -20°C.

2.2.2 Ethanol precipitation

DNA was precipitated by addition of 0.1 volume of 3M NAOAc pH5.2 and 2 volumes of absolute ethanol. The solution was mixed by pipetting up and down several times then placed at -20°C for 20 minutes, before centrifugation at 13000 rpm for 15 minutes to pellet the DNA. The pellet was washed with -20°C 70% ethanol and then repelleted by centrifugation. The supernatant was removed and the pellet air dried. The DNA was resuspended in TE or dH_2O.

2.2.3 Molecular Analysis of DNA

Type II restriction enzymes (Promega, NEB) were used to cut DNA at specific sites. Routinely, 0.5-1μg of DNA was digested with 5-10 units of enzymes in a

suitable buffer, in a total volume of 30μl at 37°C for 1-2 hrs. Reaction volumes were scaled up as required.

2.2.4 DNA modifying enzymes

DNA ligase

T4 DNA ligase (NEB) was used for the ligation of DNA fragments.

Alkaline phosphatase

Alkaline phosphatase catalyses the removal of 5' phosphate residues from DNA. Calf intestinal phosphatase (NEB) was used to remove 5' phosphate from linearised vectors to prevent self ligation during subsequent ligation reactions.

2.2.5 Agarose gel electroporesis

0.7% agarose gels were used for analysis of DNA fragments. Agarose (Cambrex) was dissolved in 1X TAE buffer by boiling. After cooling, ethidium bromide was added to a concentration of 2.5ug/ml to enable DNA to be visualised. DNA samples were mixed with loading buffer before loading into wells next to molecular weight markers (1kb ladder, Promega or NEB). DNA was visualised on a transilluminator and images recorded with a digital camera.

2.2.6 Gel purification

Restriction digest reactions were separated on an agarose gel as described and the appropriate fragment cut out of the gel using a scalpel. The DNA fragment was

then purified using the QIAGEN QIAquick Gel Extraction kit, following the manufacturer's instructions.

2.2.7 DNA sequencing

Sequencing was carried out using an automated sequencer after carrying out the reactions using ABI PRISM BigDye Terminator Cycle Sequencing Ready reaction kits following the manufacturer's instructions. For all sequencing reactions a Hybaid PCR thermal cycler was used with the following programme:

96°C for 30 secs

50°C for 15 secs

60°C for 4 minutes X 25 cycles

2.2.8 Site directed mutagenesis

Specific point mutations were made using QuikChange Site Directed Mutagenesis Kit (Stratagene) according to the manufacturer's instructions. In brief, the procedure involved the use of a dsDNA vector with the insert of interest and two oligonucleiotide primers containing the desired mutation. PfuTurbo DNA polymerase extends the two primers, each complementary to opposite strands of the vector generating a nicked plasmid with the desired mutation. The DpnI endonuclease, specific for methylated and hemimethylated DNA, is added to digest the parental DNA template. The mutated plasmid is then transformed into XL-1 Blue supercompetent cells.

Primers used to create a single amino acid mutation of glutamic acid to lysine (E190K) in the Msps protein

AB1 GCAGCTGGCTGTTAAGATTTACCGTTGG

AB2 CCAACGGTAAATCTTAACAGCCAGCTGC

Oligos were obtained from Sigma Genosys

Mismatches are underlined.

2.3 Analysis of Proteins

2.3.1 SDS polyacrylamide gel electrophoresis (SDS-PAGE)

Discontinuous SDS polyacrylamide gels were used for the separation of proteins under denaturing conditions. Discontinuous polyacrylamide gels consist of a lower resolving gel and an upper stacking gel. The 8% resolving gels and stacking gels were made following the directions described in Sambrook (1989). The Bio Mini-PROTEAN II system was used for all SDS-PAGE gels described in this work.

The BioRad Mini-PROTEAN II system was assembled following the manufacturer's instructions. The resolving gel was poured between the glass plates and overlaid with isopropanol. After the resolving gel was polymerised, the isopropanol was washed way, the stacking gel poured and a comb inserted into polymerising gel to form the wells for loading.

Once the stacking gel had polymerised, the comb was removed and the well rinsed with water to remove any unpolymerised acrylamide. Protein samples were denatured by heating at 100°C for 5 minutes in 1x SDS sample buffer (section 2.1). The gel was run in Running Buffer (see below) for 1-2hrs at 100 volts.

Running Buffer: 25mM Tris
250mM Glycine
0.1% SDS

2.3.2 Western blotting

The Mini-Trans Blot cell from BioRad was used for the electrophoretic transfer of proteins from SDS-PAGE gels to nitrocellulose membranes (Schleicher & Schuell). The apparatus was assembled according to the manufacturer's instructions and transfer carried out in Transfer Buffer for 1 hour at 100 Volts.

Transfer Buffer: 25mM Tris
250mM glycine

Staining of membranes for total protein

After electrophoretic transfer, membranes were stained with Ponceau S solution (1g Ponceau S (Sigma), 1 ml acetic acid, H_2O to 100ml) to monitor blotting efficiency.

Blocking, washing and antibody incubations.

Blots were blocked by incubation in Blocking solution (Blocking solution:1x PBS (50mM sodium phosphate, pH 7.4; 150mM NaCl) containing 0.05% Tween 20 and 3% (w/v) non-fat milk powder) for 1hr to overnight at room temperature with gentle agitation.

The blocking solution was removed and the primary antibody added at the appropriate dilution (table 2.1) in blocking solution. Incubation with the primary antibody was from one hour to overnight at room temperature with gentle agitation. After removal of the primary antibody the blot was washed three times, for 10 minutes each, in PBS-Tween (1x PBS containing 0.05% Tween 20). Horseradish peroxidase conjugated secondary antibody, diluted in blocking solution, was added at the concentrations described in table 2.1. Incubations with the secondary antibodies were for at least 1 hr at room temperature, followed by washing in PBS-Tween as before.

Detection of immune complexes

The presence of horseradish peroxidase conjugated secondary antibodies was detected using an enhanced chemiluminescent reagent (ECL™, Amersham), following the manufacturer's instructions. Signal was detected by exposure of the blot to Hyperfilm™ECL™ chemiluminescent film (Amersham) for times ranging from a few seconds up to 1 minute, depending on the strength of the signal. Antibodies used and concentrations are given in Table 2.1.

Stripping and reprobing of blots

Whenever necessary, antibodies were stripped from the blots by a 20 minute incubation in antibody removal solution (0.5M acetic acid; 0.5M sodium chloride), washed three times in PBS-Tween, and processed for incubation with a second primary antibody as before.

2.4.3 Antibody purification

Antibodies were purified based on a protocol described in (Smith and Fisher, 1984). Approximately 20μg of protein, corresponding to the antigen used to make the antibody, was run on an SDS-PAGE gel. The protein was then transferred on to nitrocellulose membrane by western blotting. The strip of membrane containing the protein was cut out into smaller strips that would fit in a 1.5 ml eppendorf. The strips were washed in PBS and incubated in blocking solution (PBS containing 0.05% Tween 20 and 3% dried skimmed milk (Marvel)) for 30 minutes. Crude antibody was then diluted 1/10 in blocking solution and incubated with the nitrocellulose strips overnight at 4°C. The antibody was now be bound to the antigen on the nitrocellulose paper. The antibody solution was removed from the nitrocellulose strips and the strips washed 4 times, for 15 minutes, with PBS containing 0.05% Tween. The antibody was eluted from the membrane by washing three times, for 30 seconds, in 400μl of elution buffer

(see below). The elution buffer neutralised immediately by addition of Na_2HPO_4 to a final concentration of 50mM. The eluted antibody was stored at 4℃.

Elution buffer

50mM glycine-HCl pH2.3
500mM NaCl
0.5% (v/v)Tween 20
100μg/ml of BSA
0.1% azide

2.4 *Escherichia coli* Manipulations

2.4.1 E.coli strain used in this study

XL1-Blue (Stratagene) *recA1 end1 gyrA96 thi-1 hsdR1 supE44 relA1 lac[F'proAB laci^{q}Z M15 Tn10(Tet^r)]*

2.4.2 Media and growth conditions

Media was prepared by the Swann Building, University of Edinburgh media service.

Luria-Bertani medium (LB)

E.coli was grown in rich LB liquid or solid media

Bacto-tryptone	10g/l
NaCl	10g/l
Yeast extract	5g/l
Glucose	1g/l

For solid medium, 15g/l Bactoagar was added before autoclaving.

2.4.3 Selective antibiotics

Ampicillin: powdered ampicillin was dissolved in dH_2O at 100mg/ml to make a stock solution. This was added to the media to a final concentration of 100μg/ml.

Chloramphenicol: chloramphenicol was dissolved in absolute ethanol at 34mg/ml to make a stock solution. This was added to the media at a final concentration of 34μg/ml.

All antibiotic stock solutions were stored at – 20°C.

2.4.4 Transformation of E.coli

Preparation of competent cells was as follows: 2 ml of XL1-Blue was grown in LB at 37°C overnight. This was added to 200ml of pre-warmed LB in a 1litre conical flask, and incubated at 37°C, with shaking, for a further 3 hours. Cells were collected by centrifugation at 4°C for 10minutes at 3000rpm (with a JLA 10,500 rotor, Beckman), resuspended in 15mls ice cold TS buffer and left on ice for 1hour.

TS buffer:	LB	20ml
	DMSO	1ml
	1M $MgCl_2$	0.2ml
	1M $MgSO_4$	0.2ml
	PEG_{4000}	2g

200μl aliquots of cells were pipetted into 1.5ml tubes on dry ice and stored a -80°C.

Transformation of cells was carried out after thawing the competent cells on ice. 100μl of cells were used per transformation with 500-1000ng DNA. After addition

of DNA to the cells, the mixture was incubated on ice for 10 minutes, and then heat shocked at 37°C for 2 minutes. Cells were again incubated on ice for 2 minutes before addition of 900µl of LB. The mixture was incubated at 37°C for 60 minutes before plating the cells on to selective plates. Plates were incubated overnight to allow colony formation.

2.4.5 Isolation of plasmid DNA from *E.coli*.

Plasmid DNA was isolated from *E.coli* using the Wizard Plus Minipreps DNA Purification System (Promega) as manufacturer's instructions.

2.5 Fly methods

2.5.1 Fly maintenance

All stocks were grown at 25°C in cornmeal media provided by the media service. Standard techniques of fly manipulation (Ashburner, 1989) were used. w^{1118} was used as a wild-type stock. Stocks used in study are given in table 2.2.

2.5.2 Genetic analysis

2.5.2.1 Fly crosses

Fly crossing was carried out with standard techniques described in Ashburner (1989). To maximise virgin collection during the screen the following pattern of collection was followed. Female virgins, recognised by their pale pigmentation and the

presence of a dark spot on the abdomen, were collected in the morning. All flies were removed from the bottles and then placed at 25℃ for 7-8 hours. As females will not mate for the first 8 hours after emergence as adults, all the female collected after 7-8 will be virgins. The bottles were emptied again and placed at 18°C overnight. At this temperature development is slower and the females that hatch will be virgins when collected in the morning.

2.5.2.2 Rescues and recombination

Stocks of *msps* mutant alleles were cleaned of other lethal or female sterile mutations on the 3rd chromosome by recombination (figure 2.1). Mutant *msps* alleles were rescued with a wild-type *msps* gene (*P267[msps$^+$w$^+$]*) (Cullen *et al.*, 1999) to ensure that the lethality was caused by the mutation in the *msps* gene and not by other mutations on the 3rd chromosome. The crossing scheme is illustrated in figure 2.2.

2.5.2.3 Determining lethal phase of mutants

Lethal phase was evaluated for all the new lethal mutants. All the mutants in this study were carried over balancer chromosomes that contained a dominant *Tubby* (*Tb*) marker. Homozygotes not carrying this marker, i.e. non-*Tb,* could be distinguished from heterozygotes carrying the *Tb* marker. Tb and non-Tb can be distinguished in the larvae from the 2nd instar onwards. If no non- Tb 2nd instars were seen, the lethal phase was classified as an early lethal, to include embryonic and 1st instar stage lethality. Otherwise, lethality was classified as occurring that the 2nd instar, 3rd instar or pupal stage.

2.5.2.4 Female sterility tests

To assess a mutant for female sterility, 5 females of the appropriate genotype were selected and crossed to 5 fertile males. The cross was left for at least 5 days and then examined for the presence of progeny.

2.5.2 EMS mutagenesis

Random chemical mutagenesis was carried out using the mutagen ethylmethane sulfonate (EMS). Approximately 400 male w^{1118} flies were collected, just after hatching, and aged in bottles for 3 to 5 days. On the day of the mutagenesis, the flies were put into 4 empty bottles (100 flies per bottle) to starve for 6 hours. Discs of filter paper were placed in the empty bottles and 1ml of EMS solution (25-35mM EMS, 2 % glucose, dH_2O) added to each bottle. The starved male flies were transferred to the bottles containing the EMS and left over night in the fume hood. In the morning, the flies were transferred to fresh food and left for another 24hrs to recover. 30 male flies were then crossed to virgin females carrying a TM6C balancer. The flies were allowed to lay for 3-4 days and then the adults were discarded. The crossing strategy is described in result section 3.2 and figure 3.1.

All tips, bottles etc that had been in contact with EMS were left in denaturing solution overnight.

Denaturing solution: 4g NaOH
500μl mercaptoacetic acid
dH_2O to 100ml

2.5.4 Sequencing from genomic fly/larvae DNA

To sequence genomic DNA several steps were carried out. The first step was to obtain genomic DNA, the second to amplify the region by PCR, and the final step, to sequence the amplified PCR fragments.

DNA extraction from fly/larvae

DNA as obtained from flies or larvae. 10 larvae or flies were placed in a 1.5 ml eppendorf and homogenised in 100μl of cold TE (25mM TrisHCl pH8, 50mM EDTA). Proteins were digested by adding, 50μl of SDS, and protease K, to a final concentration of 50μg/ml, and the mixture incubated at 65°C for 1 hour. Proteins were removed by phenol/chloroform extraction using the following method. 100μl of TE saturated phenol was added to the homogenised flies, mixed and left for 5 minutes. The tube was then centrifuged for 5 minutes and the supernatant transferred to a new 1.5ml tube containing 125μl of chloroform and mixed well. The tube was then centrifuged at 13,000rpm for 1 minute and the supernatant transferred to a new tube. Nucleic acids were precipitated from the solution as described in section 2.2.2. RNA was then digested by resuspending the nucleic acids in 50μl of water containing 100μg/ml RNase.

PCR from genomic DNA

1.5-3 kB fragments of genomic DNA were amplified by PCR. 18 base pair primers were designed to amplify overlapping fragments of the whole of the coding region (*msps* primers in Table 2.3 and *d-tacc* primers in Table 2.4). The standard PCR reaction mix described below was used.

PCR reaction

1μl genomic DNA
3μl PCR reaction mix (Roche)

0.3 mM dNTPs (Promega)
1nM primer left
1nM primer right
Upto 30ul with dH_20

PCR programme

94°C 1 minute 1 cycle

94°C 30 seconds
50°C 1 minute 30 cycles
72°C 3 minutes

72°C 5 minutes 1 cycle

Sequencing from PCR products

6µl of the PCR product was placed in a fresh tube and 2µl of Exonuclease I (Amersham, 10U/µl) and SAP (Shrimp Alkaline Phosphatase (USB, 1U/µl) added and mixed. The mixture was incubated at 37°C for 15 minutes, 80°C for 15 minutes and then placed on ice. 4µl of sequencing primer (0.8pmol/µl stock) and 8µl of sequencing mix were added, and sequencing reactions carried out in the PCR machine.

Sequence analysis

Sequences were analysed using Editview and Gene Jockey programmes. Genes from the parent stock used in the screen and mutant flies were sequenced, so that polymorphisms could be detected. In some cases heterozygotes were sequenced. Differences between the mutant and wild-type gene could be detected by the presence of double peaks in the sequencing. If a change in sequence was found, the original PCR reaction was repeated and sequenced. This was to ensure that mutations were genuine, and did not occur due to a mistake by the Taq polymerise when the PCR product was synthesised.

2.5.5. Preparing fly protein samples for SDS-PAGE

300μl of SDS protein sample buffer was added to 3 larvae/ flies. The samples were then heated for 3 minutes to inactivate proteases. The larvae/flies were then homogenised in the buffer, using a plastic homogeniser, and boiled again for 3 minutes. Protein gels were loaded with 10μl of protein sample, which corresponds to a 10^{th} of one larva/fly.

2.5.6 Cytological analysis

2.5.6.1 Immunostaining larval brains

Neuroblasts have a large number of mitotic cells, so are frequently used to examine the mitotic phenotype of mutants which die as larvae. Brains were dissected from 3^{rd} instar larvae in 0.7% NaCl plus 5mM EGTA. The brains were then transferred to a watchglass containing fix (12% formaldehyde, 0.7 % NaCl, 5mM EGTA) for 15-30 minutes. A solution of 0.7% NaCl was used to wash the brains several times for 1 hour.

Before immunostaining, the brains were blocked in PBS containing 10% Foetal bovine serum (FBS) and 0.3% Triton-X-100. The same solution was used to dilute antibodies to the appropriate concentration (see Table 2.5). Brains were incubated with the primary antibody overnight. The following day, the brains were washed every 20 minutes with PBS 0.3% Triton-X-100 for 1 hour, before incubation with the secondary antibody for at least 4 hours. Following the incubation, brains were again washed with PBS 0.3% Triton-X-100. Finally, to visualise the DNA, brains were incubated with 0.5μg/μl DAPI in PBS for 10 minutes. This was followed by 3 washes in PBS for 10 minutes each.

Brains were mounted in mounting media (2.5% propyl gallate, 85% glycerol) and the coverslips sealed using nail varnish.

2.5.6.2 Brain squashes

Larval brain squashes were carried out to observed mitotic cells in the neuroblast and calculate mitotic index, as described by (Gonzalez and Glover D.M., 1993). Briefly, brains were dissected from 3rd instar larvae, placed in NaCl, before being transferred to 45% acetic acid for 30 seconds, followed by transfer to 45% orcein. The brains were left in the orcein for 3 minutes out of the light. Taking one brain at a time, the brains were transferred to 60% acetic acid for 10 seconds and then immediately transferred to a blob of 60% orcein on a coverslip. The brain was then squashed between the coverslip and a glass slide. The brains were then observed by light microscopy.

Mitotic index was calculated as the number of mitotic cells per microscope field using a 100X objective.

2.5.6.3 Dissection and immunostaining of oocytes

To examine the structure of female meiotic spindles, oocytes were dissected, fixed and immunostained.

Females, 4-5 days old, were collected from bottles kept at 25℃ and transferred to fresh bottles containing extra yeast and a few males. This bottle was then left at 18% for 3-4 days to ages the females. As flies are not overcrowded and well fed, females become fat and have large numbers of oocytes.

20-25 fat female were selected and the head removed to kill them. 3 females at a time were placed in a watchglass, containing methanol, and the ovaries removed. The ovaries were transferred to 3mls of fresh methanol. The remaining females were then dissected, using fresh methanol each time. To remove the chorion, ovaries were

sonicated for 1 second bursts, at 38% amplitude. The ovaries were transferred to the watchglass again, and the dechorinated ooctyes picked out with forceps into fresh methanol. This process was repeated to collect as many oocytes as possible.

The oocytes were then taken through a methanol series (80%, 60%, 40%, 20% methanol in PBS) until the oocytes were in PBS. A blocking solution of 10% FBS in PBS containing 0.1% Triton-X-100 (PBST) was added to the oocytes for 30 minutes. First antibody was diluted in blocking solution blocking and left for 4 hours to overnight.

The first antibody was removed by washing three times in PBST, each wash lasting 10 minutes. The oocytes were then incubated in secondary antibody for 2 hours or longer, and then washed three times in PBST. To visualise DNA, either 0.5μg/μl of DAPI or 1μg/ml of propidium iodide diluted in PBS, was added for 10 minutes, followed by 2 washes in PBST and 1 wash in PBS.

Oocytes were mounted on a coverslip, and the coverslip picked up with a slide and sealed with nail varnish.

2.5.6.4. Immunostaining of syncytial embryos

Embryos there collected on grape plates attached to cages containing the appropriate flies. The embryos were washed off the plates into a mesh sieve using dH_2O. The embryos were dechorionated by incubation with 100% bleach for 3 minutes and then washed with dH_2O. Embryos were transferred with a brush to a small glass pot containing 3ml heptane (Sigma) and 3 ml methanol (Sigma) containing 90ul of 0.5M EGTA (pH7.5). The pot was shaken vigorously for 1 minute and then left to stand. Embryos that sank to the bottom were devitellinalised. All the heptane, and as much methanol as possible, were removed leaving the embryos at the bottom of the pot. Fresh methanol containing 3% 0.5M EGTA was added and the embryos left for 4 hours to overnight.

Embryos were rehydrated by passage through a methanol series (as described for the oocytes) and incubated in 10% FBS/PBS 0.3% Triton-X-100 for 30 minutes for blocking. Primary antibodies were diluted in blocking solution and incubated with the embryos for 4 hours to overnight. The antibody solution was removed and the embryo washed 3 times, for 10 minutes, in PBST. Incubation with secondary antibody diluted in PBST for 2 hours, was followed by washing 4 times in PBST for 10 minutes each. The final stage was to incubate with DAPI (0.5μg/μl) for 10 minutes followed by washing with PBS.

Embryos were picked up on a brush and excess PBS removed with a tissue. Approximately, 50 embryos per coverslip were mounted in the usual mounting media.

2.5.6.5 Cytological analysis of fly blood cells

To examine microtubules in the fly, haemolymph cells, were collected from wild type and *msps* mutant larvae. Third instar larvae were submerged in 100μl Schneider's media and the cuticle torn with forceps. The media was then pipetted onto a concanavilin A coated coverslip and the cells left to attach for 2 hours. Cells were then fixed and tubulin distribution examined by immunofluorescence as described for S2 cells (see section 2.6.2). The cells were viable under these conditions, as the cells attach to the concanavilin A surface, and spread in a similar manner to S2 culture cells.

2.5.6.6 Antibodies used for Immunostaining

Table 2.5 contains all the primary and secondary antibodies used for immunostaining in this study.

2.5.7 Co-immunoprecipitations from larval extract

To investigate interactions between D-TACC and Msps mutant proteins, co-immumoprecipitation experiments were carried out. The first task was to obtain a soluble protein extract. In my experiments, larvae were used as a source of protein extract.

1ml of IP buffer, at 4°C, was added to 20 third instar larvae. The larvae were homogenised on ice in this buffer and then centrifuged (13,000rpm at 4°C for 10 minutes). The supernatant was collected and the procedure repeated several times until the supernatant was clear. The volume of the protein extract was then made up to 1ml using IP buffer. A 40μl sample was removed and added to 80μl of 2X protein sample buffer. The protein extract was split into two eppendorf tubes. To one tube, 1μl of crude antibody was added, and to the other tube, 1μl of pre-immune serum. Both tubes were then incubated at 4°C with rotation for 1 hour.

Protein A beads were prepared by the following method. 50μl of bead slurry was added to 200μl of IP buffer in an eppendorf. The beads were spun down in a centrifuge and the supernatant removed. The beads were washed twice more by this method. 50μl of IP buffer was left on top of the beads after the final wash.

To each tube of protein extract, 20μl of bead slurry was added, and the tubes incubated at 4°C with rotation for 1 hour. The beads were then collected by centrifuging for 30 seconds at 13,000rpm. The supernatant was removed and the beads washed 4 times in 500μl IP buffer. Sample buffer was added to the beads and the beads boiled to remove the protein.

Samples were run on an SDS PAGE gel, western blotted and probed with the appropriate antibody.

2.5.8 Microtubule binding assay

This is an *in vitro* assay to assess the ability of a protein to bind microtubules. Protein extracts from both embryos and larvae have been used in this study and were processed in the same way. Embryos were collect overnight on a grape plate, washed, dechorionated with bleach, washed extensively with water and then once with BRB80 (see below). In the case of larvae, 20-25 were collected, and then rinsed with water and BRB80.

The embryos or larvae were homogenised in 500μl BRB80 plus protease inhibitors, and incubated on ice for 15 minutes to depolymerise microtubules. The extracts was spun several times (13000 rpm, 10 minutes, 4°C) to clear the extract. 50μl of soluble extracts was taken and added to 50μl sample buffer, boiled and stored at -20°C for later analysis. The protein extract was then divided equally and made up to 500μl using BRB80 (+ protease inhibitors). GTP (to a final concentration of 1mM) and taxol (to a final concentration of 10μM) were added to one extract. The taxol was diluted in BRB80 and added stepwise. The samples were then incubated at room temp for 30 minute on a rotating wheel, to allow microtubules to polymerise.

The microtubules were pelleted by centrifugation (13000 rpm, room temperature, 10 minutes) and a sample of the supernatant collected. The pellet was washed 5 times in 500μl BRB80 + protease inhibitors + GTP and taxol (concentrations as above). Finally the pellet was resuspended in 100μl of sample buffer. Samples were analysed by SDS-PAGE and western blotting.

BRB80 solution

80mM Pipes pH 6.9

1mM MgCl2

1mM EGTA

2.6 Tissue culture methods

2.6.1 Maintaining S2 cell cultures

Drosophila S2 cells were grown in Schneider's media (Gibco) supplemented with 10% FBS (Gibco) at 27℃. Every 5-6 days cells were diluted 1/10 in fresh media.

2.6.2 Immunofluorescence in S2 cells

To investigate the distribution of proteins within the cell immunofluorescence techniques were used.

Preparation of concanavilinA coated coverslips

To improve cytology, cells were grown on coverslips coated in concanavilin A (con A). Coverslips were prepared by the following method.

Coverslips were placed in a holder and submerged in a beaker. The coverslips were washed several times in dH_2O, before the H_2O was replaced with 0.5M HCl and left for 30 minutes. The acid was then removed and the coverslips washed several times in dH_2O. The coverslips were then dehydrated by leaving them in 100% ethanol for 30 minutes.

A con A (Sigma) solution (0.5mg/ml) was made by dissolving the powdered con A in dH_2O. After removal from the ethanol coverslips were picked up individually with forceps, the excess ethanol drained off and then dipped into the con A solution. The coverslips were left to dry on clean blotting paper. Prior to use, the coverslips were placed under a UV light for 1 hour to sterilise them.

Growing S2 cells on con A coverslips

Con A coverslips were placed into the wells of 6-well tissue culture plates. Cells were seeded at a concentration between 1-5 x 10^5 cells/ml, as this allowed cells to spread out well. Cells were grown on the coverslips for a minimum of 2 hours.

Immunofluorescence

Fixative

90% methanol
3 % formaldehyde
5mM sodium carbonate

Cooled to -80℃

Cells were routinely fixed in the methanol/formaldehyde fixative described above as this fixed microtubules very well (Rogers *et al.*, 2002). The only exception was for actin staining, in which case, a fix of 4% formaldehyde in PBS was used.

Cell culture media was removed from the coverslip and immediately 2 mls of cold fix added. The coverslips were then placed in dry ice for 10 minutes, before being allowed to heat up to room temperature. The fix was then removed and the cells washed in PBST (PBS with 0.1% Triton-X-100) three times for 3 minutes. A blocking solution (10% FBS in PBST) was then added to the cells for at least 30 minutes. Primary antibodies were diluted in blocking solution and incubated on the coverslips for at least 1 hour. The primary antibody was washed away by rinsing 3 times, for 5 minutes, with PBST. Secondary antibody was diluted in PBST and incubated on the coverslip for at least 1 hour at room temperature. Again, the cells were washed with PBST three times for 3 minutes. Cells were stained with DAPI (0.5μg/μl) for 10 minutes to visualise DNA, washed in PBST and finally in PBS.

The cells were rinsed in dH_2O, the excess liquid drained off and 10μl of mounting media dropped on the coverslip. The coverslip was the picked up with a slide and sealed with nail varnish.

2.6.3 RNA interference in S2 cells

RNA interference (RNAi) was used to deplete Msps and D-TACC proteins from *Drosophila* S2 culture cells. The protocols used were based on those described by Clemens *et al* (2000).

Selection of target region in gene

A 500-600 bp region of coding sequence in the target gene was chosen as the target for RNAi. In general the region chosen corresponded to the region covering the start codon. Exceptions were made if the exons at the start of the gene were too short to contain 500-600 bp. In this case the largest exon was chosen as the target. Occasionally the C-terminal region was deliberately targeted. The chosen region was subjected to a BLAST search, to determine if the region was similar to any other proteins. Regions were chosen that failed to pull out other proteins in the BLAST search.

Amplification of target region

Primers complementary to 18 base pairs, at each end of the target region, were designed. The primers also had an additional tag of the first 18 base pairs of the T7 RNA polymerase promoter (figure 2.3.A). All primers are recorded in table 2.6. The region was amplified from either cDNA or genomic DNA using the same PCR reaction and PCR program previously described (figure 2.3.B). Success of the PCR was checked by running 2 μl of the PCR reaction on a 0.7% agarose gel. The

remaining PCR product was purified using a Qiagen PCR Purification Kit, as directed by the manufacturer's instructions.

To add on the full T7 RNA polymerase promoter, necessary for RNA transcription, a second round of PCR using the first PCR product as a template was necessary (figure 2.3.C). The second set of primers contains the full T7 RNA polymerase promoter. At each end of the PCR product there is 18 bps corresponding to this primer. The T7 primer (oNSD33) will bind to this sequence and amplify the region, adding on the full T7 RNA polymerase sequence (figure 2.3.D). 4 reactions were carried out, the PCR products pooled and purified using the UltraClean PCR Clean-Up Kit (Mo Bio). The DNA concentration was measured using a spectrophotometer, set to measure absorbance at 260nm. A DNA concentration of 125μg/μl or greater was required.

Production of dsRNA

Ambion MEGAscript T7 kit was used to transcribe RNA from the PCR DNA template, as described by the supplied protocol. The following reagents were added to an RNAse free tube:

Xμl of nuclease free water to a final volume of 20μl
2μl 10x reaction buffer
2μl each of ATP, CTP, GTP and UTP.
1μg DNA template
2μl enzyme mix

The reagents were mixed, spun down and incubate at 37°C for 4-6 hours. RNA was precipitated using ethanol and resuspended in 40μl RNAse free dH_2O.

To anneal the two single strands of RNA, the tube was heated to 65°C for 30 minutes and then allowed to cool very slowly. dsRNA was then quantified by measuring the absorbance at OD_{260} and dsRNA concentration calculated.

dsRNA was stored at -20°C until required.

dsRNA treatment

To ensure that dsRNA addition was not the cause of any defects, control dsRNA (corresponding to the β-lactamase gene) was added to some cells, whilst dsRNA corresponding to the target gene was added to another set of cells. The same amount of dsRNA (15μg) was added in each case.

The protocol used for dsRNAi follows that described by Clemens *et al.* (2000). Briefly, *Drosophila* S2 cells were diluted to $1x10^6$ cells/ ml in serum free Schneiders medium. Place 1ml of cells were placed into each well of a 6-well 35mm plate, 15μg of dsRNA added and swirled to mix. The cells were then incubated at 27°C for 30 minutes to 1 hour. 2 mls of Schneider's media, supplemented with 10% FBS, was added and cells incubated at 27°C.

To determine the level and timing of protein depletion samples were taken every day for 5 to 6 days to perform a western blot. To ensure even loading of protein, cells were counted, and the same number of cells spun down and resuspended in protein sample buffer.

Alternatively samples were processed for immunofluorescence as described above.

2.6.4 Transfection of S2 cells

S2 cells that had been depleted of Msps by RNAi were transfected with plasmids expressing either MspsN or MspsN-E190L truncated proteins. Construction of these plasmids is described in results section 5.9.1. As dsRNA corresponding to the C-terminus of *msps* was used, RNA transcribed from the plasmids expressing *mspsN* and *mspsN-E190K* will not be destroyed.

Cells were treated with either control or *msps* C-terminal dsRNA, as described previously, and left for 2 days. The cells were then counted and diluted to between

0.5-1 x 10^6 cells per ml. Cells were transfected using Effectene Transfection Reagent (Qiagen) as described in the manufacturer's handbook. After transfection, 15μg of dsRNA was added to the cells to ensure depletion of the full length protein.

2.6.5 Drug treatment

S2 cells were treated with colchicine to depolymerise microtubules. Colchicine (Sigma) was added directly to the S2 cell media, at a high concentration (200μM), and left over night. This treatment depolymerised the majority of microtubules in control cells.

2.6.6 Microtubule dynamics in live S2 cells.

Microtubule dynamics were observed in live S2 cells expressing GFP-tubulin (a gift from Ron Vale; Goshima and Vale, 2003). The cells were treated with 15μg of control (bacterial *beta-lactamase*) or *msps* dsRNA, as described previously, but for only 2 days. The cells were then grown on con A coated (24x50mm) coverslips for 1-2 hours before observation. A square was drawn in the centre of the coverslip using a hydrophobic pen to prevent media from running off the coverslip.

Microtubule dynamics were observed on an inverted Axioplan2 (Zeiss) microscope with LSM 510 Meta confocal scan head. Images were acquired for a period of 5 minutes, at a capture rate of one frame every 5 seconds. Single confocal slices were obtained and a sum of 2 scans used to reduce bleaching. Image sequences were converted to movies and the microtubule ends tracked over time using ImageJ (http://rsb.info.nih.gov/ij/). Only microtubules that could be followed for at least 3 minutes were measured. An arbitrary point behind the tip of the microtubule was chosen as a point from which to measure changes in microtubule length. Microtubule

measurements were imported into Excel (Microsoft) and the microtubule life histories plotted.

Growth and shrinkage events were defined as net changes in length of 0.5μm. Pauses were defined as events lasting 30 seconds or more in which no significant change in length (0.5μm) occurred. Catastrophes were defined as transitions to shrinkage after growth or a pause; rescues were defined as transition to growth or pause from shrinkage. Catastrophe frequency was calculated by dividing the total number of events by the total time the microtubules spent in shrinkage or pause. Rescue frequency was calculated by dividing the total number of rescues by the total time the microtubules spent shrinking.

To calculate the transition rates between the three states of growth, pause and shrinkage, the total number of transitions were divided by the total amount of time spend in the state in question i.e. when measuring the growth to pause transition, the number of changes from growth to pause were divided by the total time spent in growth.

Dynamics of microtubule plus ends located near the cortex or internally within the cell were calculated separately. Microtubule tips 0.2μm from the cell edge were count as been at the cortex, whilst all others were counted as internal.

Comparisons of statistical significance were either by student t-test or Chi-squared.

2.6.7 FRAP

S2 cells expressing GFP-tubulin, treated with either control or *msps* dsRNA for 5-6 days, were plated on con A coated coverslips as described in the previous section. An area of microtubules, 25µm x 60µm, was bleached on 60% laser power for 50 iterations. Images were recorded prebleach, immediately after bleaching (T=0) and subsequently images were captured every 20 seconds for at least 5 minutes. The

percentage recovery of the bleached area after 5 minutes was calculated for control (n=5) and *msps* RNAi (n=5) treated cells. Regions were selected and measurements of fluorescence intensity were calculated by the LSM software. Measurements of fluorescence in the bleached area, whole cell and background were made in the pre-bleach, T=0 seconds and T=5 minutes images. Fluorescence in the bleached area was given as a ratio between the average pixel intensity of the bleached region and the average pixel intensity of the whole cell. This method takes into account the photobleaching that occurs during the collection of images. Fluorescence recovery was calculated as change in fluorescence from the first post bleach image, to the image 5 minutes after bleaching, as a percentage of the pre-bleached value.

Table 2.1 Antibodies used in Western blotting

A) Primary antibodies

Antibody	Description	concentration	Source
Msps 264, affinity purified	GST-C-terminal (1349-1784 aa) Msps, rabbit	1/50	Cullen et al., 1999
Msps 268, affinity purified	GST-Mid (746-1120aa) Msps, rabbit	1/50	unpublished
Crude D-TACC-C	MBP- C-terminal (250aa) D-TACC, rabbit	1/1000	unpublished
D-TACC-N, affinity purified	MBP-N-terminal (2-433aa) D-TACC, rabbit	1/50	unpublished
DM1A	α-tubulin, mouse monoclonal	1/500	Sigma
NHK-1 (Trip)	rabbit	1/500	(Aihara et al., 2004)

B) Secondary antibodies

Antibody	Description	concentration	Source
HRP rabbit	Peroxidase conjugated, goat anti-rabbit	1/1000-1/2000	Jackson Labs
HRP mouse	Peroxidase conjugated, goat anti-mouse	1/1000-1/2000	Jackson Labs

Table 2.2 Fly stocks used in this study

Stock	Genotype	source / reference /comment
w^{1118}	w^{1118}	Lindsley and Zimm 1992
$msps^{P}$	*yw;* $msps^{P}$ / TM6C	Cullen et al., 1999
$msps^{208}$	*yw;* $msps^{208}$ / TM6C	Cullen and Ohkura., 2001
ncd^{1}	*yw;* $Df(3R)ca^{nd1}$ / TMC6	Yamamoto et al., 1989
$d\text{-}tacc^{stella}$	*w;* $dtacc^{stella}$ / TM6B	Lee et al., 2001
$d\text{-}tacc^{stella}$ $msps^{P}$	*w;* $d\text{-}tacc^{stella}$ $msps^{P}$ / TM6C	Fiona Cullen
$msps^{P}$ ncd^{1}	*w;* $msps^{P}$ ncd^{1} / TM6C	Fiona Cullen
$msps^{D}$	*w;* $msps^{D}$ / TM6C	this study
$msps^{D}$ *rec3*	*w;* $msps^{D}$ e^{s} *ca* / TM6C	this study
$msps^{51}$	*w;* $msps^{51}$ / TM6C	this study
$msps^{51}$ *rec2*	ru^{1} h^{1} th^{1} st^{1} cu^{1} $msps^{51}$ st^{1} e^{s} ca^{1} / TM6C	this study
$msps^{S10}$	$msps^{S10}$ / TM6C	this study
$msps^{S10}$ *rec13*	*w;* ru^{1} h^{1} th^{1} st^{1} $msps^{S10}$ sr^{1} e^{s} ca^{1} / TM6B	this study
$msps^{146}$	*w;* $msps^{146}$ / TM6C	this study
$msps^{146}$ *rec3*	*w;* ru^{1} h^{1} th^{1} st^{1} cu^{1} $msps^{146}$ / TM6C	this study
$msps^{A}$	$msps^{A}$ / TM6C	this study
$msps^{C}$	$msps^{C}$ / TM6C	this study
$msps^{E}$	$msps^{E}$ / TM6C	this study
$msps^{1358}$	$msps^{1358}$ / TM6C	this study
msps rescue P267 A11	*w;* $P[w^{+},msps^{+}]$	Cullen et al., 1999

d-tacc^{S3}	*w; d-tacc^{S3}* / TM6B	this study
d-tacc^{S3} rec17	*d-tacc^{S3} sr^{1} e^{s} ca^{1}* / TM6B	this study
d-tacc^{S3} rec21	*d-tacc^{S3} sr e^{s} ca^{1}* / TM6B	this study
Df (3R) 110	*Df(3R)110, ru^{1} th^{1} st^{1} kni^{ri-1} rn^{roe-1} p^{p} e^{s} ca^{1} / TM3, Sb^{1}*	Bloomington Stock Centre uncovers *d-tacc*
ruPrca	*w; ru^{1} h^{1} th^{1} st^{1} cu^{1} sr^{1} e^{s} Pr ca^{1}* /TM6B *Hu e^{s}*	Bloomington Stock Centre
rucuca	*w; ru^{1} h^{1} th^{1} st^{1} cu^{1} sr^{1} e^{s} ca^{1}*	Bloomington Stock Centre
trp^{GT28} rec96	*ru^{1} h^{1} th^{1} st^{1} cu^{1} sr^{1} e^{s} trp^{GT28} ca^{1}* / TM6B	Fiona Cullen
FRT trp rec22	*FRT 82B cu^{1} sr^{1} e^{s} trp^{GT28}* / TM6B	Fiona Cullen
d-tacc^{stella} trp^{GT28} rec5	*d-tacc^{stella} trp^{GT28}* / TM6B	Fiona Cullen
msps^{208} trp^{GT28} rec12	*msps^{208} e^{s} trp^{GT28}* / TM6B	this study
trp^{GT28} ncd^{1} rec31	*FRT82B cu^{1} sr^{1} e^{1} trp^{GT28} ncd^{1}/ TMC6*	this study

Balancers

TM6C = In(3LR)TM6C, *cu^{1} Sb e^{1} Tb ca^{1}*

TM6B = In(3LR)TM6, *Hu e^{1} Tb ca^{1}*

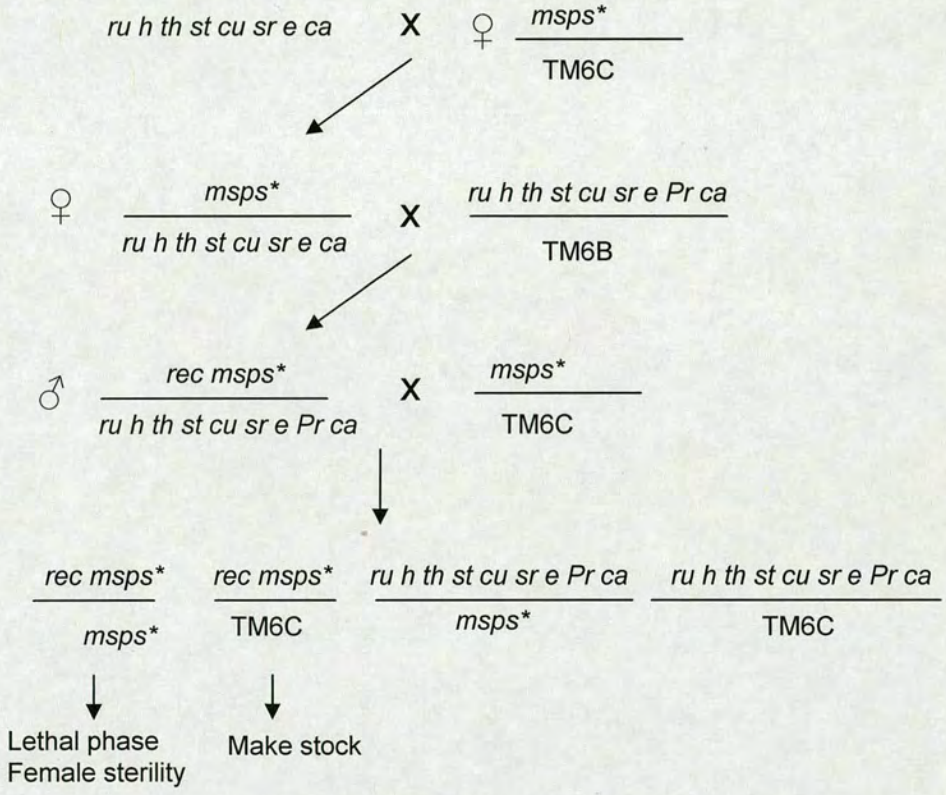

Figure 2.1 Recombination crossing strategy

The 3rd chromosomes of the new *msps* alleles were cleaned of other lethal mutations by recombination with a multiple marker chromosome (*rucuca*). The crossing strategy is outlined above. Recombinants were detected by the presence of visible markers. Retention of the mutant *msps* allele was confirmed by non-complementation with the original mutated chromosome. A stock of the new recombinant was created. The dominant *Prickle* (*Pr*) marker was used to distinguish the two classes of F2 progeny containing the TM6C balancer.

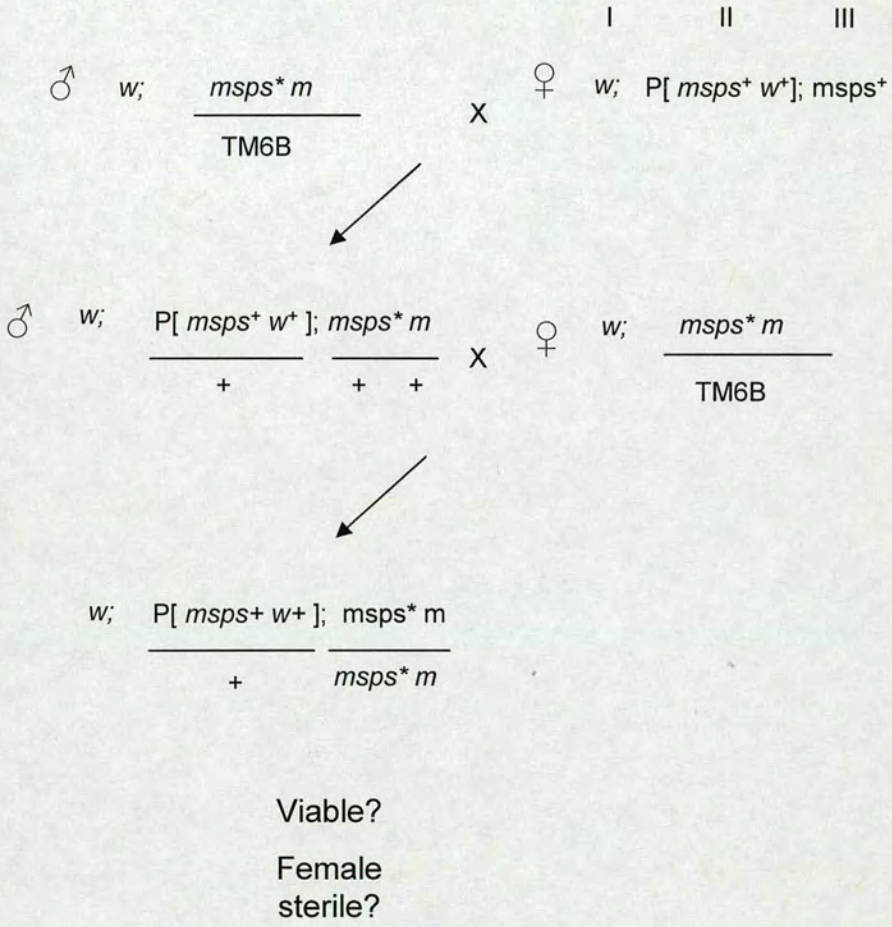

Figure 2.2 Rescue of mutant *msps* alleles.
A fly line carrying a P element insertion, containing the wild-type *msps* gene and w^+ marker (P[$msps^+$ w^+]), on the second chromosome, was crossed to the mutant *msps* allele (msps*) with a visible marker (*m*) on the 3rd chromosome. Male progeny carrying one copy of the *msps* mutant allele and a copy of the P element were crossed with the *msps* allele to obtain progeny homozygous for the mutant *msps* allele and containing a copy of the P-element. Vials were checked for viable progeny of this genotype and female sterility tests carried out.

Table 2.3 Primers used to amplify and sequence *msps* genomic DNA

name	Direction	sequence
AB3	For	GAGCTGGAGGATGAATTCGAC
AB4	For	TGCAGAAGATGATGGCGAGGC
AB5	Rev	CTGGCAGAATTTCTTCGGAT
AB6	Rev	CTACCTGGATCTGGGACT
AB7	Rev	GAGCAGGAGCCAAGTCGC
AB8	Rev	GAATGGATATCCTCCTTCGA
AB32	For	GATGACTCCGACATCCG
AB33	Rev	TACTCGCCATTCTCTAGC
AB34	For	CTCCGGCTAAGACAGTGG
AB35	For	CAATGAGGACGATGATGG
AB36	For	TTGTCGAAATCACGTGCG
AB37	For	TGGAATCCAGAAGAGTGC
AB38	Rev	ATACATAGGACGCACATC
AB39	For	GTCCTTCTATGTGTATGC
AB40	For	TTCTGCAGCATCTCAACC
AB41	For	CTACCCATTGAAAGTCAT
AB42	For	GCTATGGCATGAACATCT
AB43	For	CCATTCGGCTTGGACTCG
AB44	For	ATACCATCGGCTCAATCC
AB45	For	AACTGCAGCAGCTACTCG
AB46	For	AGATAGAGAAGCAGGAGG
AB47	For	ACTAGTCATCGTTCAGCAGC
AB48	Rev	TCGACAAAGACACACCGACG
AB49	For	CTTAGAACCAGGTGTTCG
AB50	Rev	CAGTTGTCAGTAAGTACC
AB51	For	ACTATTCATCTTCTGGAG
AB52	Rev	ACTTTGATAGGTACGCGC
AB53	Rev	ACTAGTCCCGATGCCGCACAAGG
AB54	For	GGTCTATGTATTAGCACT
AB55	For	CACAGTAGAAACGCAGCG
AB56	For	TTGCGACGAGCTTCCACC
AB57	Rev	TAATAGGCGTATCAAAGC

Table 2.4 Primers used to amplify and sequence d-tacc genomic DNA

Name	Direction	Sequence
AB9	For	CACACTGTCACTTATGCT
AB10	For	CGTTGGAAATTCGCGCA
AB11	Rev	ACCGAACACACACATATG
AB12	For	GCGATGTACATCTTGATA
AB13	For	GCCAGAAGAGCGAAGTAA
AB14	Rev	CTAAGGGAGGAATGAATG
AB15	Rev	CTAACTGGTCTAGTTCAA
AB16	For	CCTAATCAAGAGAAGCAA
AB17	For	GAAGCCATGGATGTGGAT
AB18	Rev	TGGATTCATCCACATCCT
AB19	For	CCATCAGCTTCGCTCTCA
AB20	Rev	CGTCGAGACACCATCAGG
AB21	For	GGTTCAGCCCACGAAGGA
AB22	Rev	TTCTGCTGCATGCAGAAG
AB23	Rev	GAACATTCCTTACAAACG
AB24	For	ATGCACGCGCATGTACTC
AB25	For	GCCACCTGTGGATAGAAC
AB26	Rev	TCAATGACGTCCACACTC
AB27	Rev	TACTGATCCAGGTTACAG
AB28	For	TAGCATCATACAGAGCTT
AB29	For	GTAACGAGGAATCGCTTC
AB30	Rev	TCAGTTAGACAGACACCA
AB31	Rev	TGTGATGAGGGTGAGTGC

Table 2.5 Antibodies used for immunostaining

A) Primary antibodies

Msps 264, affinity purified	C-terminal (1349-1784 aa)Msps	1/50	Cullen et al, 1999
Msps 268, affinity purified	Mid (746-1120aa) Msps rabbit polyclonal	1/50	unpublished
Crude D-TACC-C	MBP- C-terminal (250aa) D-TACC, rabbit	1/1000	unpublished
D-TACC-N, affinity purified	MBP-N-terminal (2-433aa) D-TACC, rabbit	1/50	unpublished
DM1A	α-tubulin mouse monoclonal	1/250	Sigma
Phospho histone H3	mouse monoclonal	1/500	Upstate Cell Signalling

B) Secondary antibodies

Cy3 rabbit	Cy3 conjugated donkey anti rabbit	1/2000	Jackson Labs
Alexa 488 mouse	Alexa 488 conjugated donkey anti mouse	1/500	Molecular Probes
Cy3 mouse	Cy3 conjugated donkey anti-mouse	1/2000	Jackson Labs
Cy5 mouse	Cy5 conjugated donkey anti mouse	1/500	Jackson Labs

Table 2.6 Primers used to create dsRNA for RNA interference experiments

Target gene	Primer Name	Direction	Sequence
Msps N-terminus	AB65	For	CGACTCACTATAGGGAGA-ATGGCGAGGACACAG AG
	AB66	REV	CGACTCACTATAGGGAGA-CAACGCGTTCACCTTTGA
Msps C-terminus	AB83	For	CGACTCACTATAGGGAGA-GCCTATTACGGGAGACTT
	AB84	Rev	CGACTCACTATAGGGAGA-TCTGCAGACCTTGCTGTT
D-TACC N-terminus	AB69	For	CGACTCACTATAGGGAGA-CATTCGGATTCGGATGTT
	AB70	Rev	CGACTCACTATAGGGAGA-GGCCTTTTCAGGCTCCTT
D-TACC C-terminus	AB77	For	CGACTCACTATAGGGAGA-GTACACGAAAGGCAGCAA
	nAB78	Rev	CGACTCACTATAGGGAGA-CACTAATGAGCTCTGCAA
KLP10A	AB77 A	For	CGACTCACTATAGGGAGA-GCAGAGCGTCAAGATCAA
	AB78 B	Rev	CGACTCACTATAGGGAGA-GTACCGTGGACGCTGTAA
KLP59C	AB79	For	CGACTCACTATAGGGAGA-GGACGGTAGAGTCCACTT

	AB80	Rev	CGACTCACTATAGGGAGA-GGTCTCTTCCTCACACAA
KLP59D	AB81		CGACTCACTATAGGGAGA-ACTGCCAAGAACCTGGAA
	AB82		CGACTCACTATAGGGAGA-GTTGGGATTCCCCGGATT
Bacterial beta-lactamase	oNSD38	For	CGACTCACTATAGGGAGA-TTCCTGTTTTTGCTCACC
	oNSD39	Rev	CGACTCACTATAGGGAGA-AGTGAGGCACCTATCTGA
T7 polymerase promoter	oNSD-33	Both For and Rev	GAATTAATACGACTCACTATAG GGAGA

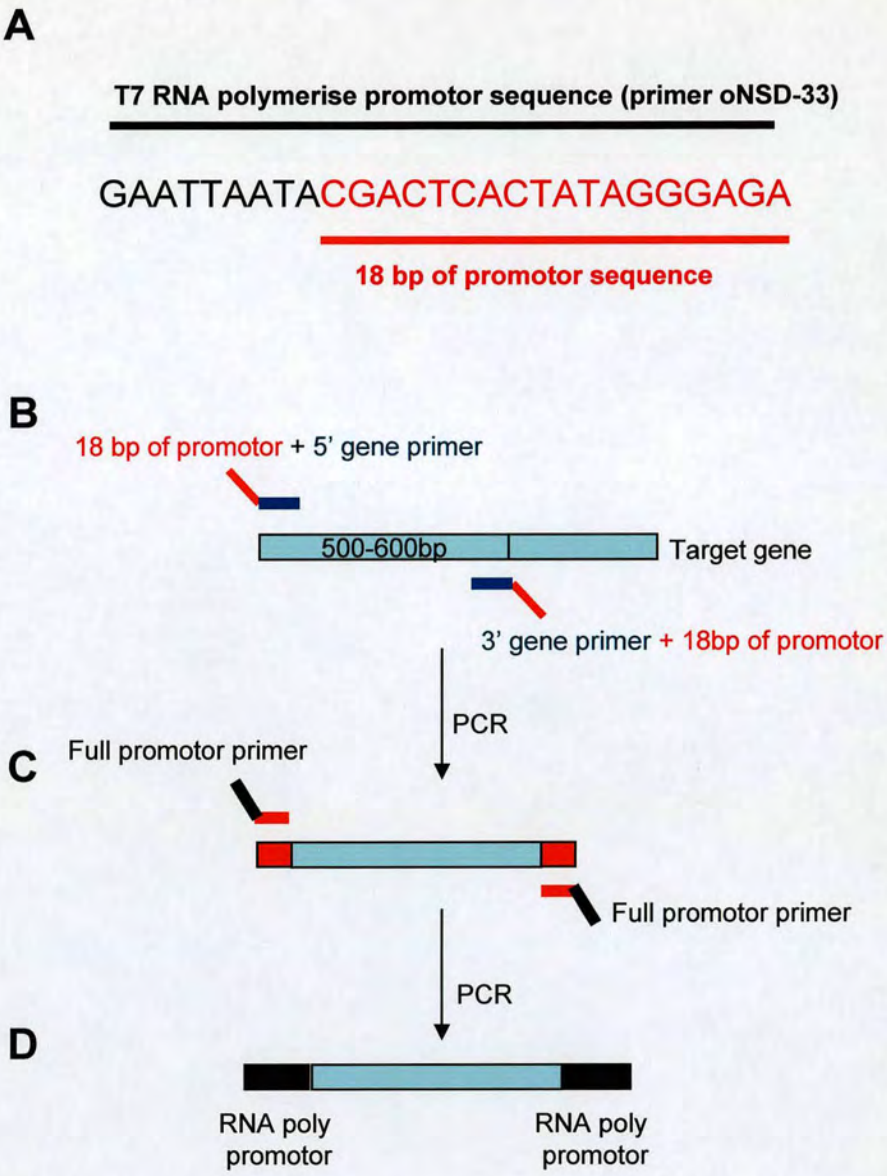

Figure 2.3 Preparation of DNA template for the transcription of dsRNA.

(A) The T7 RNA polymerase sequence. Primers, including half of the T7 RNA polymerise sequence (red), were designed to amplify a 500-600bp region of coding DNA from the target gene (B). The amplified DNA product was then used as a template for a further PCR reaction, using primers containing the full RNA polymerise sequence (C). The final PCR product will contain the RNA polymerase sequence at both ends of the gene sequence (D).

Chapter 3 Isolation of new *msps*, *d-tacc* and *ncd* alleles

3.1 Background

Understanding the role of Msps protein in both mitosis and meiosis has developed through the study of *msps* mutant alleles. The first lethal allele of *msps* identified ($msps^{P}$) has a P element insertion into the 5' UTR of the gene, reducing wild-type Msps protein to a very low level. The lack of Msps protein leads to mitotic spindle defects and subsequent lethality at the late larval stage (Cullen *et al.* 1999). Furthermore, through the study of a female sterile allele ($msps^{208}$), containing Msps protein at 10% of the wild-type level, the role of Msps in female meiotic spindle assembly was revealed.

Interaction between Msps and the centrosomal protein, D-TACC, has been demonstrated (Cullen & Ohkura 2001; Lee *et al.* 2001). D-TACC is important for localising Msps to the poles of both mitotic and female meiotic spindles. Furthermore, the minus end directed motor protein, Ncd, plays a role in the efficient localization of Msps, but not D-TACC, to the poles in female meiosis (Cullen & Ohkura 2001). Discovery of these interactions led to a model in which Ncd helps to transport Msps to the poles, followed by anchoring through an interaction with D-TACC. Mutant alleles of *d-tacc* and *ncd* were instrumental in uncovering the interplay between these three proteins.

All of the *msps* and d-tacc alleles thus far identified, cause changes in protein levels rather producing normal levels of dysfunctional protein. The *d-tacc* alleles previously isolated are all female sterile, and in one allele, $d\text{-}tacc^{stella}$, no D-TACC protein can be detected by western blotting (Lee *et al.* 2001). In the case of the microtubule motor, Ncd, a number of alleles have been isolated, including a null allele that results from a deletion most of the *ncd* gene (ncd^{1}) (Endow *et al.* 1990).

To understand more about *msps* and its interactors, *d-tacc* and *ncd*, a screen was carried out to identify new alleles of these three genes. The aim of the screen was to identify new alleles producing mutant protein with small changes in amino acid sequence. In such alleles, domains of the protein important for specific functions, such as localization and protein interactions, could be elucidated. This would provide crucial information about Msps, as the regions of the protein responsible for different functions have not been identified. In addition, new alleles may reveal novel functions or new insights into previously described functions.

3.2 Obtaining new *msps*, *dtacc* and *ncd* alleles

In this section, I describe a screen to isolate new *msps, d-tacc* and *ncd* alleles. All three genes are on the third chromosome, and double mutants, $msps^{P}$ $dtacc^{stella}$ and $msps^{P}$ ncd^{1}, are available, enabling the detection of new *d-tacc* or *ncd* alleles at the same time as new *msps* alleles. In this study, a strategy was used to create alleles with single point mutations, to try to disrupt specific domains of the proteins.

Flies were fed a chemical mutagen, ethylmethane sulfonate (EMS), to produce random mutations in the genome. EMS is an alkylating agent that will primarily produce point mutations, causing transitions from GC to AT (Ashburner 1989). To obtain mutations in the selected genes efficiently it was important to produce a high frequency of mutations in the genome. A range of concentrations of EMS were used in the initial stages of the screen, to determine the most effective concentration. It was important to find a balance between a high mutation rate and viability and fertility of the flies. Using a concentration of 35mM of EMS or above, resulted in death of over 25% of the flies. A concentration of 30mM, resulted in only a 10% death rate, and was chosen as the concentration to use for the rest of the screen.

Mutagenesis was carried out by incubating male flies over night, in bottles containing filter paper soaked in an EMS/glucose solution. After a day of recovery,

mutagenised flies were crossed to females carrying a third chromosome balancer (the crossing strategy employed illustrated in figure 3.1). From the progeny, male heterozygotes carrying a mutagenised chromosome, over the TMC6 balancer, were selected and individually crossed to virgin females carrying double mutations of either *msps*^{P} *d-tacc*^{stella} or *msps*^{P} *ncd*^{1}. Failure of the mutagenised third chromosome to complement the chromosome carrying the double mutations was recognized by either lethality or female sterility. Lethality was scored by the absence of heterozygous (mutagenised (*) chromosome/double mutant) flies, which could be distinguished by a lack of the *Tb* marker. If these flies were viable, 5 females were crossed with fertile male flies and the vials scored 5-6 days later for the presence of live offspring.

2805 chromosomes were screened for new *msps* and *dtacc* alleles and a further 1405 chromosomes were screened for *msps* and *ncd* alleles. From this screen, 7 lethal, 2 female sterile and 2 dominant female sterile alleles were obtained (Table 3.1). Complementation testing with single *msps*^{P}, *d-tacc*^{stella} and *ncd*^{1} alleles identified 8 of the new mutants as new *msps* alleles and one as a new *d-tacc* allele (Table 3.2). No new *ncd* alleles were obtained. New alleles of *msps* were obtained at a rate of 1 in 526 mutagenised chromosomes, whist *d-tacc* alleles were obtained at 1 per 2805 mutated chromosomes.

Two alleles obtained in the screen, sterile in combination with *msps*^{P}, *d-tacc*^{stella} and *ncd*^{1} (Table 3.2), were also female sterile over the TM6C balancer and a wild-type chromosome. Such behaviour demonstrates that these two mutants contain a dominant female sterile mutation. Dominant female sterile mutations could be identified in the screen, as male flies were used to carry the mutations in the crossing scheme.

To conclude, EMS mutagenesis has been used successfully to isolate new alleles of *msps* and *d-tacc*. Using a concentration of 30mM EMS, mutations that cause lethality or female sterility in the *msps* gene can be obtained at a high rate. Many more *msps* alleles were isolated in the screen than *d-tacc*, with only one new allele, and *ncd,* which produced none. This could be explained by the fact that *msps* is a larger target

for the mutagen. The *msps* coding region covers a large area (6kb) compared to the smaller regions encoded by *d-tacc* (3.7kb) and *ncd* (3.6kb).

3.3 Determining lethal phase / sterility of new mutants

The next step in the characterization of the new mutants was to determine the lethal stage of the homozygotes. Lethal stage is the time at which the organism dies due to the mutation. For example, $msps^{P}$ homozygotes die at the larval/pupal transition (Cullen *et al.* 1999). As some protein is still present in the $msps^{P}$ allele, a null allele may prove to be lethal earlier. As I have created new *msps* alleles, comparisons between the lethal stages of homozygotes can be used to reveal the relative strengths of the mutations.

Stocks of the new alleles were established and the lethal stages of homozygotes determined. Homozygous mutant larvae were distinguished from heterozygotes by the absence of the *Tb* marker, which is carried on the balancer chromosome. Many of the homozygotes were lethal early in development, as no third instars were seen (Table 3.3). Only $msps^{146}$ homozygotes survive beyond this stage and die in the pupal case.

The EMS mutagen was used at a high concentration, and consequently, more than one lethal mutation may have occurred per chromosome. It is possible that the lethality of the mutant homozygotes is due the *msps* mutation or due to a random mutation in an unrelated gene. $msps^{S10}$, for example, is viable but female sterile when heterozygous with $msps^{P}$, suggesting it is a viable allele (Table 3.1). However, the $msps^{S10}$ homozygote was found to be lethal (Table 3.3). In this case, another mutation on the third chromosome may be responsible for this lethality. The third chromosomes carrying the new alleles must be cleaned of other lethal mutations, so that the true lethal phase that results from the msps mutation can be determined.

3.4 Recombination of new mutants to remove extra chromosomal mutations

The effects of extra mutations on the chromosome can be removed by two methods: the use of a deficiency that uncovers the region containing the gene or by removal of unwanted mutations by recombination. No deficiency uncovering the *msps* gene is available, so a recombination strategy was used.

The chromosomes carrying the new *msps* and *d-tacc* alleles were cleaned of other mutations by recombining them with the multiple marker chromosome *rucuca* (Fig 3.2). *msps* maps cytologically to 89B and *d-tacc* to 82D, so recombinants were selected that had recombined outside these regions (as indicated in figure 3.2). The recombinants were tested to see if they had retained the lethal or female sterile *msps* or *d-tacc* mutations and a stock made. The new stocks were observed to see if there was a change in lethal phase of the homozygotes (Table 3.3).

An improvement in lethal phase indicates the removal of an extra lethal mutation. This proved to be the case for $msps^{51}$, which showed an improvement in lethal phase from early lethal to 3rd instar lethal (Table 3.3). Similar improvements were seen for $msps^{D}$, $msps^{S10}$ and $d\text{-}tacc^{S3}$. Some *msps* alleles did not show an improvement in lethal phase following recombination. There are two possible explanations for this: either lethal phase results from the *msps* allele or an extra lethal mutation lies very close to the *msps* gene and has not been removed by recombination.

To confirm that other mutations had been removed, *msps* mutants were rescued using a wild-type *msps* gene (Table 3.3). Recombinants of $msps^{D}$, $msps^{51}$, $msps^{146}$ and $msps^{S10}$ were all rescued by the full length wild-type *msps* construct. Therefore, all other mutations resulting in lethality or female sterility have been removed. The remaining *msps* alleles were not recombined or rescued due to time constraints and the fact that subsequent characterisation (see chapter 4) indicated that these alleles were of less interest.

It is clear from this data that mutagenesis with a concentration of 30mM EMS results in more than one mutation per chromosome in the majority of cases. Removal of extra mutations on the third chromosome revealed that the new *msps* alleles are lethal as early third instars or later.

3.5 Genetic analysis of new alleles

The extent to which protein function is disrupted in the new alleles will influence the severity of the phenotype, and subsequently, the lethal stage of the fly. The relative strengths (i.e. degree of loss of function) of the various *msps* alleles may be determined by creating heterozygotes of the different alleles and examining lethal phase.

The new alleles were crossed to each other and to *msps* mutants that had previously been isolated. The lethal phase and female sterility were analysed. $msps^{A}$, $msps^{D}$, $msps^{C}$, $msps^{E}$ and $msps^{1358}$ all seem to be of a similar strength. When in combination with each other they were all lethal as 2nd instars (Table 3.4). $msps^{51}$ homozygous larvae can survive until the early 3rd instar stage in combination with $msps^{A}$, $msps^{D}$, $msps^{C}$ and $msps^{1358}$ alleles. This suggests that $msps^{51}$ is a weaker allele that the other five and retains more function. These 6 new lethal alleles appear to be stronger than the previously identified lethal allele, $msps^{P}$. Many $msps^{P}$ homozygotes die at the larval-pupal transition (Cullen *et al.* 1999), but when $msps^{P}$ is heterozygous with any of these 6 new alleles, the larvae die as 3rd instar. Therefore, I have isolated alleles that are stronger than any previously identified.

$msps^{146}$ is unique among the lethal alleles as homozygotes survive to the pupal stage, unlike the other lethal alleles which all die as larvae. This allele retains sufficient function to survive larval development and is the weakest of the lethal alleles.

The new female sterile *msps* allele, $msps^{S10}$, appears to be weaker than the previously identified female sterile $msps^{208}$ allele. This is indicated by the fact that $msps^{S10}$ is viable when heterozygous with other lethal *msps* alleles, whereas $msps^{208}$ will die in the pupal case.

Genetic analysis reveals that a range of alleles of varying strength, different from those previously isolated, have been obtained in this screen. None of the combinations of alleles complement each other, signifying that disruption of Msps function in one allele can not be restored by any of the other alleles.

3.6 Determining DNA mutations of *msps* and *d-tacc* alleles

One of the reasons to create new alleles was to investigate regions of the proteins important for function. Therefore, it was important to understand the molecular nature of the new alleles. I sequenced the alleles to determine the mutation at the DNA level, and from this data, mutant protein sequences were predicted.

Genomic DNA was isolated from either homozygous mutant larvae or heterozygous flies carrying the mutation. The 15 kb of genomic *msps* DNA was amplified in 1.5 to 3kb sections using PCR (fig 3.3.A and B). Internal primers were then used to sequence the PCR products (fig 3.3.C.). The wild-type *msps* gene, from the parental strain used in the screen, was also sequenced to compare with the new alleles. Mutations found in both the parental gene and new alleles were excluded as polymorphisms. If heterozygotes were used, differences in sequence are indicated by double peaks in the sequencing, with one base referring to the wild-type gene sequence and the other referring to the new allele. Changes in sequence were confirmed by repeating the PCR and sequencing, to ensure that the change in sequence did not result from a mistake made by the TAQ enzyme when the PCR product was synthesized. A similar strategy was used to sequence the new *d-tacc* allele.

Sequencing revealed that the new alleles result from a mix of point mutations and small deletions (Table 3.5). The point mutations result from transitions from G to A or C to T. These transitions are the most frequent changes observed with the EMS mutagen (Ashburner, 1989). In addition, a number of small deletions were created. No mutation was found in the coding sequence of $msps^{E}$ suggesting a mutation has occurred in a non-coding region.

All of the DNA mutations result in premature stop codons, either due to a point mutation or a small deletion producing a frame shift (Table 3.5). The new alleles are predicted to produce a series of Msps protein truncations (figure 3.4). The smallest predicted protein, $Msps^{D}$, has a premature stop codon after only 20 amino acids. The largest predicted protein, $Msps^{S10}$, is missing the final 79 amino acids.

The $d\text{-}tacc^{S3}$ allele has a point mutation at base pair 16920, resulting in a premature stop codon (Table 3.5). The predicted protein will be truncated, with the C-terminal 304 amino acids missing. The C-terminal region has been shown to be involved in binding microtubules and is also the domain through which D-TACC binds to Msps (Gergely *et al.* 2003; Lee *et al.* 2001). The $d\text{-}tacc^{S3}$ allele is viable, despite lacking both the microtubule and *msps* binding domain, indicating that these interactions are not essential for viability of the fly.

All but one of the alleles were predicted to produce truncated proteins rather than full length protein with an amino acid substitution. This result demonstrates that there is a lower chance of randomly mutating an amino acid and disrupting protein function, than there is of producing a stop codon and subsequent truncation. It is unsurprising that deletion of large regions of the protein will have serious consequences for protein function. As mutagenesis was random, mutants resulting in amino acid substitutions will have occurred, but failed to affect protein function sufficiently to cause lethality or female sterility.

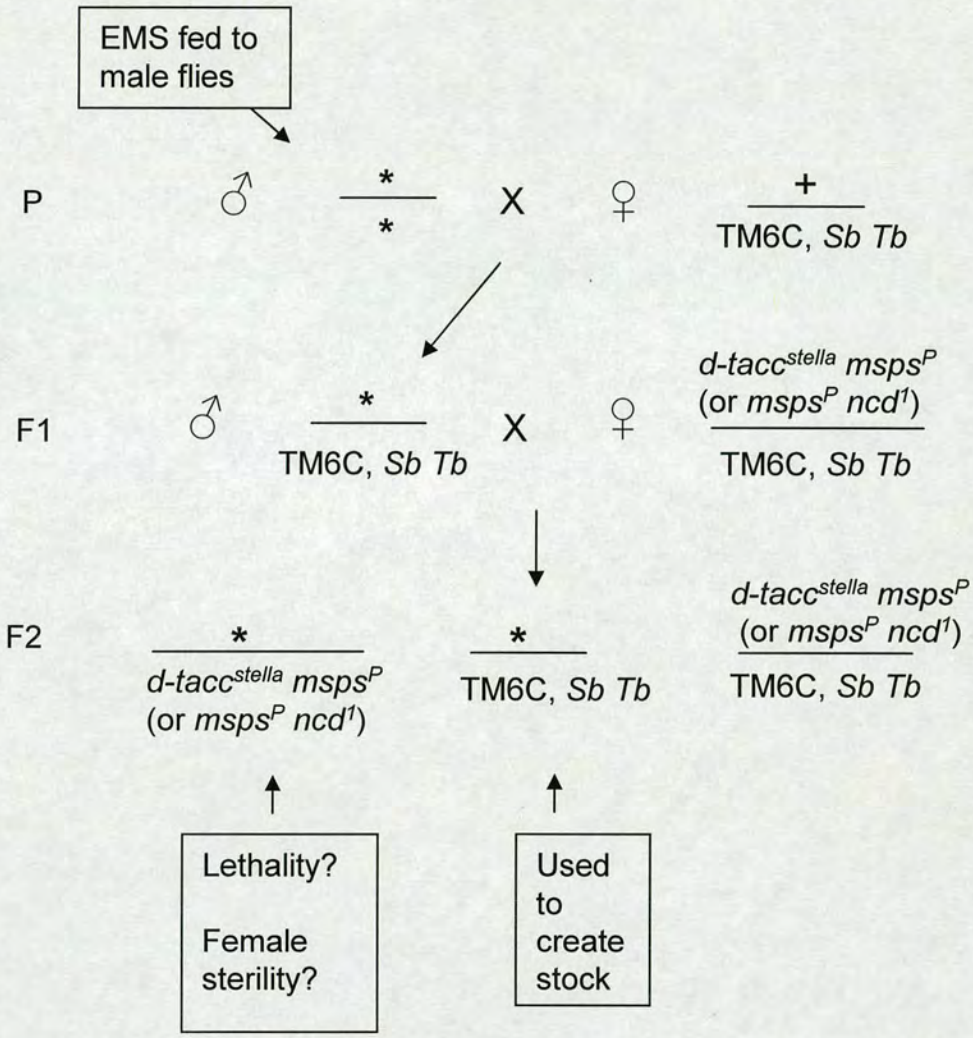

Figure 3.1. The crossing scheme used to isolate new *msps, ncd* and *d-tacc* alleles.

EMS was fed to male wild-type flies which were then crossed to females carrying the TM6C balancer. In the F1 generation, single males carrying a mutagenised 3rd chromosome (*) over the TM6C balancer were crossed *to d-tacc^{stella} msps^{P} (*or *msps^{P} ncd^{1})* mutant females. F2 progeny were examined for failure to complement the double mutant chromosomes. Lack of complementation was indicated by lethality or female sterility. The flies used had a *white* background so that the two types of F2 generation progeny carrying the TMC6 balancer could be distinguished. Both *d-tacc^{stella}* and *msps^{P}* alleles were created by insertion of a P-element containing a copy of the *w+* gene, resulting in red eyes flies. Flies carrying the mutated chromosome over the TMC6 balancer have white eyes and could be selected to create a stock.

A

Name of mutant	mutant / *dtacc*^{stella} *msps*^{P}
A	Larval lethal
S3	Viable – female sterile
51	Larval lethal
146	Pharate lethal
1358	Larval lethal
S6	Viable – female sterile
S8	Viable – female sterile

B

Name of Mutant	mutant / *msps*^{P} *ncd*^{1}
C	Larval lethal
D	Larval lethal
E	Larval lethal
S10	Viable female sterile

Table 3.1. Mutants identified in EMS screen.
Mutants failing to complement a chromosome carrying (A) the *d-tacc*^{stella} and *msps*^{P} alleles or (B) *msps*^{P} and *ncd*^{1} alleles. Failure to complement was indicated by lethality or female sterility.

	single mutants		
New mutants	***msps^{P}***	***d-tacc^{stella}***	***ncd^{1}***
A	Lethal	+	+
C	Lethal	+	+
D	Lethal	+	+
E	Lethal	+	+
51	Lethal	+	+
146	Lethal	+	+
1358	Lethal	+	+
S3	+	Female sterile	+
S6	Female sterile	Female sterile	Female sterile
S8	Female sterile	Female sterile	Female sterile
S10	Female sterile	+	+

Table 3.2. Lethality/viability of the newly isolated alleles heterozygous with single *msps^{P}*, *d-tacc^{stella}* and *ncd^{1}* alleles.

Complementation (viable, fertile) is indicated by +. If non-complementation occurred the phenotype is given (either lethality or female sterility).

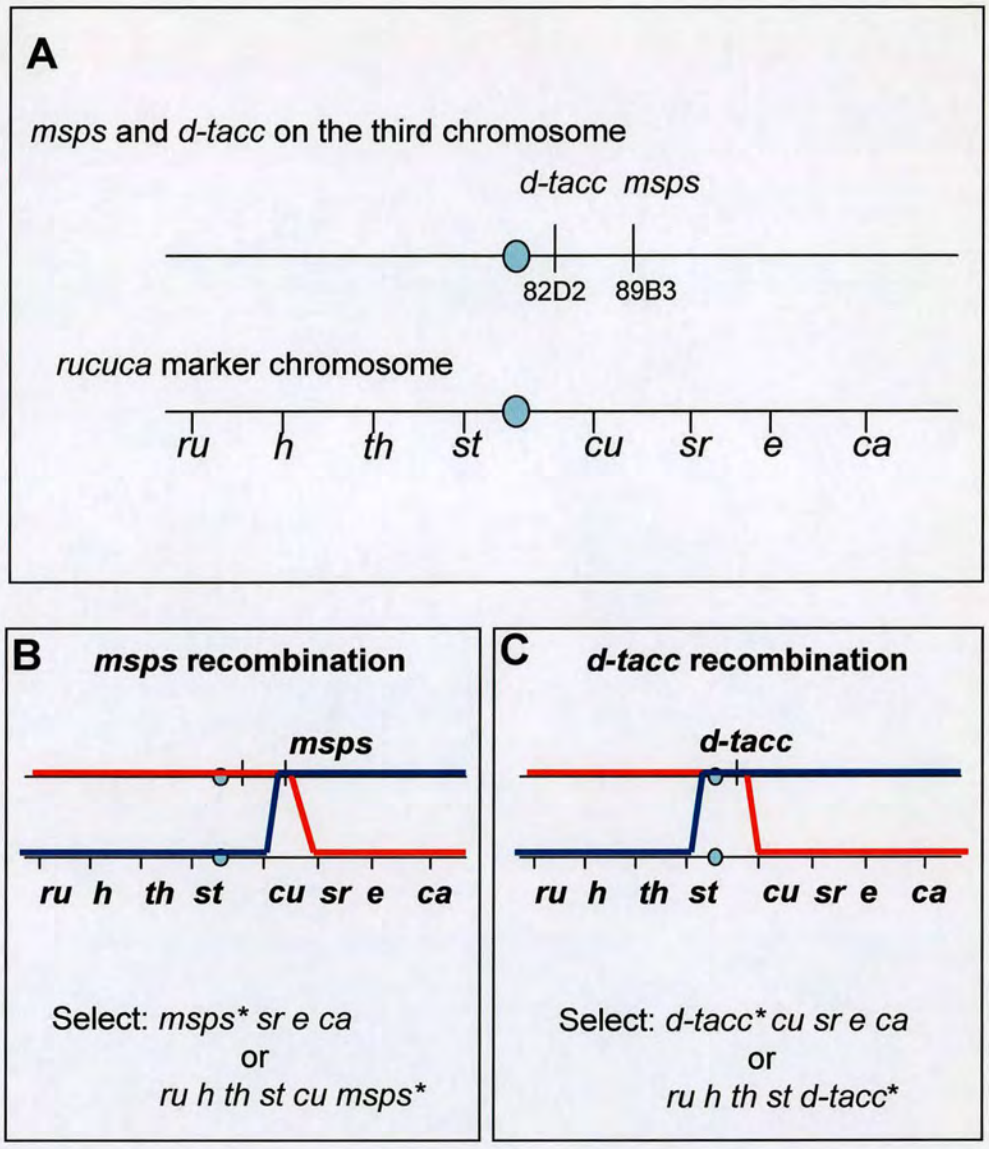

Fig. 3.2 Recombination strategy for *msps* and *d-tacc* mutants to remove other unwanted mutations.

(A) The cytological location of the *msps* and *d-tacc* genes on the third chromosome. Location of the multiple marker genes of the *rucuca* chromosome are also shown.

(B & C) The use of multiple markers allowed recombinants to be selected that had recombined either side of the *msps* (B) or *d-tacc* (C) gene.

msps / *d-tacc* allele	Lethal phase of original stock	Recombinant	Lethal phase/female sterility of recombinant	Recombinant rescued by wild-type gene?
$msps^{D}$	Early lethal	rec 3	2nd instar larval lethal	yes
$msps^{51}$	Early lethal	rec 2	Early 3rd instar larval lethal	yes
$msps^{146}$	Pupal lethal	rec 3	Pupal lethal	yes
$msps^{S10}$	Early lethal	rec 13	Viable - Female sterile	yes
$msps^{A}$	Early lethal	n/d	-	n/d
$msps^{C}$	Early lethal	n/d	-	n/d
$msps^{1358}$	Early lethal	n/d	-	n/d
$msps^{E}$	Early lethal	n/d	-	n/d
$d\text{-}tacc^{s3}$	Early lethal	rec 21	Viable – female sterile	n/d

Table 3.3 Lethal phase and rescue of recombinants created to clean up chromosomes of new mutant alleles.

Early lethal refers to lethality before the 3rd instar stage

alleles	A	C	D	E	51	146	1358	S10	P	208
A	?	**L** 2L	**L** 2L	**L** 2L	**L** Early 3L	**L** Ph	**L** 2L	**f.s.**	**L** Late 3L	**L** Ph
C		?	**L** 2L	**L** 2L	**L** Early 3L	**L** Ph	**L** 2L	**f.s.**	**L** Late 3L	**L** Ph
D			**L** 2L	**L** 2L	**L** Early 3L	**L** Ph	**L** 2L	**f.s**	**L** Late 3L	**L** Ph
E				?	**L** Early 3L	**L** Ph	**L** 2L	**f.s**	**L** Late 3L	**L** Ph
51					**L** Early 3L	**L** Ph	**L** Early 3L	**f.s**	**L** Late 3L	**L** Ph
146						**L** Ph	**L** Ph	**f.s**	**L** Ph	?
1358							?	**f.s**	**L** Late 3L	**L** Ph
S10								**f.s**	**f.s.**	**f.s**
P									**L** L/P	**L** Ph
208										**f.s**

Table 3.4 Viability and female sterility of combinations of *msps* mutant alleles.

The new *msps* alleles were crossed to each other and the lethal phase/female sterility tested. Lethality (**L**) was classified as either 2nd instar larval (2L), early 3rd instar (early 3L), late 3rd instar larvae (late 3L), larval/pupal transition (L/P) or pharate (Ph). Viable flies were tested for female sterility (f.s). Combinations for which viability or lethal phase was not determined are marked with a question mark (?).

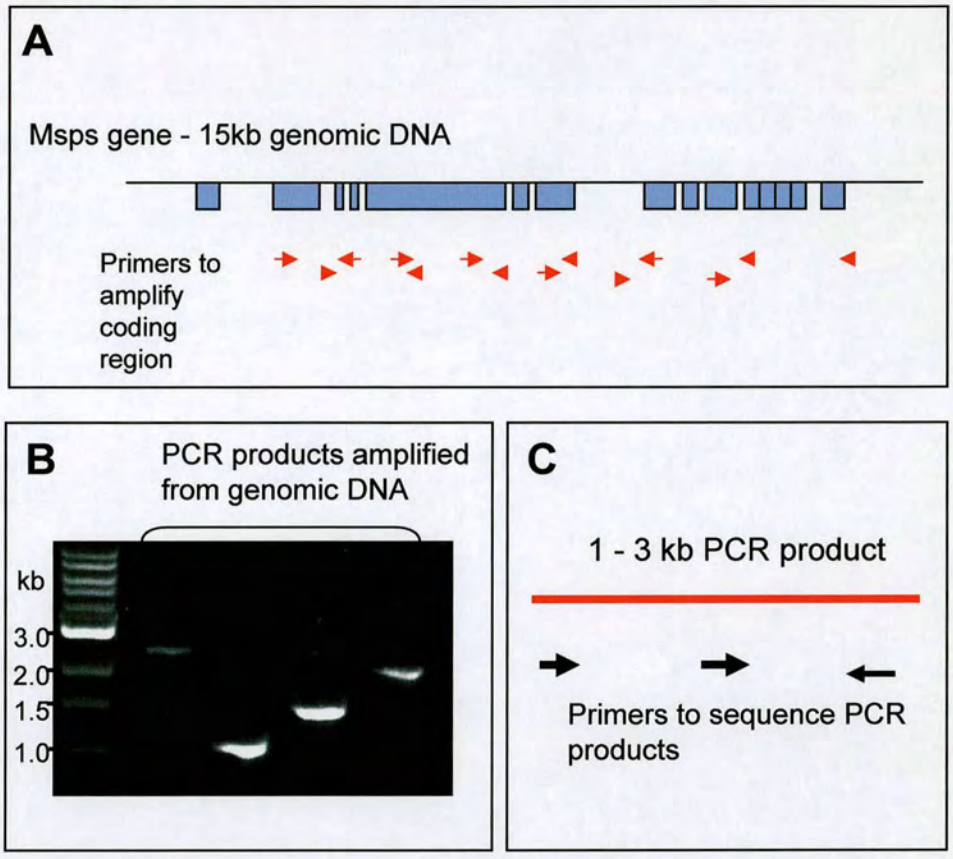

Figure 3.3. Strategy for sequencing the new *msps and d-tacc* alleles.

(A) Primers were designed to amplify 1-3 kb fragments of *msps* coding sequence from genomic DNA extracted from flies. (B) 2µl of the PCR reaction was run on an agarose gel to check the size of band was correct. (C) The DNA fragments were purified and then sequenced using internal sequencing primers. A similar strategy was used to sequence the new *d-tacc* allele.

allele	Description of DNA mutation	Protein alteration
msps^{A}	Deletion of bps 3958-3977	Frame shift resulting in premature STOP
msps^{C}	Deletion of 4 bps: 6976-6979	Frame shift resulting in premature STOP
msps^{D}	G to A at 2755bp	Premature STOP
msps^{E}	No mutation found in coding	-
msps^{51}	C to T bp 8143	Premature STOP
msps^{146}	Deletion bps 3889-3903	Removal of 5 prime splice site of intron 4. Failure to splice intron will result in frame shift and premature STOP
msps^{1358}	G to A at bp 5964	Premature STOP
msps^{S10}	G to A at bp 10075	Premature STOP
d-tacc^{S3}	C to T at bp 16920	Premature STOP

Table 3.5 DNA mutations and resulting amino acid changes in new *msps* and *d-tacc* alleles.
Sequencing of genomic DNA revealed the DNA changes in the new *msps* and *d-tacc* alleles. Alterations in amino acid sequence were deduced from the DNA changes. Nucleotide at position one corresponds to the first nucleotide of the *msps* gene sequence (Accession number AJ249115)

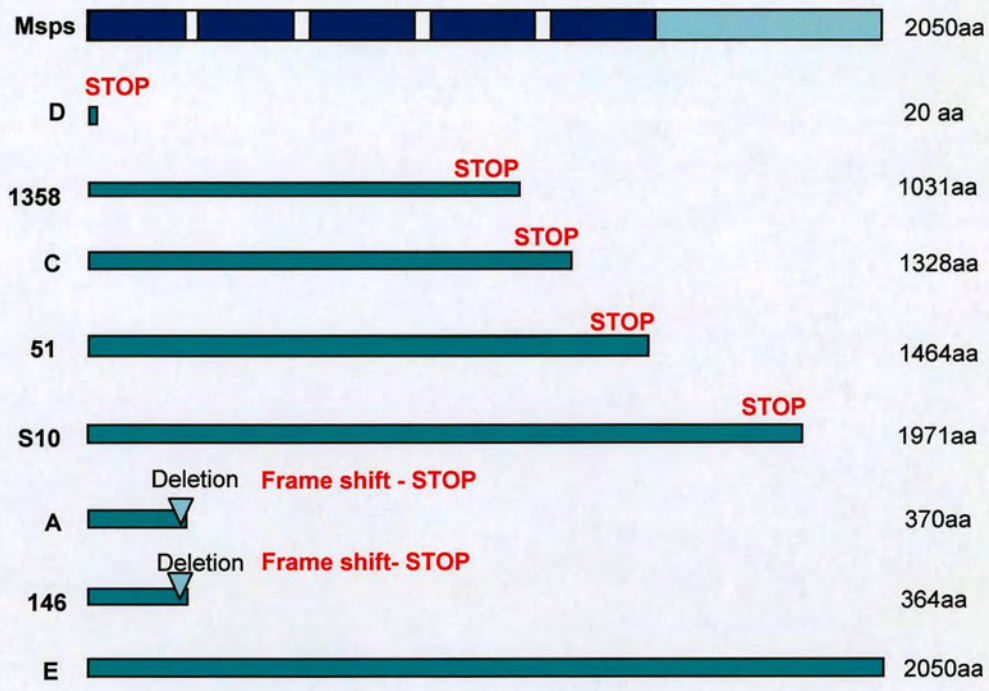

Figure 3.4. Predicted mutant Msps proteins produced by new *msps* alleles.

The length of the mutant proteins were predicted from the DNA sequences of the *msps* alleles. Protein length is given in amino acids (aa).

Chapter 4 Protein and cytological analysis of new *msps* and *d-tacc* alleles

4.1. Background

In this chapter, I describe the analysis of a number of new *msps* and *d-tacc* alleles, created to reveal novel functions and domains of the proteins important for function, localisation and interaction with other proteins. In order to carry out this analysis, a number of steps had to be taken. Firstly, the levels and sizes of the predicted mutant proteins of these new alleles were established. Secondly, the mutant phenotype was analysed to establish if the different mutant proteins had different changes in function. Thirdly, protein localisation and interaction with other proteins were analysed. The final step was to link these aspects together, to determine what regions of the protein are responsible for different aspects of protein function.

4.2. Presence and level of mutant Msps protein

The newly isolated *msps* alleles are caused by a range of different mutations. Sequences for each of the mutant proteins have been predicted (figure 4.1.A), but to confirm the presence and levels of the mutant proteins western blots were carried out.

Mutant larvae were collected as late or early third instars depending upon the lethal stage of the mutant. Care was taken to ensure only live larvae were selected. The larvae were homogenised in protein sample buffer and boiled for 5 minutes. SDS-PAGE gels were loaded so that 10% of the protein extract from one larva was loaded per lane, and western blots were carried out to detect Msps protein. In the western blots in fig 4.1, the Af268 Msps antibody, raised against the middle of the protein (figure 4.1.A), was used to detect Msps protein. Wild-type Msps protein gives a single band at approximately 220kD. In figure 4.1.B, $msps^{P}$ and $msps^{208}$ homozygous larvae, with known protein levels, were loaded alongside

the new mutants. The blot shows that very little Msps protein is present in the *msps*^{P} mutant, whilst msps^{208} contains approximately 10% of the level of wild-type Msps protein. These results confirm those previously described using another antibody (Cullen & Ohkura 2001; Cullen *et al.* 1999).

DNA sequencing data revealed that the *msps*^{S10} allele has a premature stop codon, predicted to remove the final 79 amino acids of the protein (figure 4.1.A). As expected, the Msps antibody recognised a protein, slightly smaller than wild-type, in the *msps*^{S10} homozygous larvae (figure 4.1.B). The level of Msps^{S10} protein is approximately equivalent to wild-type levels.

Sequencing of the *msps*^{146} allele revealed a deletion removing the 5' splice site of intron 4 (table 3.5). Failure to remove the intron will result in a frame shift, leading to a premature stop codon and predicted protein of 364 amino acids (figure 4.1.A). Unexpectedly, *msps*^{146} homozygotes contain a protein of similar size and intensity to wild-type protein (figure 4.1.B), despite the deletion of the splice site. It is possible that an alternative splice site has been used and the intron has been removed. Clearly the protein is dysfunctional, as the larvae die in the pupal case, but the change in protein sequence is unknown.

msps^{51} homozygotes die as small 3rd instar larvae, therefore protein samples from wild-type and *msps*^{51} homozygotes were made from small 3rd instars so that a fair comparison of protein levels could be made. The *msps*^{51} allele contains a premature stop codon and is predicted to produce a protein of 1462 amino acids (figure 4.1.A). The truncation removes the conserved C-terminal domain and half of the final TOG domain. In *msps*^{51} homozygotes a smaller Msps protein of approximately 120kD is present, corresponding to the mutant protein (figure. 4.1.B). This band is weaker than wild-type Msps, indicating a lower level of protein in the mutant.

The *msps*^{D} allele has a premature stop codon after only 20 amino acids (figure 4.1.A). The blot shows that no protein can be detected (fig 4.1.C). However, the 268 antibody used in this blot was raised against the middle of Msps protein (figure 4.1.A), and will not be able to recognise the small 20 amino acid

peptide if it is present. Nevertheless, it confirmed that there was no Msps protein of significant size in the mutant larvae.

msps^{D} proved to be useful in examining protein levels of the four *msps* mutants, *msps*^{A}, *msps*^{C}, *msps*^{E} and *msps*^{1358}. The third chromosomes of these 4 alleles have not been cleaned of other lethal mutations and all the homozygotes die before the 2nd instar larval stage. When these alleles were heterozygous with *msps*^{D}, 2nd instar larvae were obtained, and protein samples could be prepared for western blotting. Protein samples from these heterozygotes contain no detectable Msps protein (figure 4.1.C). The allele *msps*^{A}, like *msps*^{D}, is predicted to produce a protein that is too short to be recognised by antibody 268. Msps^{C} and Msps^{1358} proteins, 1031 and 1328 amino acids long respectively, were predicted to be detected by this antibody but no bands were seen on the blot (figure 4.1.C). Due to the truncations, the proteins may be folded in unstable conformations that result in the proteins breaking down. No mutation was found in the coding region of *msps*^{E}, however, no protein is present in the mutant homozygotes (fig. 4.1.B). This suggests that a mutation has occurred in a non-coding region, resulting in a reduced level of protein.

To conclude, three of the new *msps* alleles produce mutant protein that can be detect by western blotting. The remaining alleles appear to produce no protein, or at a level that is not detected by western blotting. In the case of *msps*^{A} and *msps*^{D}, short proteins not recognised by the available antibodies could be present. Proteins that include all or most of the N-terminal domain (Msps^{S10} and Msps^{51}) are more stable than those that are truncated before the 5th TOG domain (Msps^{C} and Msps^{1358}).

4.3 Cytological defects of *msps* alleles and mutant protein localisation

The new *msps* alleles that produce mutant protein, *msps*^{S10}, *msps*^{51} and *msps*^{146}, were selected for further analysis to determine protein localisation and phenotype, with the aim of identifying domains of the protein important for Msps function.

4.3.1. *msps*^{51} cytological analysis

Msps^{51} protein is missing the C-terminal 586 amino acids of the full length protein. The allele is lethal, indicating that removal of the C-terminal region has serious consequences for protein function. Determining protein localisation and examining phenotype will give insight into the role of the C-terminus.

The larval neuroblasts from 3rd instar larvae contain many dividing cells in which spindle morphology can be examined (Gonzalez & Glover D.M. 1993). Whole brains were dissected from homozygous *msps*^{51} larvae, fixed and immunostained with tubulin, to examine spindle structure, and Msps antibody, to investigate Msps^{51} protein localisation.

The mitotic phenotype in larval neuroblasts of *msps*^{51} mutants was very similar to the phenotype originally described for the *msps*^{P} mutant (Cullen *et al.* 1999b). The most common phenotype was the presence of more than one bipolar spindle (59%) (figure 4.2). Most chromosomes align at the metaphase plate and are associated with a bipolar spindle, while a few of the chromosomes become separated and associate with a smaller bipolar spindle (figure 4.2: class I). The mini-spindle usually shares one pole with the main spindle. In 34% of cases the spindle is so disorganised the structure could not be determined (figure 4.2: class II). There is no striking difference between the spindle defects seen in *msps*^{51} cells and the defects reported for *msps*^{P}. The phenotype is perhaps more severe with fewer normal bipolar spindles seen in the *msps*^{51} mutant (14%) than in the msps^{P} mutant (28%) (Cullen *et al.* 1999b).

Wild-type Msps protein localises to the centrosomes and spindle in mitotic cells in larval neuroblasts (figure 4.3.A). Staining with the Msps antibody revealed that the Msps^{51} protein is unable to localise to either the centrosome or spindle and remains cytoplasmic (figure 4.3.D).

To conclude, removal of the C-terminal domain of the Msps protein disrupts centrosome and spindle localisation during mitosis. The spindle defects seen in *msps*^{51} larvae are similar to those seen with the previously characterised

msps^{P} allele, a mutant expressing a low level of Msps protein. This suggests that protein function is severely compromised in the Msps^{51} protein.

4.3.2 *msps*^{146} cytological analysis

The allele *msps*^{146} unexpectedly produced a protein of similar length to wild-type despite a mutation that was expected to produce a truncated protein (figure 4.1.A and B). This allele differs from the other lethal alleles, as homozygotes die in the pupal case rather than as larvae. Mitotic phenotype and Msps protein localisation was examined in this mutant to understand the reason behind this later lethality.

Mitotic spindle morphology and Msps protein localisation were examined in the *msps*^{146} homozygous larvae as described previously. Msps^{146} protein localisation is unaffected, as both spindle and centrosome localisation was seen in mutant neuroblasts (figure 4.3.C). No obvious spindle defects were observed but a larger number of mitotic cells were seen. Brain squashes were carried out to obtain an accurate estimation of mitotic index. This procedure involved the squashing of whole brains treated with orcein to stain the chromosomes. Metaphase and anaphase cells can be identified by their chromosome pattern. In *msps*^{146} brain squashes, mitotic index rose from the 5.3% found in wild-type to 7.8%.

In conclusion, the gross spindle defects seen in *msps*^{51} were not present in the *msps*^{146} mutant brains, perhaps explaining why *msps*^{146} homozygotes are lethal much later in development than *msps*^{51} homozygotes. Localisation appears to be unaffected in the Msps^{146} protein; nevertheless, some aspect of protein function must be compromised, indicated by the rise in mitotic index.

4.3.3 Msps^{S10} cytological analysis

4.3.3.1. Somatic mitotic phenotype of msps^{S10} larvae

Msps^{S10} protein has a C-terminal truncation removing the final 79 amino acids of the protein. The *msps^{S10}* allele was examined to determine how Msps protein function and localisation is affected by this small truncation.

To reach adulthood, the organism undergoes many mitotic divisions in which a functional spindle must be formed. Msps is essential for this spindle formation as demonstrated by the study of the *msps^{P}* allele (Cullen *et al.* 1999a). The *msps^{S10}* allele is viable, so must retain sufficient function to enable the fly to reach adulthood. Cuticle defects or fewer bristles can indicate slight mitotic problems, however no such defects are present in the *msps^{S10}* homozygous flies. Neuroblasts from *msps^{S10}* larvae showed no mitotic defects and the mutant protein displays the same localisation pattern as wild-type protein (figure 4.3.B).

Msps^{S10} protein appears to be able to carry out the mitotic functions of the Msps protein in somatic cells, enabling the flies to reach adulthood.

4.3.3.2. Female meiosis in msps^{S10} oocytes

Msps plays a vital role in maintaining bipolarity of female meiotic spindles, where it localises to the accentrosomal poles and spindle (Cullen & Ohkura 2001). Female meiosis was examined in the *msps^{S10}* allele to determine if the female sterility of the allele results from defects in meiosis. To examine female meiotic spindles, oocytes were dissected from flies that had been aged at 18℃ for 3-5 days. The oocytes were dissected directly in methanol to fix the tissue and then immunostained with antibodies against alpha-tubulin and Msps.

In the case of *msps^{208}*, a viable *msps* allele containing Msps protein at 10% of the level of wild-type, one third of spindles are tripolar. However, this phenotype occurred less frequently (14%) in the *msps^{S10}* mutant (figure 4.5.B). In addition, Msps^{S10} mutant protein localised to the spindle and accentrosomal poles

with the same frequency as wild-type Msps (figure 4.5 A and C). Even when tripolar spindles occurred, Msps^{S10} was still able to localise to the poles and spindle (figure 4.5.A). Msps^{S10} protein retains sufficient function for spindle bipolarity to be retained in the majority of cases.

4.3.3.3. Embryonic mitosis in msps^{S10} embryos

To examine if problems occurred following meiosis, embryos laid by *msps^{S10}* mutants were examined for mitotic spindle defects. Eggs were collected overnight, fixed and stained for Msps, tubulin and DNA. *msps^{S10}* mutant females lay eggs but at a reduced rate compared to wild-type flies. The majority of eggs had arrested with only one or two nuclei of DNA, and only 1% of embryos went through further divisions. An example of an embryo that underwent multiple rounds of cell division is given in figure 4.6. Msps^{S10} protein can be seen localising to the spindle and centrosomes. However, a number of spindle defects are present. The spindles do not have a strong robust shape and microtubules appear to be weaker than wild-type.

The Msps^{S10} protein retains the centrosome and spindle localisation of its wild-type counterpart, both in female meiosis and mitosis (syncytial and somatic), indicating that removal of the final 79 amino acids of the protein is not essential for this localisation. Animals with this mutation are viable but female sterile, indicating that the protein maintains the functions required for mitosis to create an adult fly. Some loss of activity must have occurred, as indicated by the failure of embryos to develop. The oocytes are able to form bipolar meiosis I arrested spindle in the majority of cases indicating that problems must occur after this stage but before the syncytial mitotic division of the embryo. Therefore, Msps^{S10} is lacking a function required for either meiotic progression, pronuclear migration or the early embryonic divisions but has sufficient function for the later mitoses later in development. This allele has revealed that Msps plays a different role in embryonic development from its role in somatic mitosis.

4.4 Mutant Msps protein binding to D-TACC

Interaction between Msps and the centrosome localising protein, D-TACC, has been demonstrated by co-immunoprecipitation experiments (Cullen & Ohkura 2001; Lee *et al.* 2001). The C-terminal TACC domain of D-TACC protein appears to be responsible for Msps binding (Lee *et al.* 2001), but the D-TACC binding domain of Msps has not been defined. The availability of truncated Msps proteins provided an opportunity to examine this question.

In *C. elegans*, depletion of Zyg-9 (the Msps homologue) by RNAi causes a decline in the level of TAC-1 (D-TACC) protein. However, the level of D-TACC protein is not as severely affected in the *msps* mutants (figure 4.6). $msps^{S10}$ homozygous larvae contain the same level of D-TACC protein as wild-type flies. There appears to be a reduction in the amount of D-TACC protein in the $msps^{51}$ mutant but at least half remains.

To examine if the physical interaction between D-TACC and the mutant Msps proteins was maintained, co-immunoprecipitation experiments from larvae extracts were carried out. Soluble protein extracts were obtained from wild-type and *msps* mutant third instar larvae by homogenisation on ice, followed by centrifugation at 13000rpm to pellet cell debris. D-TACC protein was immunoprecipitated, using a polyclonal D-TACC antibody raised against the C-terminal of the protein. As a control, pre-immune serum was added to an identical protein extract.

Western blotting revealed that wild-type Msps and $Msps^{S10}$ protein are co-immunoprecipitated with the D-TACC antibody but not the pre-immune serum (figure 4.7.A). $Msps^{51}$ protein is not pulled down by the D-TACC antibody. Unfortunately, I could not confirm that D-TACC protein was pulled down specifically with the anti D-TACC antibody as I had technical problems with the D-TACC western blot.

$Msps^{S10}$ protein maintains binding, indicating the final 76 amino acids of Msps are dispensable for D-TACC binding. $Msps^{51}$, lacking the entire C-terminal domain and half of the final TOG domain can not bind D-TACC. These results

demonstrate that the C-terminal region is important for Msps binding to D-TACC protein.

4.5 Microtubule binding

The region of Msps that binds to microtubules has not been determined. In addition to localising to microtubules, Msps has previously been shown to co-pellet with microtubules in embryo extract in a microtubule binding assay. Msps^{51} protein does not localise to microtubules in mitosis in the larval neuroblasts, suggesting that removal of the C-terminal region abolishes microtubule binding. Many of my homozygous mutants die as 3rd instar larvae preventing the collection of embryo extract. Therefore, in order to examine the ability of the Msps mutant proteins to bind microtubules, I repeated the microtubule sedimentation experiment using larval extract.

In this experiment, 25-30 wild-type larvae were homogenised and incubated on ice to depolymerise microtubules. Insoluble protein was then removed by repeated centrifugation at 13,000rpm. Taxol and GTP were added to the soluble protein extract to repolymerise microtubules, and after 30 minutes at room temperature the polymerised microtubule and soluble fractions were separated by centrifugation. These protein fractions were analysed by immunoblotting against alpha-tubulin and Msps protein.

Msps protein was found to remain in the supernatant and did not associate with the microtubule pellet (figure 4.8.A). In embryo extracts the same experiment results in the majority of Msps associating with the microtubule pellet (Cullen *et al.* 1999b). Msps protein from larval extract behaves differently in this assay, therefore, it can not be used to examine the microtubule binding capacity of the mutant Msps proteins.

An alternative approach using embryo extract from heterozygous flies was used to examine microtubule binding of the Msps^{51} protein. The embryo extract will contain a mixture of full length and truncated protein. As Msps^{51} protein is smaller than wild-type, it can be recognised as a separate band on the western blot.

This experiment could not be carried out for Msps^{S10} and Msps^{146}, as the proteins are of a similar size to wild-type Msps protein.

Embryos from wild-type or *msps*^{51}/TM6C flies were collected overnight and then process as for the previous experiment. In both extracts, full length Msps protein was associated with the pellet of microtubules (figure 4.8.B). In addition, a band the size of Msps^{51} was associated with the microtubule pellet, indicating that the truncated protein has some affinity for microtubules.

Msps protein from larval extract behaves differently in the microtubule binding assay compared to protein from embryo extracts. This suggests that there may be some kind of developmental or cell cycle regulation of microtubule binding affinity. Msps^{51} protein co-sedimented with microtubules in the *in vitro* pull down assay, indicating that there is a region within the protein with an affinity for microtubules. Full microtubule binding is not present, as indicated by the failure of the protein to localise to microtubules in the cell. The truncated protein must not be totally misfolded as it has retained some microtubule binding function.

4.6 Characterisation of the new *d-tacc*^{S3} allele

Sequencing revealed that the newly isolated *d-tacc*^{S3} allele has a mutation causing a premature stop codon, removing the last 304 amino acids of the protein. Previous studies have demonstrated that the C-terminus is required for centrosome localisation and microtubule binding (Gergely *et al.* 2000), and can bind to Msps (Lee *et al.* 2001), suggesting that D-TACC^{S3} protein will be defective in these functions.

Whole wild-type and *d-tacc*^{S3} flies were homogenised in protein sample buffer, run on a 10% SDS-PAGE gel and western blotted using D-TACC-N antibody. The blot in figure 4.9.A demonstrates that no full length D-TACC protein is present in either *d-tacc*^{S3} over a deficiency known to uncover the gene, or homozygous flies (recombinants 17 and 21). Extra bands, at approximately 100kD, present in all three *d-tacc*^{S3} mutant lanes but not in the wild-type lane, corresponds

to the truncated D-TACC^{S3} protein. The truncated protein band is weaker than wild-type, suggesting the mutant protein is unstable and thus present at a low level.

The *d-tacc*^{S3} allele is viable but female sterile, laying eggs that do not hatch. Female meiosis was examined in the mutant as described previously. In *dtacc*^{stella} ooctyes one third of spindles are tripolar (Cullen & Ohkura 2001), however, 100% of spindles (35 spindles examined) in the homozygous *d-tacc*^{S3} mutant were bipolar (figure 4.9.B). Two batches of oocytes for each recombinant (recombinant 17 and 21) were examined but neither showed any tripolar phenotype.

Antibodies to the C-terminus of D-TACC have demonstrated that wild type D-TACC protein localises to the acentrosomal poles and spindle in female meiosis. Using an antibody raised against the N-terminal of D-TACC (D-TACC-N), no concentration of protein is seen in wild-type oocytes indicating that this antibody does not detect wild-type D-TACC protein in oocytes. Consequently, an antibody recognising the D-TACC^{S3} protein in female meiosis is unavailable and its localisation can not be determined.

The new dtacc^{S3} allele does not have defects in bipolar spindle formation in female meiosis, unlike the *d-tacc*^{stella} flies. The tripolar phenotype of *d-tacc*^{stella} results from failure to recruit Msps to poles (Cullen & Ohkura 2001). No tripolar spindles were observed in *d-tacc*^{S3} oocytes suggesting that Msps is still being recruited to the poles in this mutant. This would be unexpected, as in mitosis, the C-terminal TACC domain that is missing from *d-tacc*^{S3} is sufficient for centrosome localisation. However, the region of the protein responsible for D-TACC localisation to the acentrosomal poles has not been determined, so, the mutant protein may still localise to the poles and recruit Msps. Immunostaining of Msps protein localisation has not been examined in *d-tacc*^{S3} mutant oocytes and this needs to be carried out if the lack of phenotype in this mutant is to be explained.

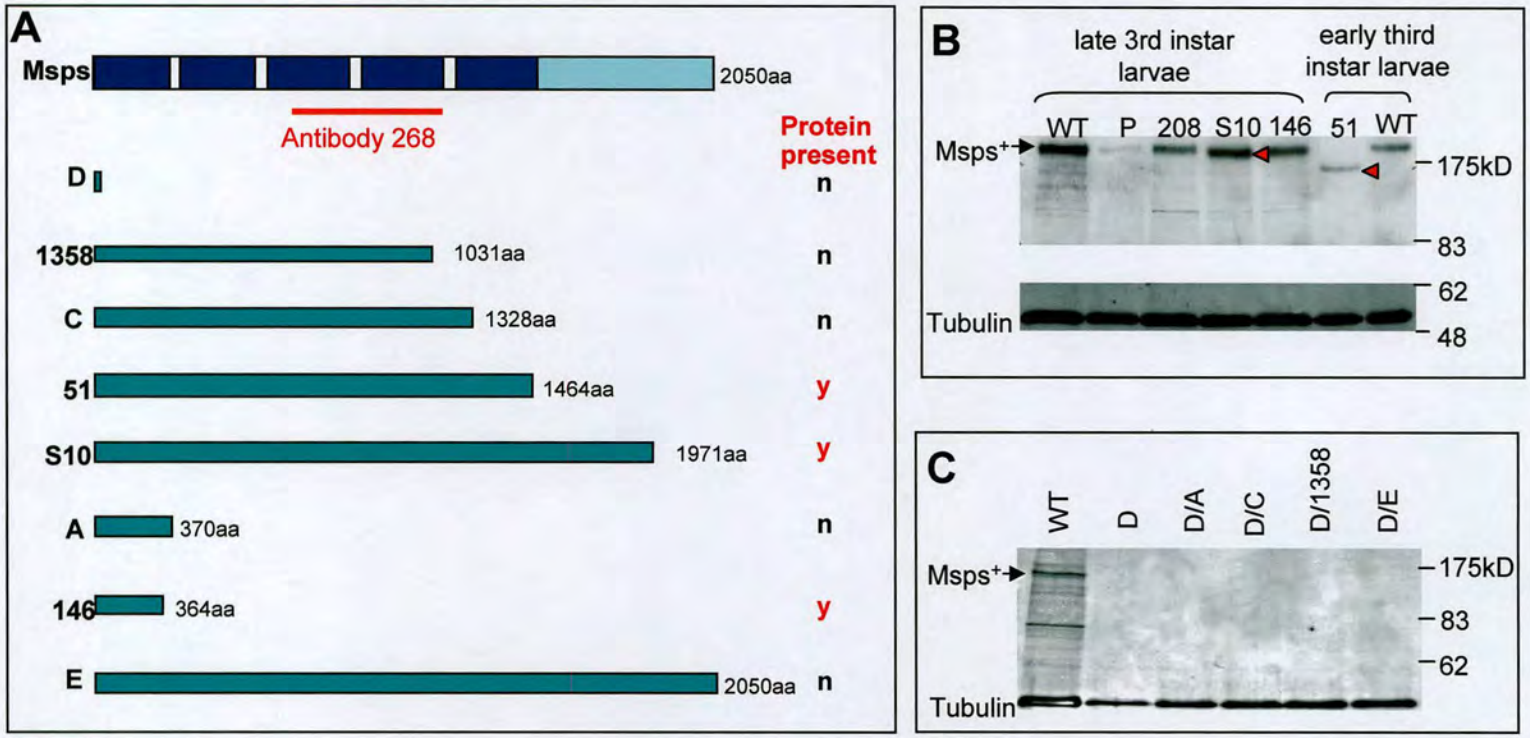

Figure 4.1 Wild-type and mutant Msps proteins in wild-type and *msps* mutant larvae.

(A) Length of predicted proteins for the 8 sequenced *msps* alleles. The region of the protein used to raise Msps antibody 268 is indicated in red. The presence or absence of mutant protein, as determined by western blotting is indicated. (B+C) Western blots using anti-Msps antibody Af 268 to detect mutant Msps proteins in either homozygous or heterozygous (*msps**/ *msps*^{D}) mutant larvae. Wild-type Msps protein is shown with an arrow. Mutant proteins of different sizes are indicated by a red arrowhead. α-tubulin was detected as a loading control.

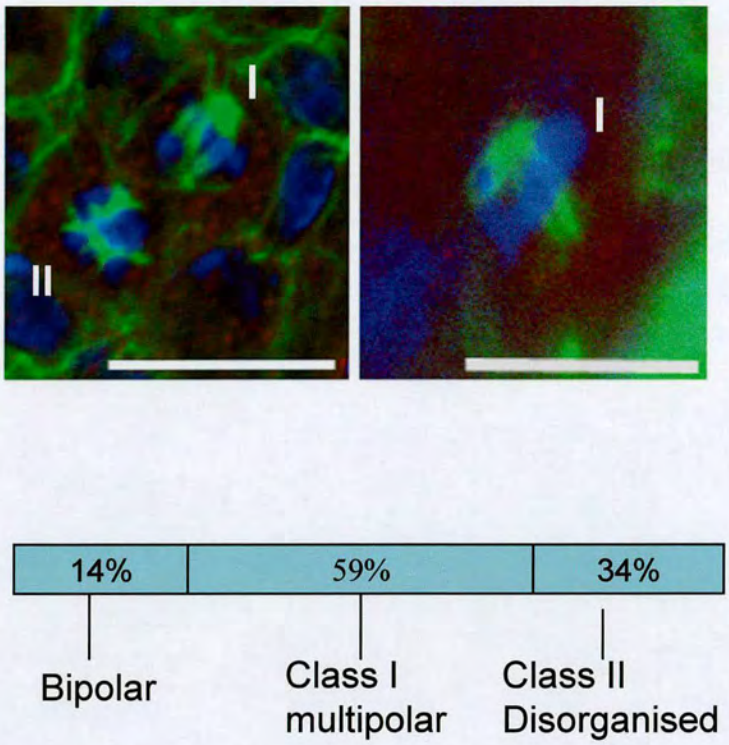

Figure 4.2 *msps*^{51} larval neuroblasts contain mitotic spindle defects.

Whole mount preparations of larval central nervous system were prepared from *msps*^{51} homozygous larvae and stained to reveal tubulin (green) and DNA (blue). (A) The two main classes of mitotic defect are shown. Class I (indicated on the figure by I): mitotic figure consisting of a bipolar spindle but with an extra smaller bipolar spindle. Class II: spindles were so disorganised a structure could not be distinguished.
(B) Frequencies of each type of spindle observed. Scale bar is 10μm.

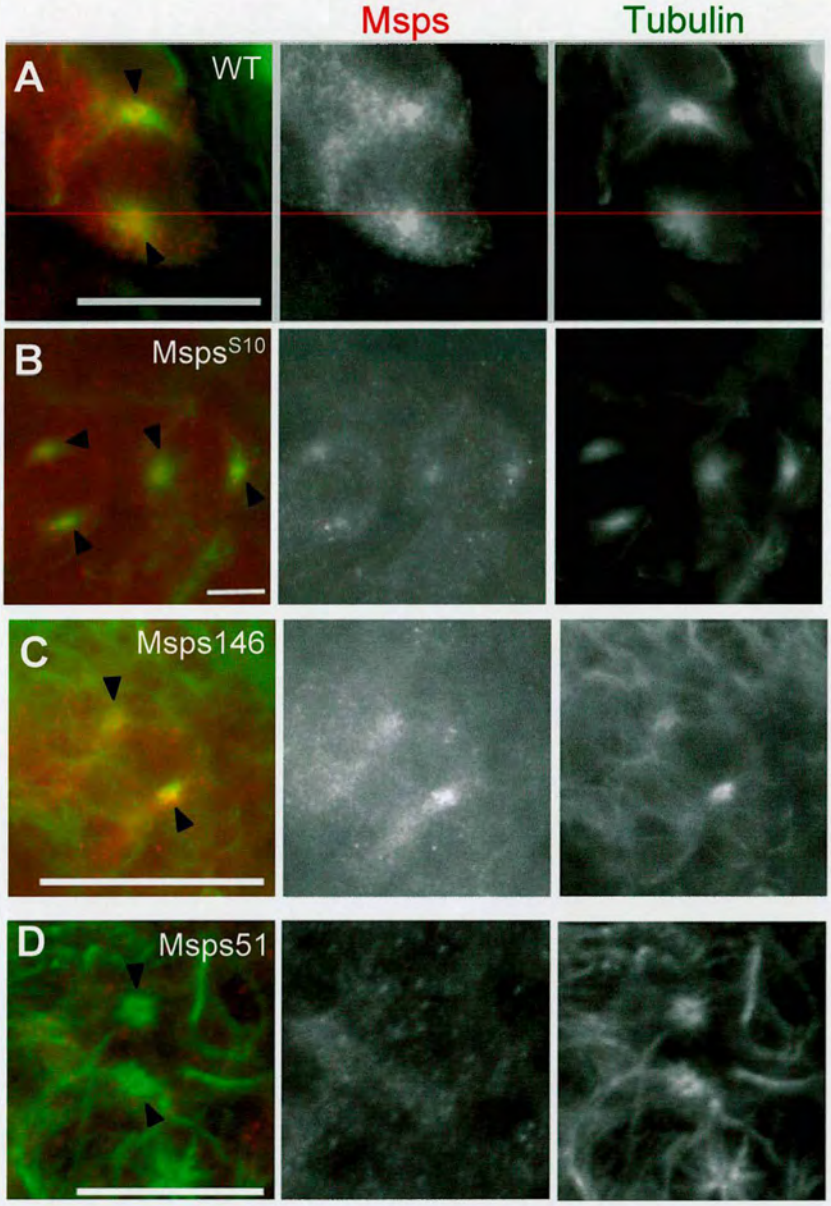

Figure 4.3. Msps51 protein does not localise to mitotic centrosomes in larval neuroblasts.

Whole mount preparations of larval central nervous system from wild-type (A), *msps^{S10}* (B), *msps^{146}* (C) and *msps^{51}* (D) homozygous larvae were stained to reveal tubulin (green), Msps (red) and DNA (blue). The black arrows point to the centrosomes. (A) Wild-type Msps protein localises strongly to the centrosomes in prometaphase, as do Msps^{S10} (B) and Msps^{146} (C) mutant proteins. Msps51 protein (D) remains cytoplasmic and does not localise to the centrosomes.
Scale bar is 10μm.

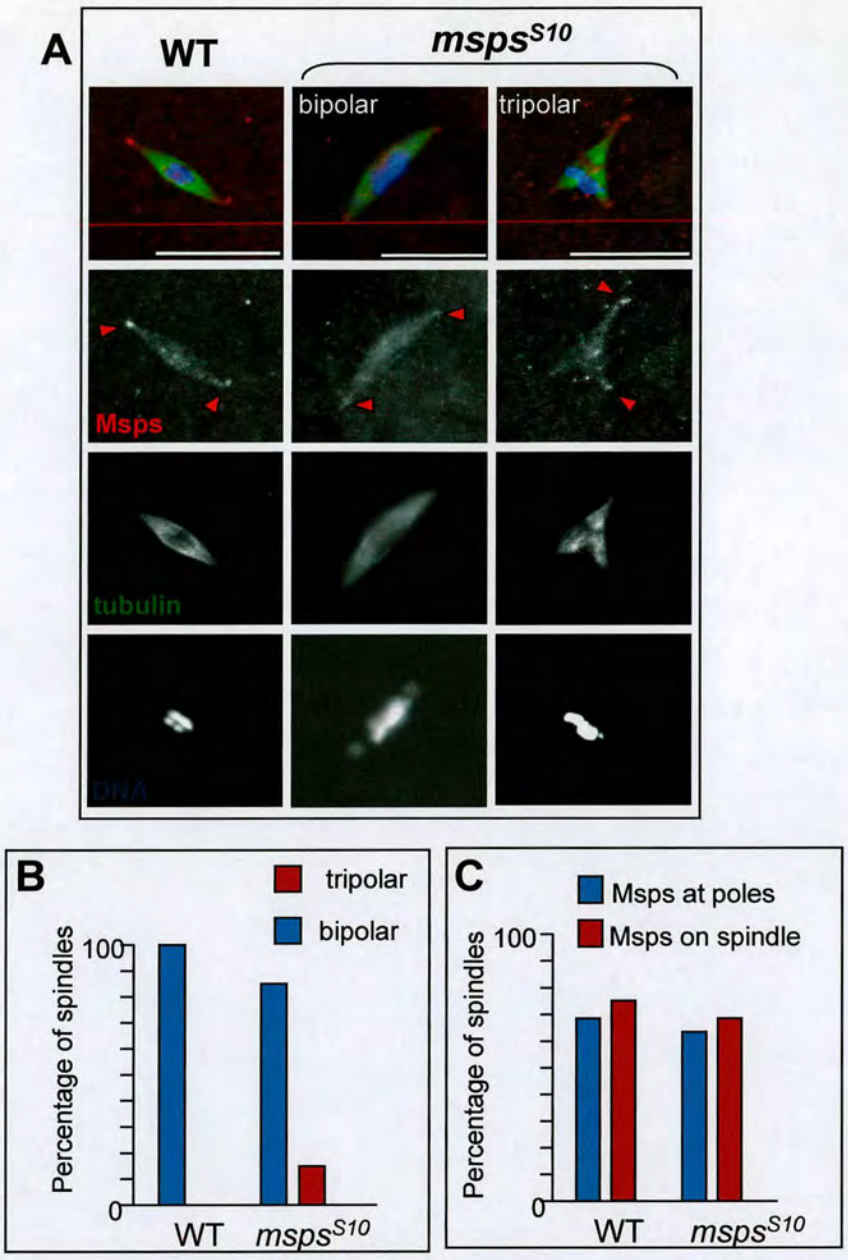

Figure 4.4. Msps^{S10} female meiotic phenotype and protein localisation.

(A) Wild-type Msps and Msps^{S10} mutant protein localise to the poles and microtubules of the female meiotic spindle. Both bipolar and tripolar spindles were seen in *msps^{S10}* mutant oocytes. Msps^{S10} protein will still localise to the poles of tripolar spindles. Pole localisation is marked with red arrows. Scale bar = 10μm. (B) Frequencies of spindles that were bipolar and tripolar in wild-type and *msps^{S10}* mutant oocytes. (C) Percentage of poles and spindles at which wild-type Msps and Msps^{S10} localises. 30 spindles of each genotype were examined.

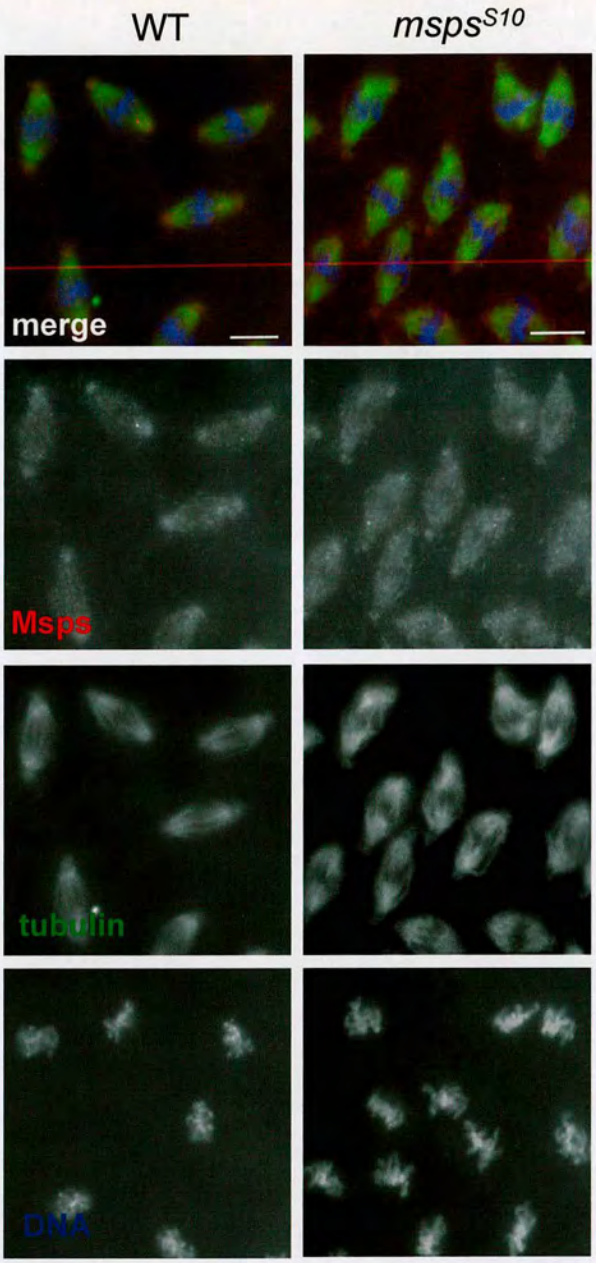

Figure 4.5. Msps^{S10} protein localises to spindle microtubules and centrosomes in embryonic mitosis.

Embryos were stained for alpha-tubulin (green), Msps (red) and DNA (blue). Wild-type Msps protein localises to the centrosomes and microtubules of the spindle in embryonic mitosis. In *msps^{S10}* mutant embryos, the mutant Msps^{S10} protein also localises to the centrosomes and spindle, however, mitotic spindles appear weaker than wild-type and do not maintain a symmetrical robust structure. Scale bar is 10μm.

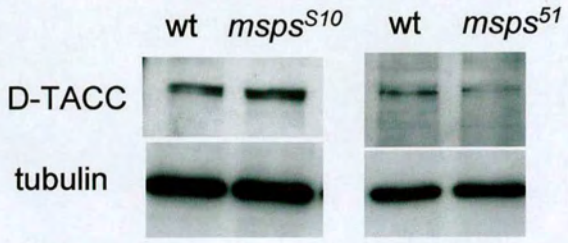

Figure 4.6 D-TACC protein levels are not severely affected in *msps* mutants.
Western blot of *msps* mutant homozygous larvae to detect D-TACC protein levels. D-TACC protein is present in both of the *msps* mutants. The level of D-TACC appears to be slightly reduced in *msps*^{51}. Alpha tubulin was detected as a loading and blotting control.

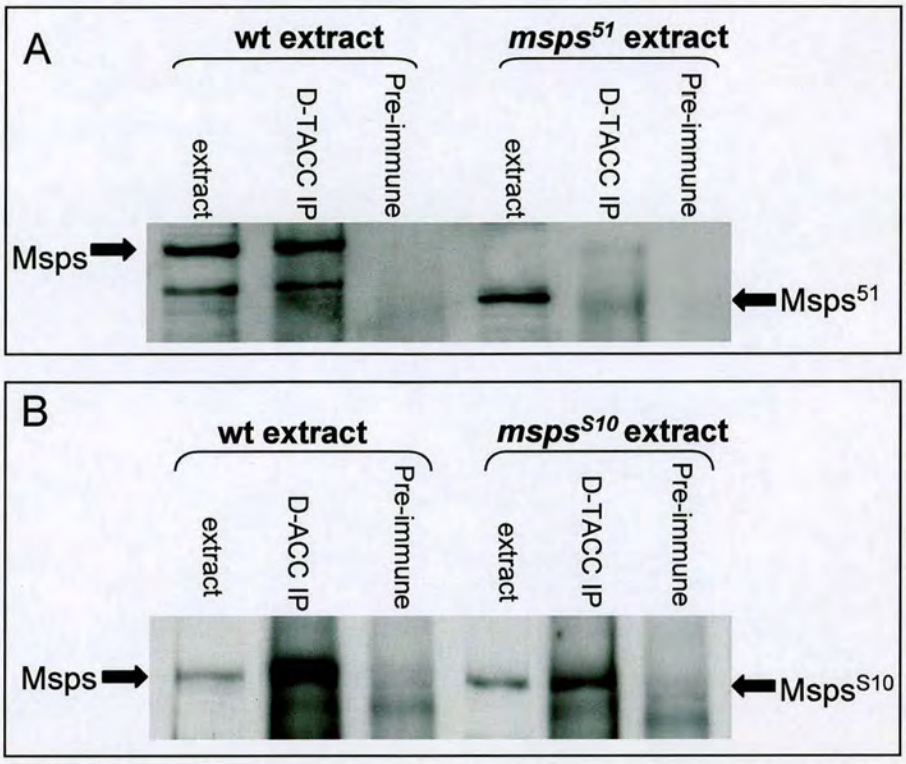

Figure 4.7 Truncation of the C-terminal 588 amino acids of Msps abolishes D-TACC binding.

D-TACC protein was pulled down using an anti-D-TACC antibody (D-TACC–C) from larval extracts. Pre-immune serum was added to another extract to act as a control. Western blots were then carried out to detect if wild-type and mutant Msps protein were co-immunoprecipitated.

(A) Western blot using Msps antibody against the middle of the protein (Af268) to detect $Msps^{51}$ co-immunoprecipitation. Msps51 is not pulled down with the D-TACC antibody or with the control pre-immune serum.

(B) Western blot using Msps antibody against the C-terminus of the protein (Af 264) to detect $Msps^{S10}$ co-immunoprecipitation. $Msps^{S10}$ is pulled down with the D-TACC antibody but not with the pre-immune serum.

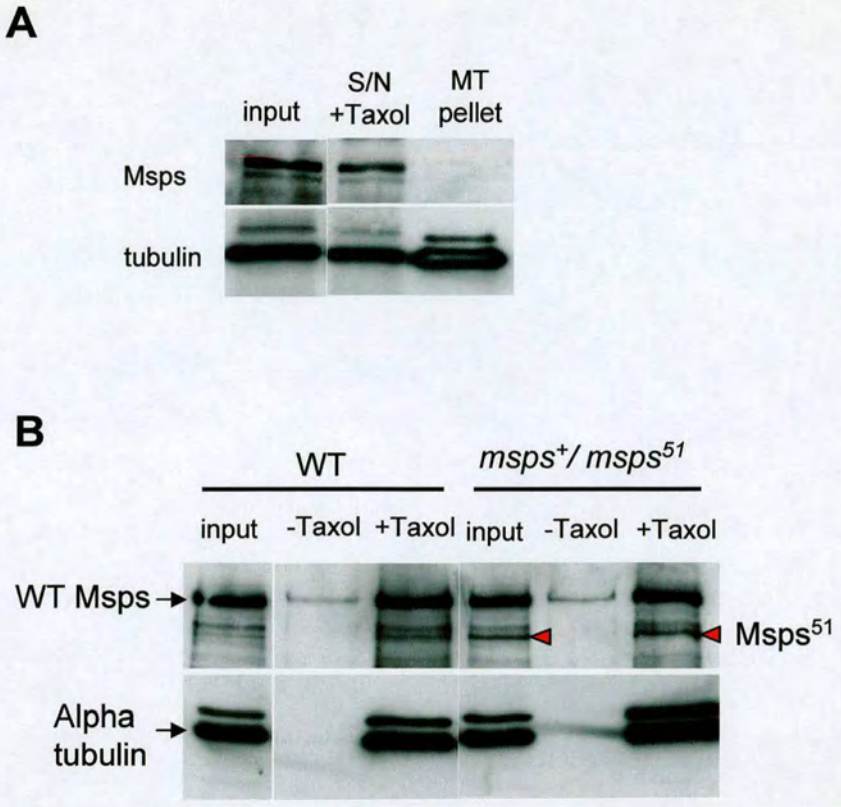

Figure 4.8 Msps^{51} protein is pulled down with tubulin in a microtubule binding assay.

(A) Msps does not pellet with microtubules from larval extract. Microtubules were polymerised in larval protein extracts by the addition of taxol. Microtubules were pelleted by centrifugation. Supernatant (S/N) and pellet were examined for the presence of Msps by western blotting. The pellet contains tubulin, as indicated by the strong band of alpha-tubulin on the western blot. Msps protein is not co-pelleted with the tubulin and remains in the supernatant.

(B) Embryos from wild-type or *msps^{51}*/TM6C flies were collected overnight. A microtubule binding assay was carried out, as above, but with embryo extract rather than larval extract. Full length Msps protein is pulled down with the microtubule pellet. Msps51 protein (red arrow) is also pulled down.

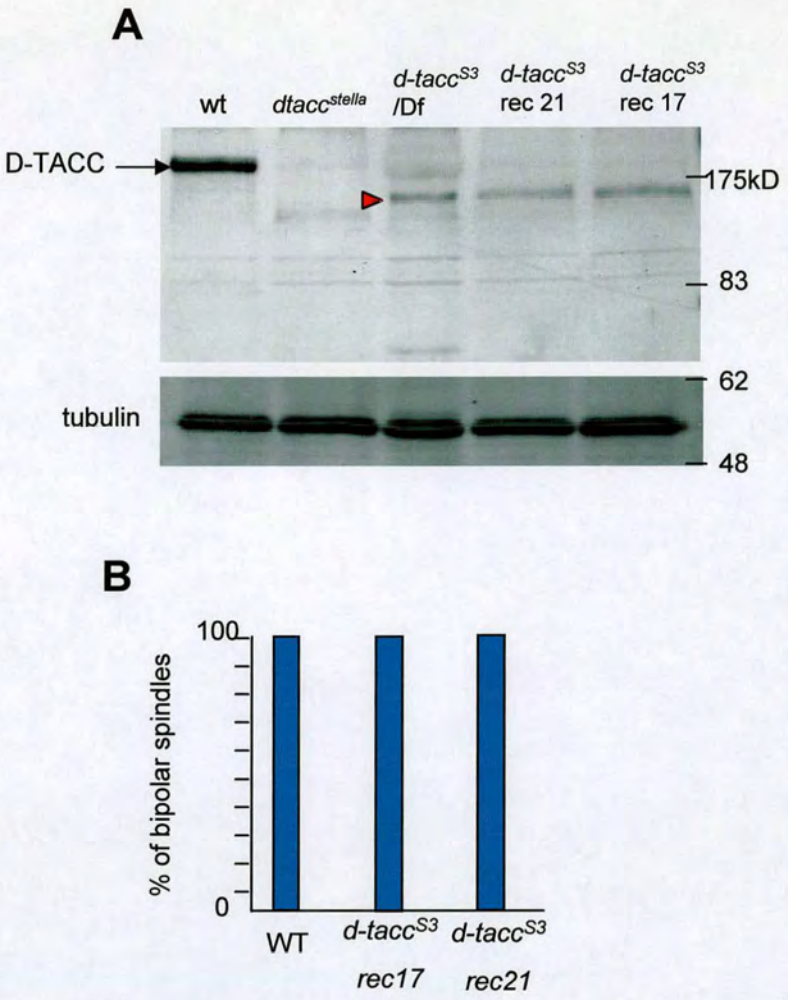

Figure 4.9. Analysis of the *dtacc^{S3} allele*

(A) *d-tacc^{S3}* flies contain a truncated mutant protein. D-TACC protein from adult flies was detected using an antibody against the N-terminus of the protein (Af D-TACC-N). Protein samples were prepared from wild-type, *d-tacc^{S3}* homozygotes and *d-tacc^{S3}* / Deficiency flies. Wild-type D-TACC protein is labelled with an arrow. A smaller band in the *d-tacc^{S3}* mutant flies is indicated by an arrowhead. Tubulin was detected as a loading control. (B) *d-tacc^{S3}* oocytes contain bipolar meiotic spindles. Meiotic spindles in oocytes from wild-type, and homozygous *d-tacc^{S3}* flies were examined by immunostaining with alpha-tubulin. All spindles examined were bipolar (>25 spindles examined for each genotype).

Chapter 5 The role of Msps in interphase microtubule regulation

5.1 Background

To date, the majority of studies examining Dis1/TOG function have focused on microtubule regulation in mitosis, with interphase microtubule regulation receiving little attention. Even so, in plants, *Dictyostelium* and yeast, interphase microtubule defects have been displayed following disruption of Dis1/TOG protein function (Whittington *et al.*, 2001; Nakaseko *et al.*, 2001; Kosco *et al.*, 2001; Graf *et al.*, 2003). A role for Msps function in interphase microtubule regulation has recently been uncovered with the discovery of microtubule disorganisation in *msps* mutant oocytes effecting the localisation of bicoid RNA (Moon and Hazelrigg, 2004). In this chapter, I describe a detailed analysis of Msps function interphase microtubule regulation, including the involvement of known Msps interactors.

In addition, to investigating the role of Msps in interphase microtubule organisation, I analysed the effect of the protein on microtubule dynamics. There has been recent controversy regarding the role of the Dis1/TOG proteins in microtubule regulation, with both microtubule stabilising and destabilising activity demonstrated *in vitro* (Popov *et al.*, 2001; Shirasu-Hiza *et al.*, 2003; van Breugel *et al.*, 2003; Tournebize *et al.*, 2000). In animal cells, the effect of these proteins in regulating microtubule dynamic has not been examined. Therefore, to shed light on the role of the Dis1/TOG proteins *in vivo*, I analysed the effect of Msps depletion on interphase microtubule dynamics.

5.2 Msps localisation in *Drosophila* S2 culture cells

Drosophila S2 cells provide a unique opportunity to study the interphase microtubule network. These cells are spherical in culture, but when grown on coverslips coated with concanavilin A (con A), the cell spreads producing a flat disc with a raised centre containing the nucleus and organelles. As the cell spreads, the interphase microtubules extend outwards to the cell periphery, enabling visualisation of individual microtubules in the flattened region of the cell. Msps distribution was examined in these cells, as microtubule localisation could point towards a role for Msps in microtubule regulation.

Exponentially growing S2 cells were cultured on con A coated coverslips, for at least two hours, to allow them to adhere and form a spread morphology. Cells were fixed with a mixture of methanol and paraformaldehyde, a mixture that found to preserve microtubule structure well (Rogers *et al.*, 2002). Protein localisation was then examined by immunostaining using antibodies against Msps protein and alpha-tubulin.

During mitosis Msps concentrated on the centrosomes and spindle microtubules (figure. 5.1.A) as seen in *Drosophila* embryos. During interphase, a high level of Msps staining is seen in the central region of the cell where microtubule density is high (figure 5.1.B-D). Punctate staining was also seen along individual microtubules that extend out toward the cell cortex (figure. 5.1.D). Additionally, Msps staining can be seen strongly on the plus ends of microtubules at the edge of the cell (figure 5.1.D and E).

Msps protein localises to microtubules, both in mitosis and interphase, in *Drosophila* S2 culture cells, indicating that it may play an important role in microtubule organisation in these cells.

5.3 RNAi depletion of Msps protein from S2 cells

Studies of *msps* mutant flies have demonstrated the importance of Msps in the formation of bipolar spindles in both mitosis and meiosis (Cullen and Ohkura, 2001; Cullen *et al.*, 1999). A role for Msps in interphase microtubule regulation has only recently been described (Moon and Hazelrigg, 2004). The clear microtubule network that can be visualised in S2 cells, along with the robust success of RNAi in these cells, provided an opportunity to study the *in vivo* role of Msps on interphase microtubule regulation.

Msps protein was depleted from S2 cells using RNA interference (RNAi) methods. Double stranded RNA (dsRNA) corresponding to a 600 bp sequence of the *msps* gene, covering the start codon, was created by *in vitro* translation. A dsRNA, corresponding to the bacterial *beta-lactamase* gene, not found in *Drosophila,* was made as a control, to account for effects resulting from dsRNA addition to the cells. Control or Msps dsRNA were mixed with serum starved S2 cells, which are known to take up the dsRNA effectively. After 1 hour, serum containing media was added to the cells and the cells incubated at 27°C. Protein samples were taken every 24 hrs for 5 days to monitor protein depletion by western blotting.

A change in the level of Msps protein can be seen at 24hrs, and by 92 hours most of the protein has disappeared (figure 5.2.A). Dilutions of control cells were run on a blot along side cells treated with Msps dsRNA (figure. 5.2.B) to estimate the degree of depletion. After 48 hours, more than 70% of the protein has been depleted, whilst at 120 hours greater than 95% has been depleted. No change in Msps protein level was detected in the cells treated with the control dsRNA. Immunostaining with Msps antibody confirmed that Msps protein could not be detected in Msps RNAi cells.

Studies in *C. elegans* (Le Bot *et al.*, 2003; Bellanger and Gonczy, 2003; Srayko *et al.*, 2003) found that depletion of the Msps homologue, Zyg-9, by RNAi resulted in a reduction of TAC-1 (the D-TACC homologue) protein. Reminiscent of the *C. elegans* studies, western blotting revealed that the level of D-TACC protein was

reduced in *msps* RNAi cells (figure 5.2.A). A time lag occurs before the level of D-TACC decreases, and at 92 hours post dsRNA addition, D-TACC protein is still detected.

To conclude, Msps protein can be successfully depleted from *Drosophila* S2 cells using RNAi methods. The level of D-TACC protein is reduced in Msps depleted cells indicating that without its binding partner, D-TACC is less stable.

5.4 Mitotic phenotype in Msps depleted cells

A mitotic phenotype has been described in larval neuroblasts in *msps* mutants and also in human culture cells following ch-TOG RNAi (Cullen *et al.*, 1999; Gergely *et al.*, 2003; Holmfeldt *et al.*, 2004; Cassimeris and Morabito, 2004). To see if this was the case for cells depleted of Msps by RNAi, cells were assessed for spindle abnormalities.

Microtubule organisation was examined in Msps depleted cells by immunostaining with antibodies against alpha-tubulin, at 3 time points, during the RNAi depletion. In mitotic cells, abnormal spindles were observed and classified into four categories (figure.5.3.A-D). The first class of spindles, seen at early time points during depletion, were bipolar spindles but with poles that appeared to be broader than in wild-type spindles (figure. 5.3.A). The second class were bipolar spindles with extra mini-spindles attached to a shared pole (figure 5.3.B). Chromosomes are aligned at the metaphase plate and associated with a bipolar spindle, but a few chromosomes separate and are associated with a smaller bipolar spindle. Another class was found to be made up of many small spindles, but with a dominant pole that is shared by all (figure 5.3.C). Finally, the fourth category found were monopolar spindles, a single pole and no small spindles visible (figure 5.3.D). Corresponding to the appearance of spindle abnormalities, an increase in mitotic index from 3.6% in control cells to 8%, in Msps RNAi cells was seen 120 hours after dsRNA addition (figure. 5.3.E).

Spindle phenotypes were scored in control and Msps depleted cells at 4 time points (0, 48, 72, 120 hours) during deletion (figure. 5.4). Early in the time course, broad bipolar spindles are common, peaking at approximately 25%, but this phenotype disappears at the end of the experiment. The number of multipolar spindles rises and becomes the dominant phenotype (77%) by 120 hours. The number of monopolar spindle also rises as Msps is depleted, but remains at a lower level than the multipolar phenotype.

As in the fly, Msps protein is essential for bipolar spindle formation. The multipolar spindles found in the culture cells are similar to those seen in *msps* mutant neuroblast (section 4.3.1 and Cullen *et al.*, 1999) Time course analysis, suggests a gradual decline in pole stability as Msps protein is depleted. With partial depletion (48hours), the first phenotype seen is the presence of broad bipolar spindles. This is followed by increasing numbers of multi-polar and mono-polar spindles, as more of the protein is depleted. Such phenotypes could be explained by failure of the minus ends to remain tightly associated with the centrosomes. If the minus ends of microtubules detach from the centrosomes, but remain associated with the chromosomes, they could be bundled into small poles to form the mini-spindles. Alternatively, microtubule plus end stability may be required to maintain spindle pole integrity. The mechanism by which the multipolar spindles form has yet to be fully elucidated

5.5 Interphase microtubule defects in Msps depleted cells

The role of Msps in interphase has not been addressed in the fly. The spread morphology of S2 cells grown on con A, provides a good opportunity to investigate the role of Msps in interphase microtubule regulation. Cells treated with *msps* or control dsRNA were grown on con A coverslips and microtubule organisation

examined by immunostaining with alpha-tubulin. To ensure that Msps had been depleted, cells were also stained with Msps antibody.

In control cells, a mass of microtubules resides in the centre of the cell, but in addition, microtubules extend towards the cell periphery in the thin layer of membrane that spreads out following plating on con A (figure.5.5.A 'extended'). Msps depletion dramatically altered this microtubule organisation. Following Msps depletion, cells appeared in which the microtubules were only in the centre of the cell and did not have microtubules extending out to the periphery (figure. 5.5.A 'compact'). In addition, thick bundles of microtubules, also predominantly in the centre of the cell were seen (figure. 5.5.A 'bundled').

A time course experiment was carried out to determine when these microtubule phenotypes appeared during depletion (figure 5.5.B). After 72hrs depletion more than half of cells (57%) had compact microtubules in the centre of the cell. Additionally, at 72hours, in 14% of cells, microtubules formed thick bundles. At the final time point of 120 hours, microtubule bundling was more common and found in 34% of cells.

The failure of microtubules to extend was not due to the cells being unable to spread out on the con A coated surface. Immunofluorescence of tubulin and phase contrast microscopy was used to determine the ability of the cell membrane and microtubules to spread in control and Msps depleted cells. Cells that were able to form a flat membrane extension outside of the raised central region were counted as spread cells. No difference in the ability of cells to attach and flatten on the con A coated surface were detected between the control and Msps depleted cells (94% versus 90%). Furthermore, this result indicates that Msps microtubule localisation is not required for cells to attach and spread on the con A surface.

In my typical protocol, cells were fixed after culturing them for 2 hours on a con A coated surface. Therefore, it is possible that Msps depletion is affecting the speed of microtubule rearrangement and extension towards the cell periphery after cell membrane spreading. To exclude this possibility, S2 cells were continuously cultured

on a con A coated surface from the start of Msps depletion. The same microtubule defects were observed in cells spread from the beginning of the experiment, as those seen with 2 hours' spreading (figure 5.6). Therefore, Msps is important for normal microtubule organisation of the cell and not just the rearrangement seen when the cell spreads.

5.6 Cell shape and actin localisation in Msps depleted cells

The dramatic change of microtubule organisation in *msps* RNAi cells could have secondary effects on the cell. To investigate potential effects on cell structure, actin distribution in Msps depleted cells was examined. Cells were fixed with 4 % paraformaldehyde and stained with Texas red X-phalloidin, a probe that selectively binds filamentous actin. In wild-type cells, actin has a distinct localisation pattern; a dense peripheral network, and a central zone of lower actin density composed of filaments. Msps depleted cells showed the same pattern of staining as wild-type cells (figure 5.7). The ability of the cells to spread and produce a normal actin network is unaffected by the microtubule rearrangement in Msps depleted cells.

5.7 Co-depletion of KinI microtubule destabilisers with Msps

Vertebrate homologues of Msps are known to antagonise the activity of a catastrophe factor, MCAK/XKCM1, which belongs to the KinI family of kinesin-like proteins (Tournebize *et al.*, 2000; Desai *et al.*, 1999). Three members of the KinI family have been identified in *Drosophila*, known as Klp10A (Kinesin like protein), Klp59C and Klp59D (Rogers *et al.*, 2004). To test if these KinI kinesins mediate the effects of Msps depletion on interphase microtubule organisation, RNAi was carried out on the three homologues in combination with Msps.

When the three KinI proteins were depleted singly, they produced no obvious interphase microtubule phenotype. Although reductions in protein levels were not checked by western blotting, RNAi in S2 cells is very robust, and routinely over 90% of the target protein is depleted (Goshima and Vale, 2003; Rogers *et al.*, 2003). Additionally, the reported mitotic phenotypes of Klp10A and Klp59C depletion (Rogers *et al.*, 2004) were observed, indicating that RNAi treatment was successful in this study. It was reported that successful depletion of Klp59D produces no mitotic phenotype and this result was confirmed here. The possibility that Klp59D was not depleted in this study can not be excluded but this is unlikely as Klp59D has been successfully depleted in another study, showing it to be amenable to RNAi treatment.

Individual depletion of each of the three KinI proteins in combination with Msps did not rescue the microtubule phenotype (figure 5.8). Klp10A co-depletion with Msps, in fact, increased in severity of the microtubule phenotype, bundling rising from 24% in cells singly depleted of Msps to 58% in cells doubly depleted of Msps and Klp10A.

To exclude the possibility that there is some functional redundancy between the KinI proteins, simultaneous depletion of all three proteins with Msps was carried out. S2 cells are able to respond efficiently to such tetra duple RNAi experiments (Goshima and Vale, 2003). Depletion of all three KinI proteins did not rescue the interphase microtubule defects resulting from Msps depletion, signifying that the defect is caused by a mechanism independent of KinI proteins (figure 5.8). The triple KinI depletion with Msps, gave the same phenotype as the Klp10A and Msps co-depletion. Therefore, the increased microtubule bundling in the triple KinI depletion is likely due to the depletion of Klp10A; the depletion of the two other KinI proteins having no additional affects.

In conclusion, Msps activity does not antagonise the activity of the KinI proteins in regulating interphase microtubule organisation. In fact, one of the KinI proteins, Klp10A, appears to enhance the microtubule phenotype produced by Msps depletion.

5.8 D-TACC depletion does not result in interphase microtubule defects

Msps localisation to the spindle poles in female meiosis and early embryonic mitosis is dependent upon D-TACC (Cullen and Ohkura, 2001; Lee *et al.*, 2001). The role of D-TACC in interphase, including its role in Msps localisation to interphase microtubules, was examined by depletion of the protein from S2 cells.

D-TACC was depleted using dsRNAi and levels of D-TACC and Msps monitored by western blotting (figure. 5.9). D-TACC depletion began at 24 hours and was well depleted by 120 hours. The amount of Msps protein was unaffected by D-TACC depletion. In the blot, Msps levels are lower at 0 and 24 hours but this is due to under loading of protein samples, as shown by the tubulin loading control.

Microtubule organisation was examined in D-TACC depleted cells by immunostaining with antibodies against alpha-tubulin. No mitotic defects were seen in D-TACC depleted cells and mitotic index was unaffected (figure 5.10.A and C). D-TACC appears to be dispensable for mitosis in S2 cells. Furthermore, Msps localises to the spindle and centrosomes independently from D-TACC in these cells (figure 5.10.B).

No interphase microtubule organisation defects were observed in the D-TACC depleted cells (figure 5.11.B). Additionally, Msps protein was able to localise to interphase microtubules in D-TACC depleted cells (figure. 5.11. C and D). These results indicate that Msps protein function in interphase microtubule organisation is independent of D-TACC.

Whilst both Msps and D-TACC localise to interphase microtubules, Msps does not require D-TACC for this localisation. Furthermore, D-TACC has no obvious role in regulating microtubule organisation in S2 cells.

5.9 Expression of the N-terminal region of Msps partially rescues Msps depletion

Whilst the C-terminal region of Msps is involved in binding to D-TACC (section 4.4) the role of the N-terminal region of the protein has not been defined. The N-terminal region contains well defined structural motifs, consisting of 5 repeated TOG domains, each containing 4-5 HEAT repeats. The N-terminal half of Msps, containing 4 of the TOG repeats, was expressed in S2 cells, to determine if the fragment can rescue the defects of Msps depletion. The same fragment but with a point mutation in a conserved residue was also expressed.

5.9.1 Construction of Msps C-terminal deletion construct and mutation at a conserved residue

A plasmid was constructed to express the N-terminal (1133 amino acids) of Msps protein (figure 5.12). The DNA encoding the C-terminal 917 amino acids was cut out, by restriction digestion with KpnI, from the full length genomic sequence and the plasmid relegated, leaving the N-terminal of *msps* under its endogenous promoter (*mspsN*).

A conserved amino acid was mutated in *mspsN*, using site directed mutagenesis, producing a point mutation at amino acid 190 (MspsN-E190K) (figure 5.13.A). An equivalent mutation in plant *mor1* results in a temperature sensitive allele, producing cortical microtubule defects at the restrictive temperature. The mutated residue and the surrounding HEAT repeat are highly conserved between species (figure 5.13.B), but the importance of the residue in the fly protein is unknown. By replicating this mutation I hoped to affect MspsN function.

3.9.2 Expression of Msps N-terminal constructs in Msps depleted cells.

The Msps N-terminal domain protein (MspsN and MspsN-E190K) were expressed in cells depleted of full length Msps protein. To avoid dsRNA destroying the RNA encoding the N-terminal fragment, dsRNA corresponding to the C-terminal region was used for depletion of endogenous Msps protein.

Cells were treated with dsRNA against the C-terminal region of *msps*, and incubated for 48hours, before the cells were transfected with plasmids expressing either MspsN or MspsN-E190K. More dsRNA was also added at this point to ensure endogenous Msps protein was well depleted. The cells were left for a further 48hours. Samples were taken to monitor protein depletion and expression by western blotting (figure 5.14.A). Full length Msps was successfully depleted and the N-terminal fragments expressed.

To examine interphase microtubules, cells were plated onto con A coverslips, fixed and immunostained using antibodies against alpha-tubulin. To confirm that full length Msps is depleted, cells were stained using a C-terminal Msps antibody (Af264) to recognise full length protein. No concentrations of full length Msps were found in the dsRNA treated cells. An N-terminal Msps antibody that will recognise the expressed fragment was used to stain cells (figure 5.15). The MspsN fragment was found to localise through out the cytoplasm but with some granular spots, possibly aggregates of protein caused by overexpression (figure 5.15.A). Consistent with results from the *Xenopus* homologue, this fragment does not localise to the spindle poles. Fragment MspN-E190K was also localised throughout the cytoplasm (figure 5.15.B).

Microtubule phenotype was scored in control and Msps RNAi cells with and without MspsN and MspsN-E190K expression. Of the transfected cells, only those staining positive with the Msps Af268 antibody were counted to ensure that only cells expressing the truncated proteins were included. Expression of the N-terminal

fragments in control cells did not disrupt microtubule organisation (figure 5.14.B). Expression of MspsN in Msps RNAi cells reduced the percentage of cells with abnormal microtubule organisation compared to untransfected cells. Expression of the MspsN protein reduced cells with microtubule bundling from 38 % to 14% in Msps RNAi cells (figure 5.15.B). The mutation in MspsN-E190K abolished the ability of the protein to rescue the defects of Msps depletion.

These results indicate that the N-terminal fragment, which lacks the centrosome localisation domain, can partially, rescue the defects caused by Msps depletion. This domain contains an activity that is important for Msps regulation of interphase microtubules. Mutation of a residue in a conserved HEAT repeat removed this activity.

5.10 Microtubule dynamics in Msps depleted cells

To understand the mechanisms behind the defects in interphase microtubule organisation seen in Msps depleted cells, microtubule dynamics in live cells were observed. For real time analysis of microtubule dynamics, a cell line stably expressing GFP-tubulin was used. Depletion of Msps in this cell line produced microtubule defects similar to those observed in S2 cells, with very compact or bundled microtubules that do not extend out to the cell periphery. Under such conditions, individual microtubules can not be observed to make measurements of dynamics. Therefore, cells were observed 48 hours after dsRNA addition, at which time microtubule organisation is only mildly effected. Msps protein is known to be at least 70% depleted after 48 hours (figure 5.2).

The behaviour of microtubules in control and Msps partially depleted cells were followed by live-cell fluorescent microscopy. Cells were grown on a con A coated surface, and images taken every 5 seconds for a total of 5 minutes. Individual microtubules were tracked to measure dynamics. Microtubules that could be clearly followed for at least 3 minutes were tracked and life history plots drawn.

Microtubules in untreated control cells exhibited dynamic instability, alternating between growth and shrinkages phases (figure 5.16.A and C). Microtubules behave differently at the cortex compared to microtubules away from the edge (figure 5.16.A). Internal microtubules tend to grow fairly continuously with few catastrophes (0.22 events per minute). When microtubules reach the cortex the time they spend in a paused state rises from 29.7% internally to 48.4% at the cortex (figure 5.17.A) and catastrophe frequency more than doubles (0.52 events per minute).

Microtubule behaviour is very different in Msps depleted cells. The most significant change is the increase in the amount of time spent pausing (figure 5.16.B) For internal microtubules in control cells, on average, 29.7% of their time is spend pausing, whilst internal microtubules in Msps depleted cells are paused for 71.4 % of their lives (figure 5.17.A). Microtubules that reach the cortex also spend more time in a paused state than control cells (76.1% vs 48.4%).

Life history plots of microtubules from Msps depleted cells show that long periods of pause are interspersed with short grow periods or shrinkage events (figure 5.16.D). Unlike control cells, it was rare to see consistent periods of growth followed by shrinkage. The speed of growth in Msps depleted cells (2.3μm/min) is not significantly different from control cells (2.1μm/min) but the shrinkage rate is reduced (10.5μm/min to 4.3μm/min) (figure 5.17.A).

Partial depletion of Msps results in a shift from a state of growth and shrinkage to pause. To analyse this process further, transition frequencies between the three states of growth, pause and shrinkage were calculated. For internal microtubules, a significant increase in the number of transitions from growth to pause, and a significant decrease in transitions from pause to growth were seen (figure 5.17.B). Overall this will result in a shift towards the paused state from a growth state. Differences between other transition frequencies were not proved to be statistically different.

Despite the significant amount of Msps that still remains, a dramatic impact on microtubule dynamics is seen. Msps depletion shifts microtubules from a state of dynamic instability to a static paused state.

5.11 Microtubule bundles induced by Msps depletion are very stable

Individual microtubule dynamics could not be observed in cells well depleted of Msps. Therefore, two alternative strategies, use of a depolymerising drug and FRAP (fluorescent recovery after photo bleaching) analysis, were employed to gain insights into microtubule dynamics in cells with over 90 % Msps depletion.

Firstly, I compared the stability of microtubules between control and Msps depleted cells by monitoring resistance to the microtubule depolymerising drug colchicine. In control cells nearly all microtubules were depolymerised when exposed to 200μM of colchicine for 16 hours (figure 5.18). However, in Msps depleted cells 60% of cells still contained some residual microtubules (figure 5.18.B). This result indicates that microtubules are stable in Msps depleted cells in terms of resistance to a microtubule destabilising drug.

A second approach for assaying microtubule dynamics was to examine turnover of tubulin dimers in microtubule bundles by FRAP. The GFP-tubulin expressing line was used again in these experiments. An area of microtubules were bleached in the cell and the recovery followed by time lapse photography (figure.5.19.A). The percentage recovery after 5 minutes was measured for control and *msps* dsRNA treated cells. After 5 minutes, control cells had recovered, on average, to 57% of the prebleach level, whilst after the same time period, Msps depleted cells had recovered, on average, to 23% of the prebleach level (figure 5.19.B.). Msps microtubule bundles have a lower turnover of tubulin dimmers, indicating an attenuation of microtubule dynamics.

These results from drug and FRAP experiments are consistent with real time observations of individual microtubule dynamics which indicate that microtubules are stabilised by depletion of Msps.

5.12 Defective organisation of interphase microtubules in blood cells from *msps* mutant larvae

This study demonstrates that Msps protein is a major regulator of interphase microtubule organisation in S2 culture cells. To confirm the role of Msps in interphase microtubule regulation, I looked for evidence of microtubule defects in *msps* mutant flies.

Haemocytes were isolated from wild-type and *msps* mutant third instar larvae, and incubated than on a con A coated surface. The blood cells attached and spread out producing similar cell morphology to that see with the S2 cells. Microtubules in these cells were examined by immunostaining. In wild type cells, microtubule distribution was similar to that of S2 cells, producing an extended microtubule network reaching the cortex (figure.5.20.A 'left'). Blood cells were obtained from a number of *msps* mutants. The strong mutants, $msps^{D}$ and $msps^{51}$, produced very few blood cells (perhaps due to defects in mitosis) so were not analysed. However, $msps^{P}$ and $msps^{146}$ were found to produce enough cells to investigate the microtubule phenotype. Both *msps* mutants showed a reduction in the number of cells with an extended microtubule array, and a rise in the number of cells with a compact circle of microtubule in the centre of the cell (figure 5.20.B). The more severe phenotype was demonstrated by $msps^{P}$ from which 60% of cells had compact microtubules, compared to less than 15% from wild type flies. Additionally, 15% of $msps^{P}$ cells showed bundling of microtubules, whist none were seen in wild-type cells.

These defects are similar to those in Msps depleted S2 cells. These results from *msps* mutants indicated that Msps is a major regulator of interphase microtubule organisation in flies as well as culture cells.

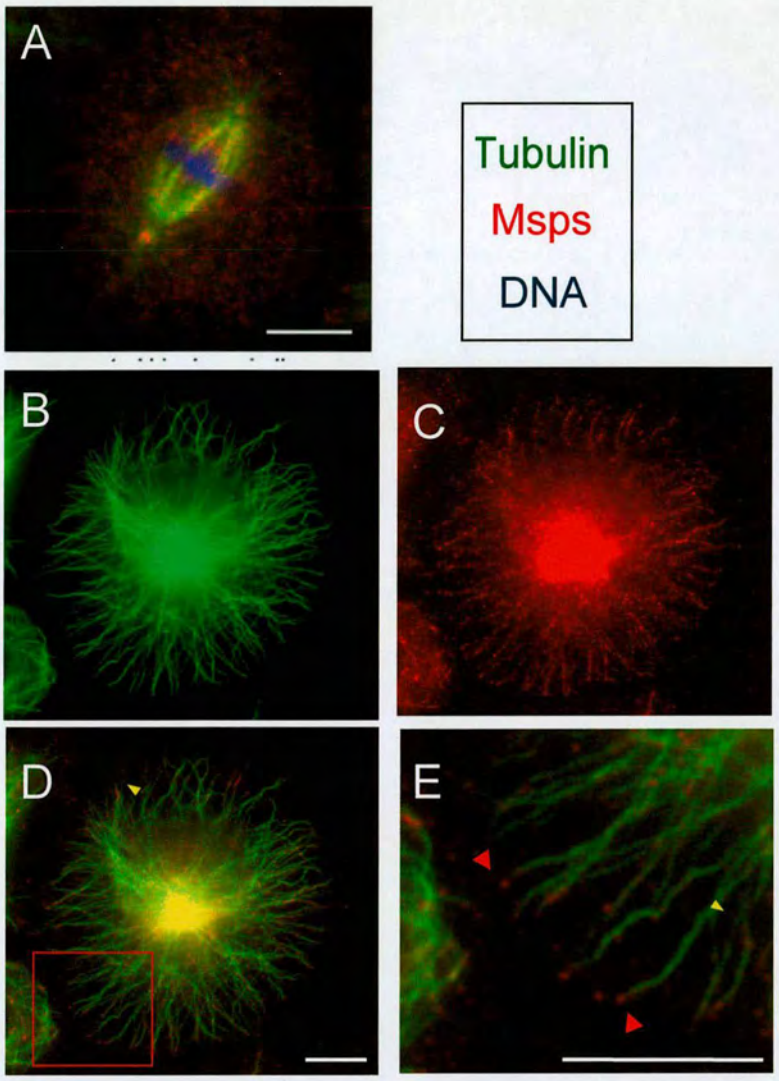

Figure 5.1. Msps microtubule localisation in S2 cells.

S2 cells were grown on con A coverslips, fixed and stained with antibodies against Msps (red) and alpha-tubulin (green) and DNA counterstained with DAPI (blue). Msps protein localises to the centrosome and spindle in mitosis (A). In interphase Msps localises along the microtubules (B-E) (E) is an enlargement of the region in the red box in (D). It highlights the Msps microtubule plus end localisation seen in these cells. Red arrows indicate plus end localisation

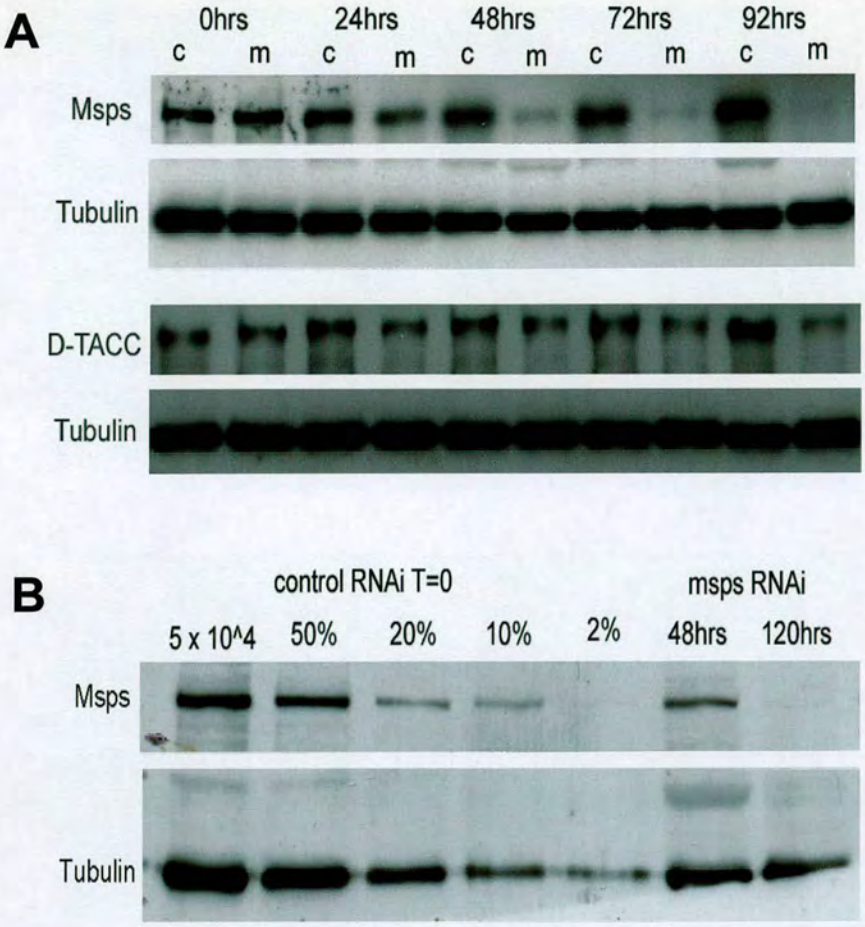

Figure 5.2. D-TACC and Msps protein levels decrease in cells treated with *msps* dsRNA.
(A) Samples from cells treated with control and *msps* dsRNA were collected every 24 hours for 5 days. Western blots were carried out against Msps and D-TACC, and alpha-tubulin as a loading control. Msps protein was depleted by the *msps* RNAi treatment but not in the control RNAi experiment. D-TACC protein levels were also affected by Msps depletion.
(B) The level of Msps depletion was estimated by running dilutions of control cells next to cells treated with *msps* dsRNA for 48 and 120 hours. After 48 hours, approximately 70% of Msps was depleted and after 120 hours, less than 5% remained.

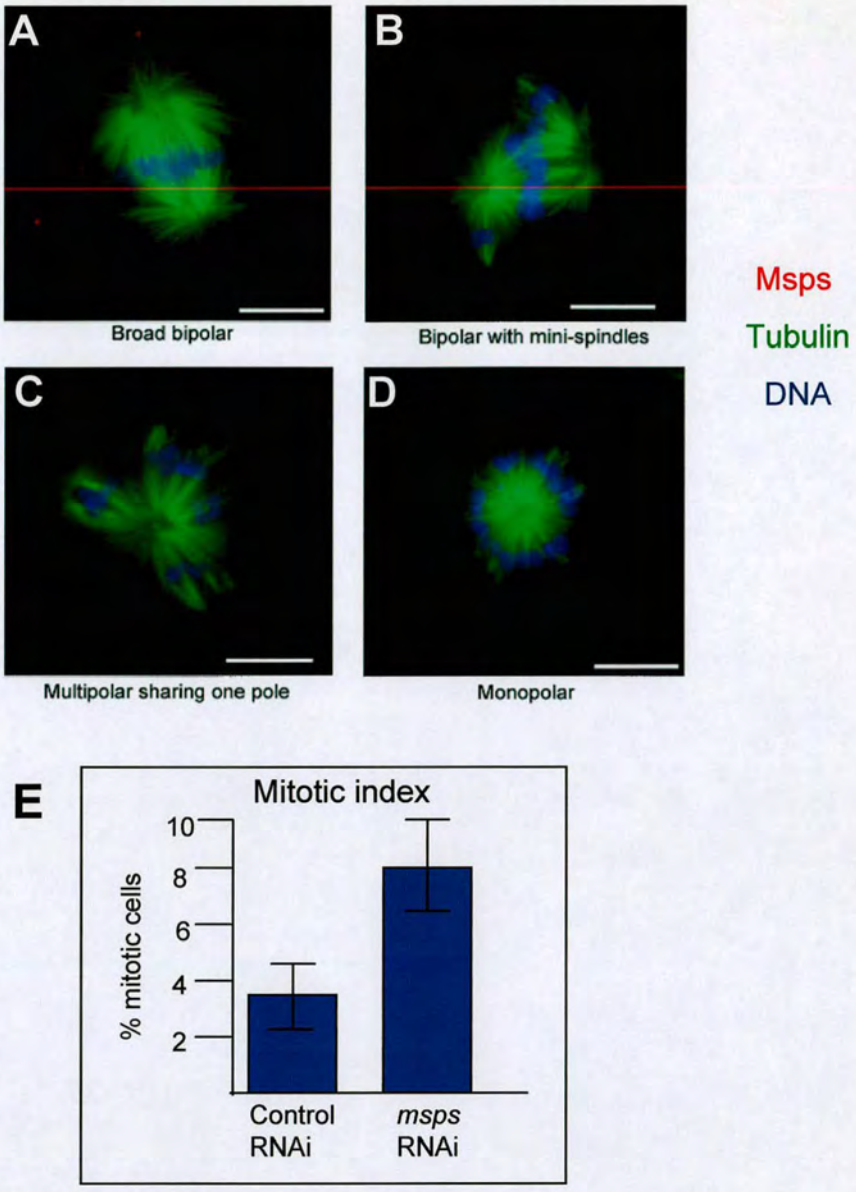

Figure 5.3. Msps depletion results in mitotic spindle defects

Cells treated with control or *msps* dsRNA were fixed and stained for alpha-tubulin (green) and DNA (blue) Spindle phenotypes seen in Msps depleted cells include, broad bipolar spindles (A), bipolar spindles with extra mini spindles sharing poles with a main spindle (B), multiple spindles all sharing one pole (C) and monopolar spindles (D). (E) Mitotic index in Msps depleted cells is higher than in control cells. Mitotic index was calculated as the percentage of mitotic cells (n>100) in the population, as an average of three experiments. Bars indicate standard deviation.

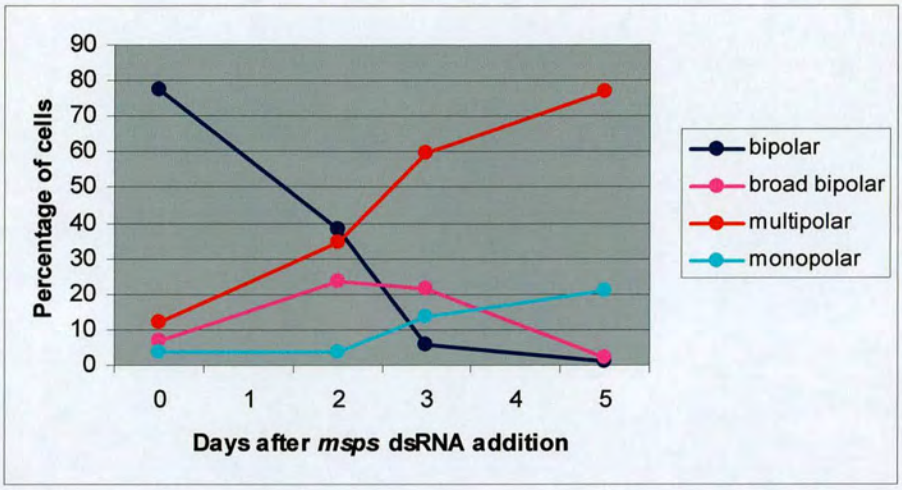

Figure 5.4. Time course of mitotic spindle phenotype in *msps* RNAi cells

Samples from control and *msps* dsRNA treated cells were fixed and stained for alpha-tubulin at 0, 48, 72 and 120 hours. At least 100 spindles were counted at each time point and categorised as either bipolar, broad bipolar, multipolar and monopolar. Data points at 0 hours refer to control RNAi cells. Control cells at later time points gave similar results to those at 0 hrs so were not shown.

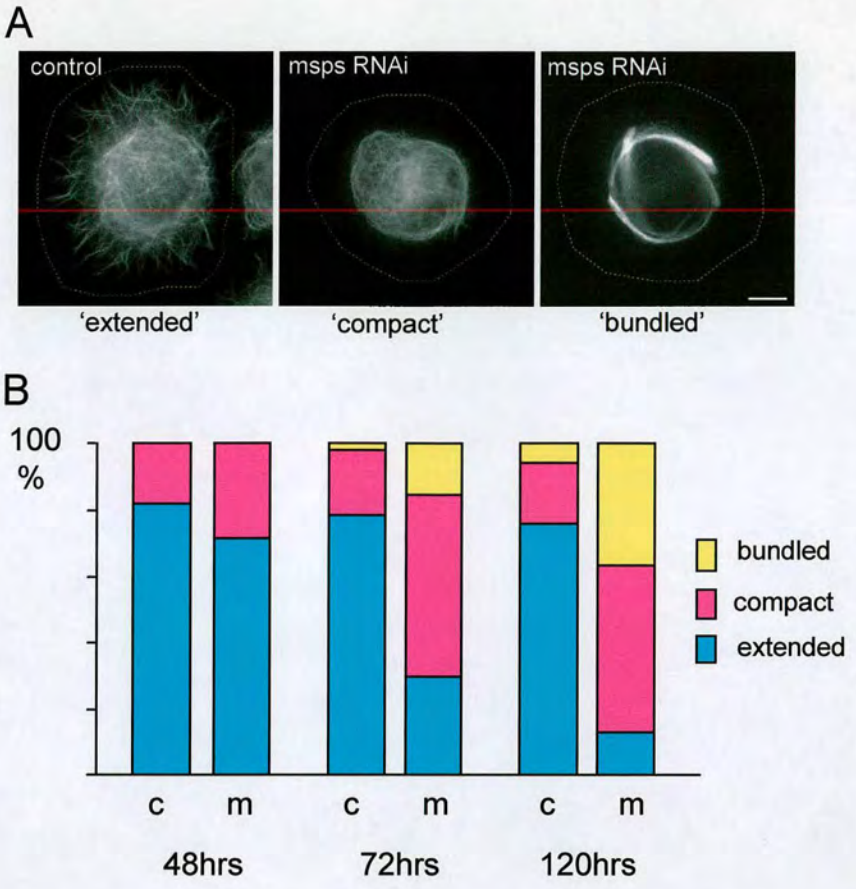

Figure 5.5. Interphase microtubule organisation is altered after Msps depletion.

Interphase microtubule organisation was observed by immunofluorescence at 48, 72 and 120 hours after control and *msps* dsRNA addition. (A) Microtubule organisation was divided into three categories: microtubules extending out towards the cell cortex ('extended'), compact microtubule structures in the centre of the cell ('compact'), and bundled microtubules ('bundled'). Yellow dotted line denotes the edge of the cell. Scale bars equal 10μm.

(B) At 48, 72 and 120 hours, interphase phenotypes were scored in control (c) and *msps* (m) RNAi cells.

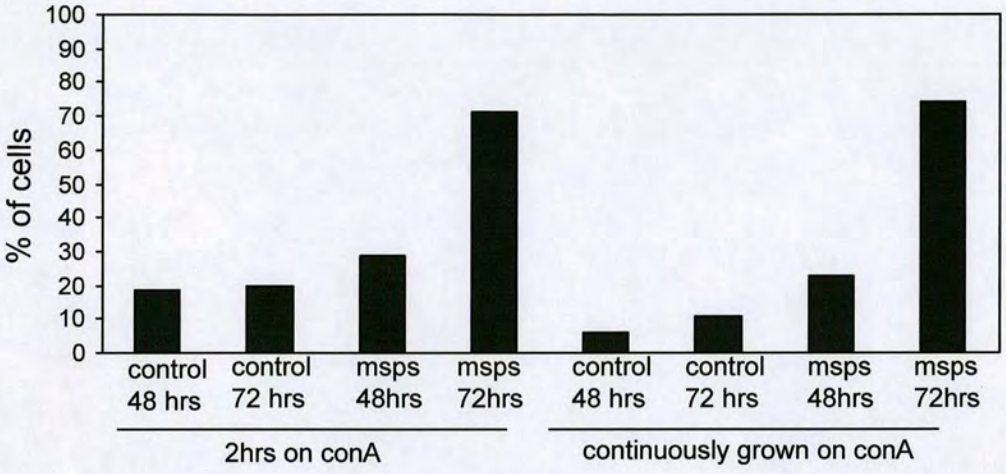

Figure 5.6. Interphase microtubule phenotype remains when *msps* RNAi cells are grown continuously on con A.

Control or *msps* RNAi cells were either grown on con A coverslips immediately after dsRNA addition or cultured on a plastic surface, followed by 2 hours growth on a con A coated surface. After 48 and 72 hours cells were fixed and processed for immunofluorescence and stained for alpha-tubulin. Cells (n>100) were scored for the presence of compact and bundled interphase microtubules. There was no difference in phenotype between the two experiments.

	edge	projections	multiple bands	long bands
	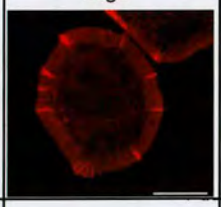	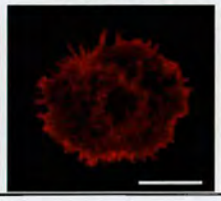	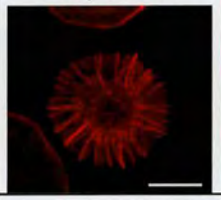	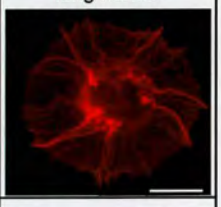
Control RNAi	94.9 (±1.1)	3.9 (±1.7)	1.1 (±0.9)	0.13 (±0.1)
msps RNAi	90.2 (± 4.1)	7.7 (±5.0)	1.4 (±1.1)	1.3 (±1.2)

Figure 5.7. No difference in the actin staining pattern is observed in control and *msps* RNAi treated cells.
After 5 days, cells treated with control or *msps* dsRNA were grown on con A coverslips and stained for filamentous actin. In both control and *msps* RNAi cells 4 types of actin staining were observed; narrow peripheral staining with strong bands (A), projections from the cell membrane (B), many strong bands around edge (C) and very long bands from the nuclear region to periphery (D). Bar = 10μm. Percentages of cells showing these patterns were determined for control and *msps* RNAi cells. At least 300 control and *msps* RNAi cells were scored in 3 separate experiments. Standard deviations are given in brackets.

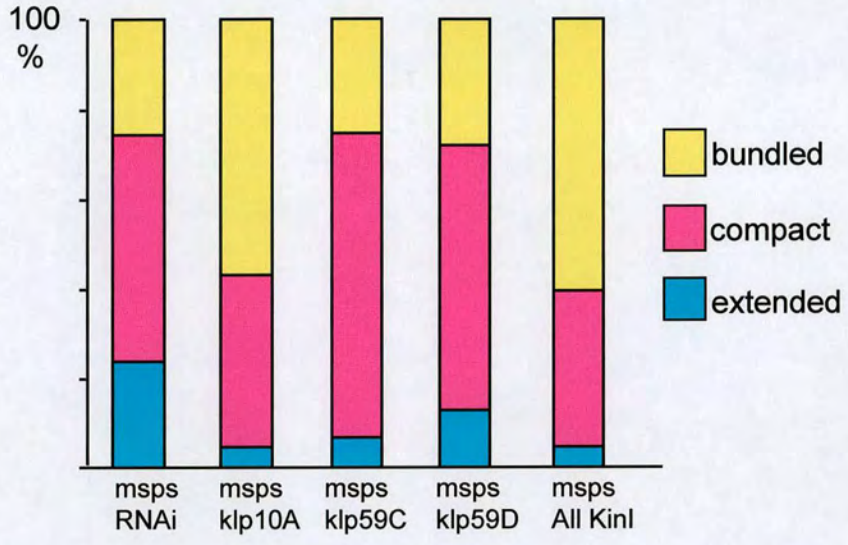

Figure 5.8. Co-depletion of destabilising KinI proteins with Msps does not restore a normal microtubule array.

The three identified KinI protein were depleted individually in conjunction with Msps using RNAi. Additionally, all three KinI proteins were depleted at once along with Msps. Cell were stained for alpha-tubulin and the interphase microtubule organisation scored in the population (n>100).

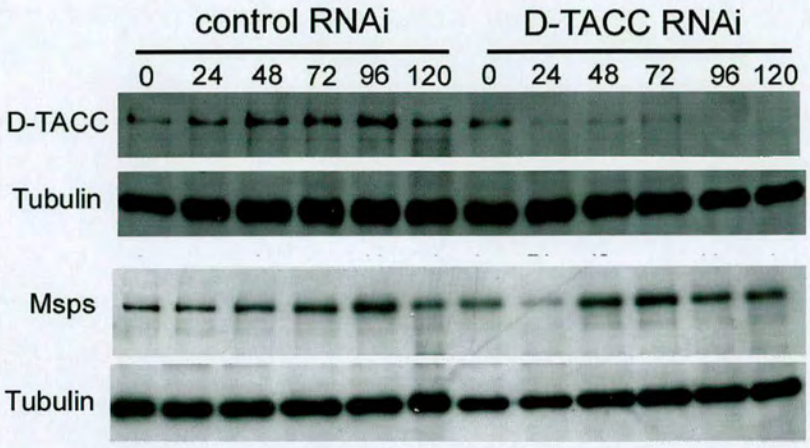

Figure 5.9. D-TACC but not Msps is depleted by addition of *d-tacc* dsRNA to S2 cells.
Samples from cells treated with control and *d-tacc* dsRNA were collected every 24 hours for 5 days. Western blotting indicated that D-TACC protein was depleted by the *d-tacc* dsRNA treatment, but was unaffected by the control dsRNA. Msps protein levels were not effected by D-TACC depletion.

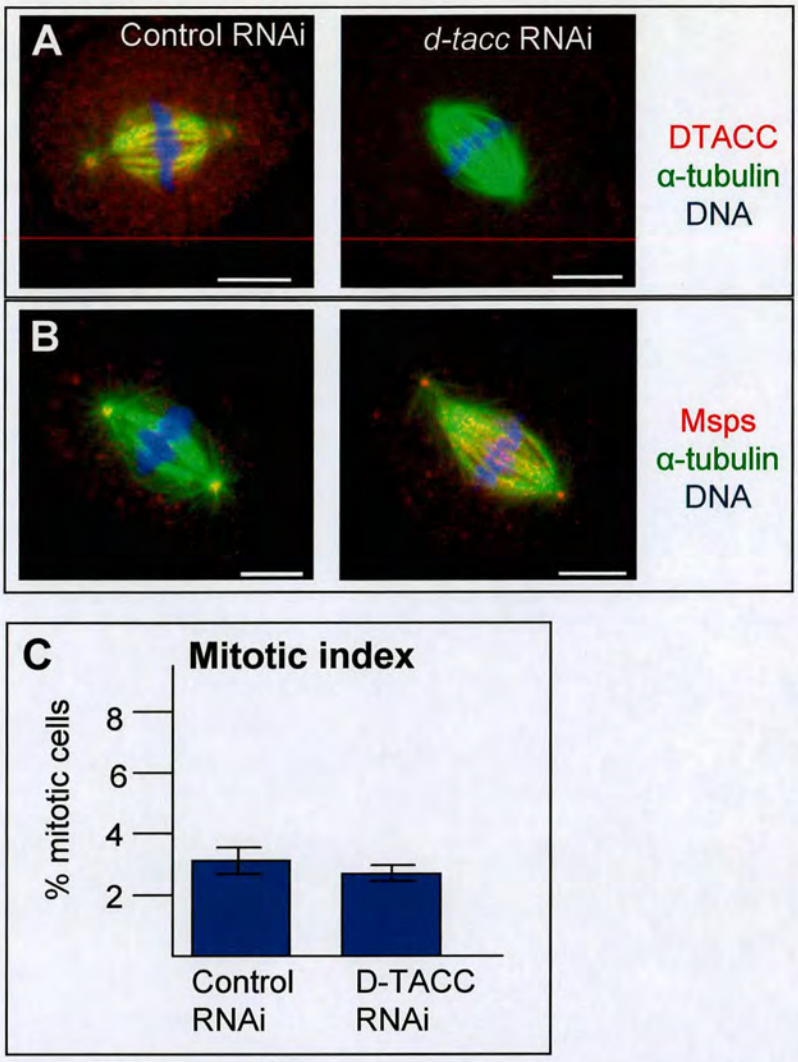

Figure 5.10 D-TACC depletion does not effect mitotic spindle formation or Msps localisation to the spindle and centrosomes.

Cells treated with control or *d-tacc* dsRNA were fixed and stained with antibodies against (A) alpha-tubulin (green) and D-TACC (red) or in (B) alpha-tubulin (green) and Msps (red). DNA was stained using DAPI (blue).

(A) D-TACC localises to the poles and spindle in control RNAi cells. D-TACC staining can no longer be seen in *d-tacc* RNAi cells but normal mitotic spindles are formed.

(B) Msps localisation to the poles and spindle was unchanged in *d-tacc* RNAi cells.

(C) Mitotic index in control and *d-tacc* RNAi cells was not significantly different.

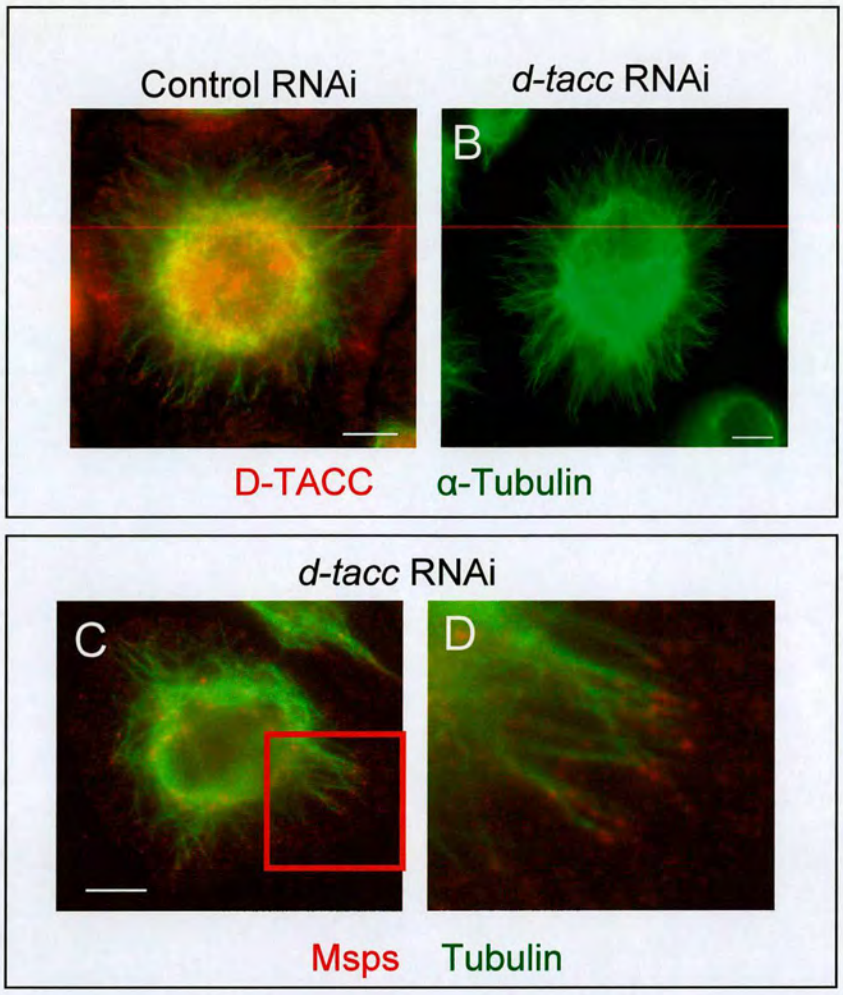

Figure 5.11. D-TACC depletion does not alter interphase microtubule organisation or Msps localisation.

Cells treated with control or *d-tacc* dsRNA were processed for immunofluorescence after 5 days.
(A+B) Control and D-TACC depleted cells were stained for alpha-tubulin (green) and D-TACC (red). (A) D-TACC localises along interphase microtubules. (B) D-TACC depletion does not obviously effect interphase microtubule organisation.
(C+D) Msps (red) still localises to microtubules in D-TACC depleted cells, and as the close up in (D) demonstrates, Msps plus ends staining is retained.

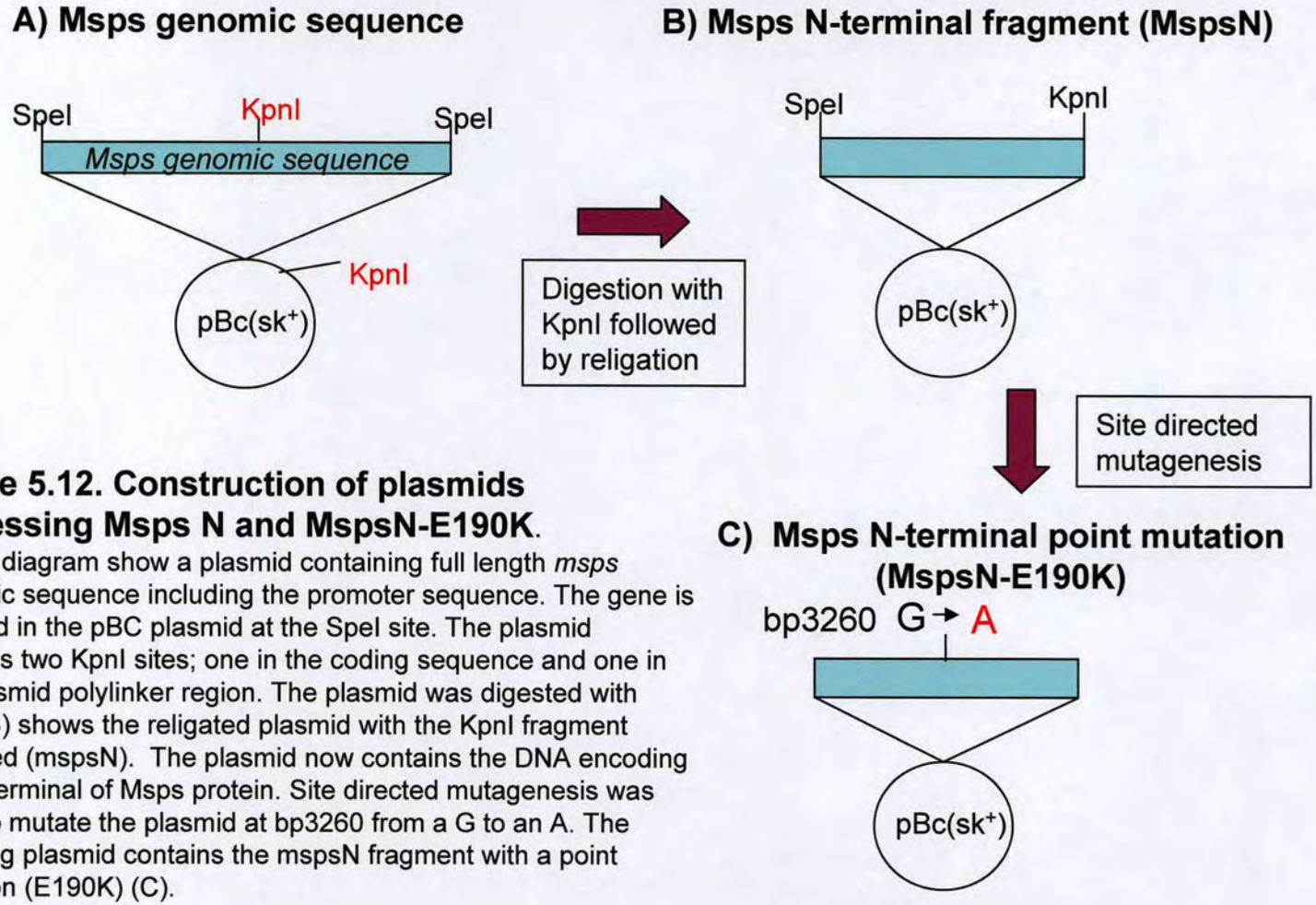

Figure 5.12. Construction of plasmids expressing Msps N and MspsN-E190K.
A) The diagram show a plasmid containing full length *msps* genomic sequence including the promoter sequence. The gene is inserted in the pBC plasmid at the SpeI site. The plasmid contains two KpnI sites; one in the coding sequence and one in the plasmid polylinker region. The plasmid was digested with KpnI. B) shows the religated plasmid with the KpnI fragment removed (mspsN). The plasmid now contains the DNA encoding the N-terminal of Msps protein. Site directed mutagenesis was used to mutate the plasmid at bp3260 from a G to an A. The resulting plasmid contains the mspsN fragment with a point mutation (E190K) (C).

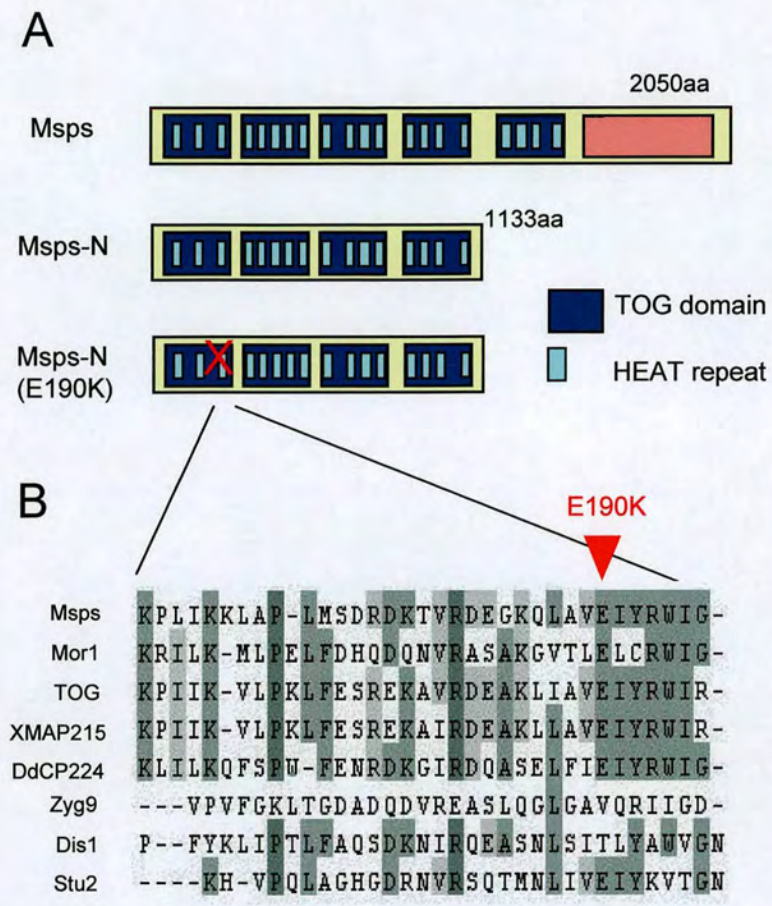

Figure 5.13. Point mutation in conserved residue of Msps.

(A) Domain structure of Msps protein and mutants used in this study. Constructs were made to express the N-terminal 1133 amino-acids (Msps-N) and the same region with one mutation (MspsN-E190K), which results in a change (glutamine to lysine) of the conserved 190th amino acid. (B) Sequence comparison of the last HEAT repeat of the first TOG domain among Msps homologues. E190 in Msps is well conserved.

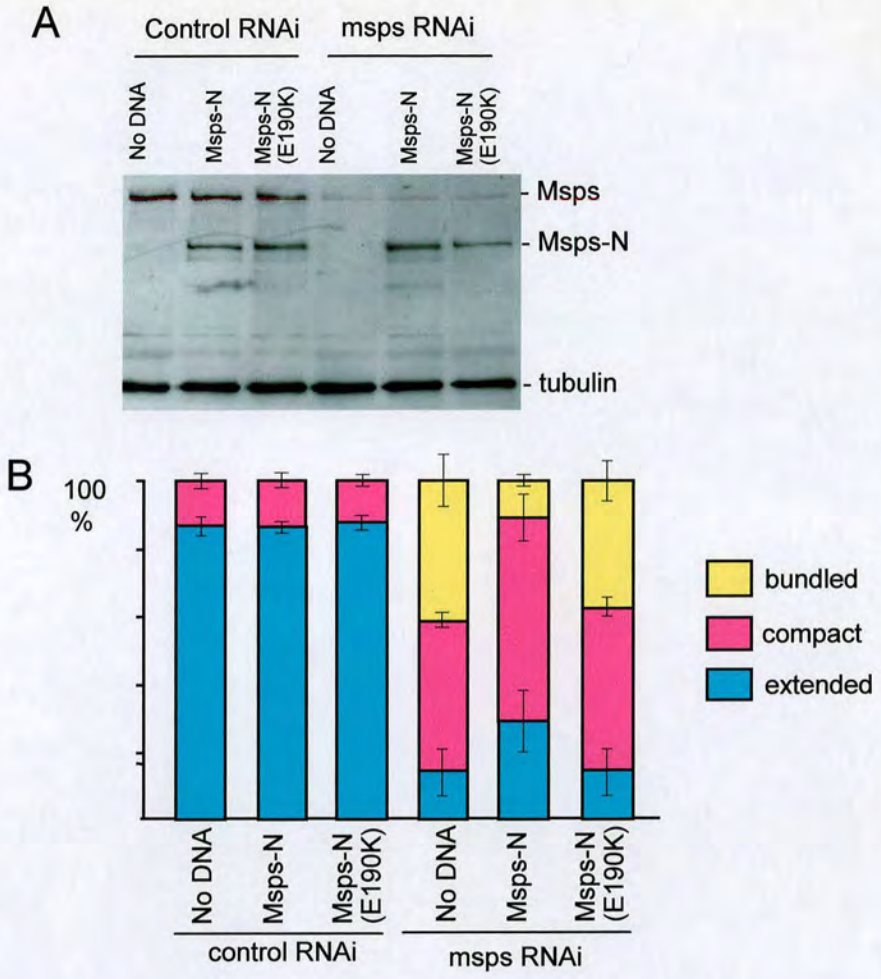

Figure 5.14. N-terminal region of Msps partially rescues depletion of endogenous Msps.

(A) Endogenous full length Msps was depleted (*msps* RNAi) using dsRNA which corresponds to the C-terminal region. dsRNA corresponding to the *B-lactamase* gene was used as a control. Msps-N and Msps-N[E190K] were expressed under the native *msps* promoter by transfection of plasmids. Msps proteins were detected by an antibody that recognises the N-terminal half of the Msps protein. Alpha-tubulin was used as a loading and blotting control. (B) Partial rescue of Msps depletion by the N-terminal region of Msps. Interphase microtubule phenotypes were examined 4 days after addition of dsRNA. Standard deviations are indicated by lines at the top of each bar (>100 cells were scored in three separate experiments). Defects caused by Msps depletion is partially rescued by expression of Msps-N, but not Msps-N[E190K].

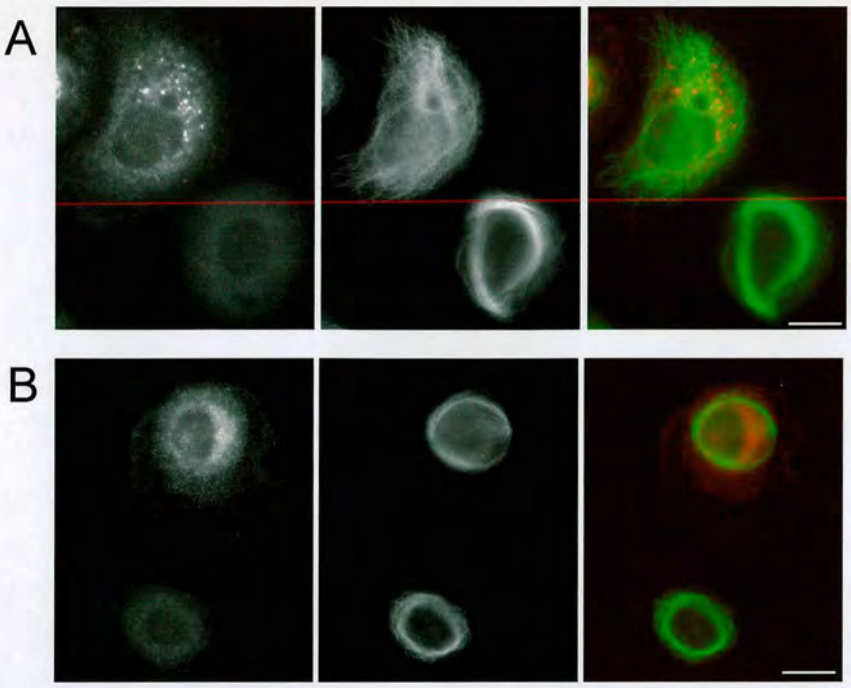

Figure 5.15. Truncated Msps proteins, MspsN and MspsN-E190K, do not localise to microtubules in S2 cells.

After 5 days of treatment with *msps* dsRNA, cells were transfected with plasmids expressing either the N-terminal fragment of Msps (MspsN) (A) or the N-terminal fragment with a point mutation (MspsN[E190K]) (B). Expression of the Msps proteins was detected using antibody recognising the middle of the protein.
(A) The cell at the top is expressing the MspsN protein and has an extended microtubule network. The MspsN protein does not show microtubule localisation but is spread in the cytoplasm with some strong granular staining. The cell at the bottom is not expressing the Msps protein and has a bundled microtubule network. (B) The cell at the top is expressing the MspsN[E190K] point mutant protein, whilst the cell on the right is not. Both cells show a bundled microtubule phenotype. The MspsN[E190K] protein does not localise to microtubules. Bar = 10 μm.

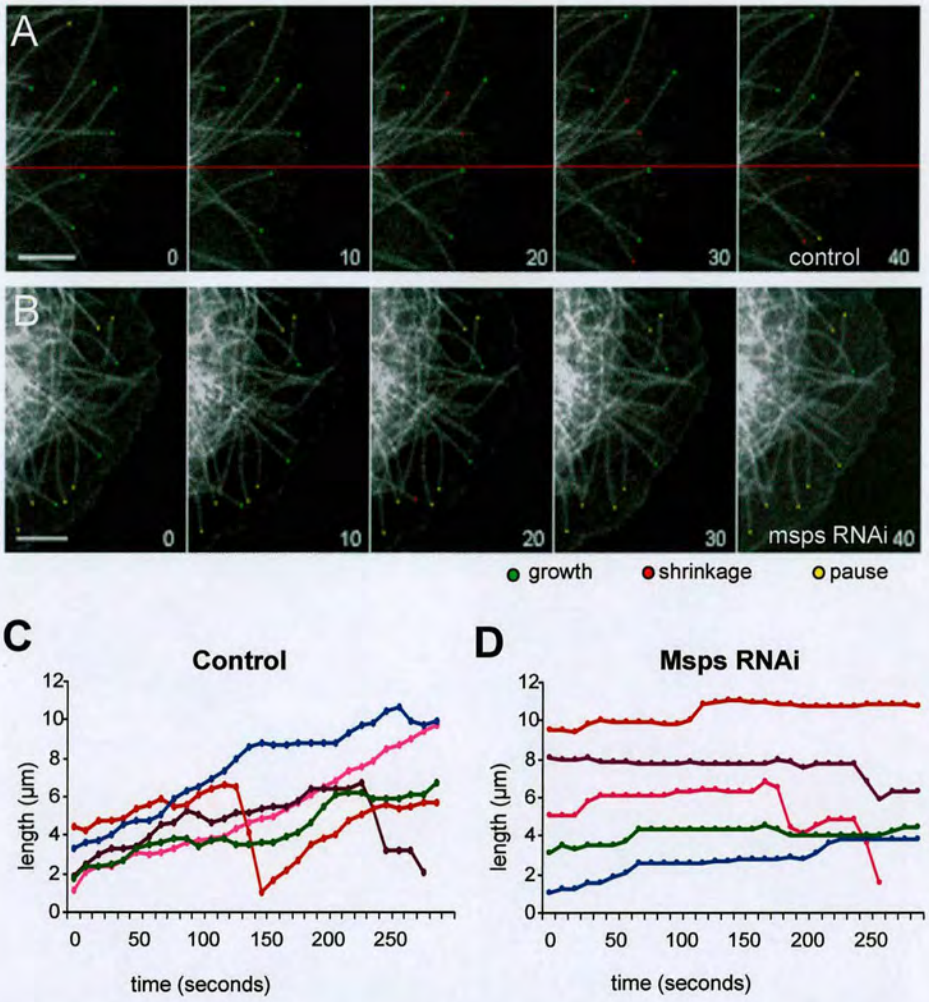

Figure 5.16. Extensive microtubule pausing results from Msps depletion.

(A) Time lapse images of microtubule plus ends in control GFP-tubulin cells. Growing, shrinking and pausing ends were marked with green, red and yellow dots. Numbers in the bottom left represent time in seconds. Microtubules show dynamic instability with occasional pauses. Bar = 10μm. (B) The dynamics of microtubule ends in a cell partially depleted of Msps. Cells were observed 48 hours after dsRNA addition. Microtubule plus ends exhibit prolonged pausing. (C) Life history plots of microtubules in control cells. Microtubule plus ends show persistent growth and occasional shrinkages with some pausing. (D) Life history plots of microtubules partially depleted of Msps. Microtubules spent most of their time pausing with occasional growth and shrinkage.

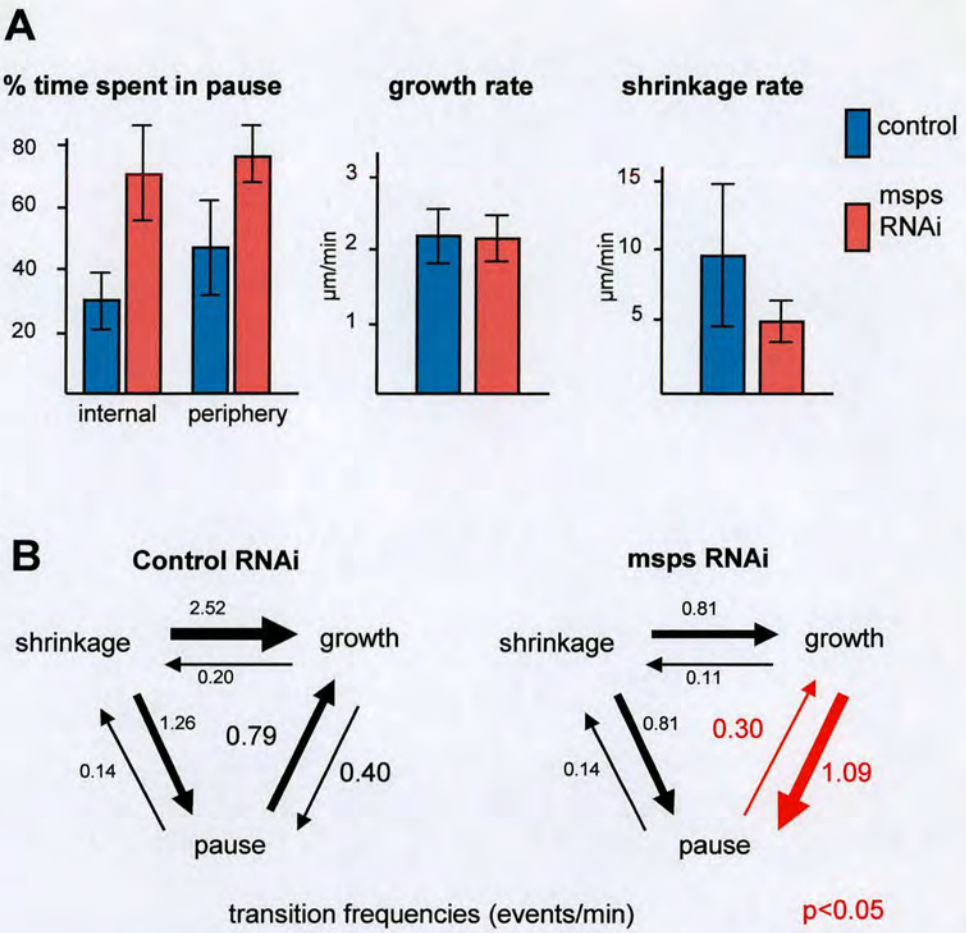

Figure 5.17. Pausing increases in Msps depleted cells but growth rate is unaffected.

(A) Parameters of microtubule dynamics. Time spend pausing was measured for >25 microtubules in 5 different cells treated with control or msps dsRNA for 48 hours. Average time spent in pause per cell is shown as a percentage. In control cells, microtubule plus ends near the cell periphery (within 0.2µm) spent more time in pause than those inside of the cell (internal). In both cases, Msps partial depletion increases time in pause ($p>0.05$ as determined by student t-test). Average growth and shrinkage rates were shown with standard deviations (lines). (B) Transition frequencies between the three microtubule states of growth, shrinkage and pause. Only the transition frequencies marked with red arrows and numbers were significantly different in Msps-depleted cells from those of control cells ($p<0.05$). The transition from pause to growth significantly decreased and the transition from growth to pause increased. Transition frequencies from shrinkage to growth or pause may be increased, but they were not proved to be statistically significant due to small sample size of time microtubules spent in shrinkage.

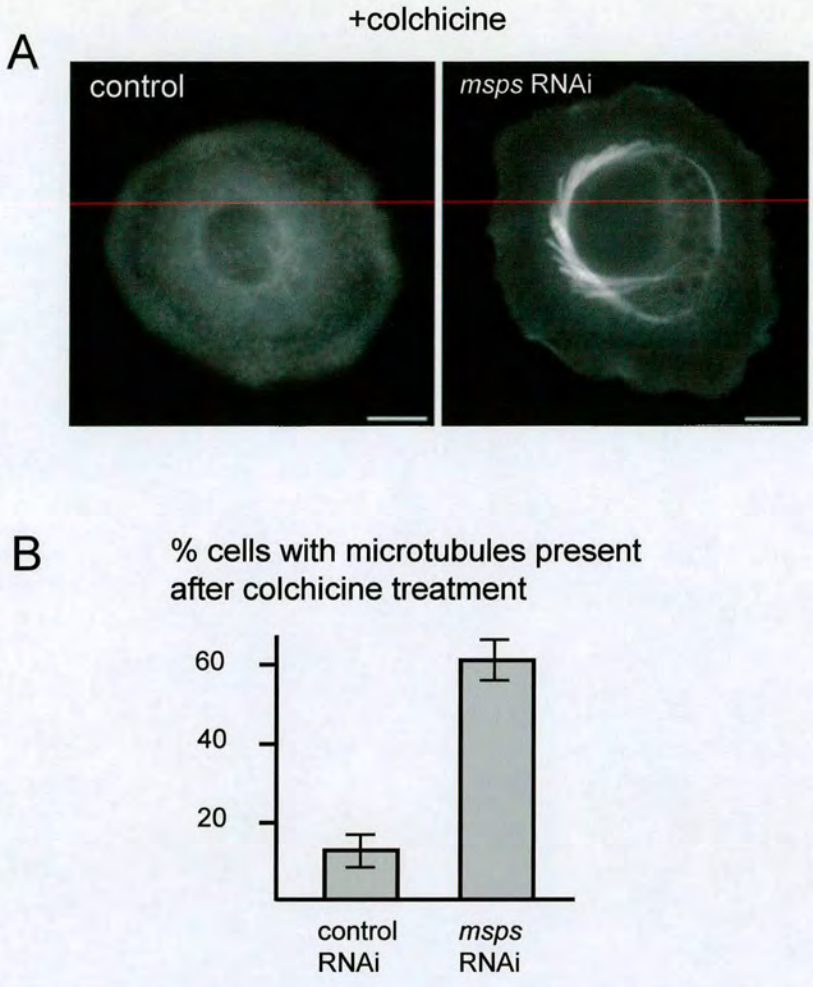

Figure 5. 18. Microtubules in Msps depleted cells are stable against the activity of a depolymerising drug.
(A) Microtubule organisation after addition of colchicine, a microtubule destabilising drug. Control and Msps depleted cells (120hours after dsRNA addition) were observed after 16 hours' incubation with colchicine. Some microtubules remained in Msps depleted cells, while nearly all microtubules were depolymerised in control cells. (B) Frequencies of cells which have residual microtubules after colchicine treatment. Lines indicate standard deviations from three independent experiments.

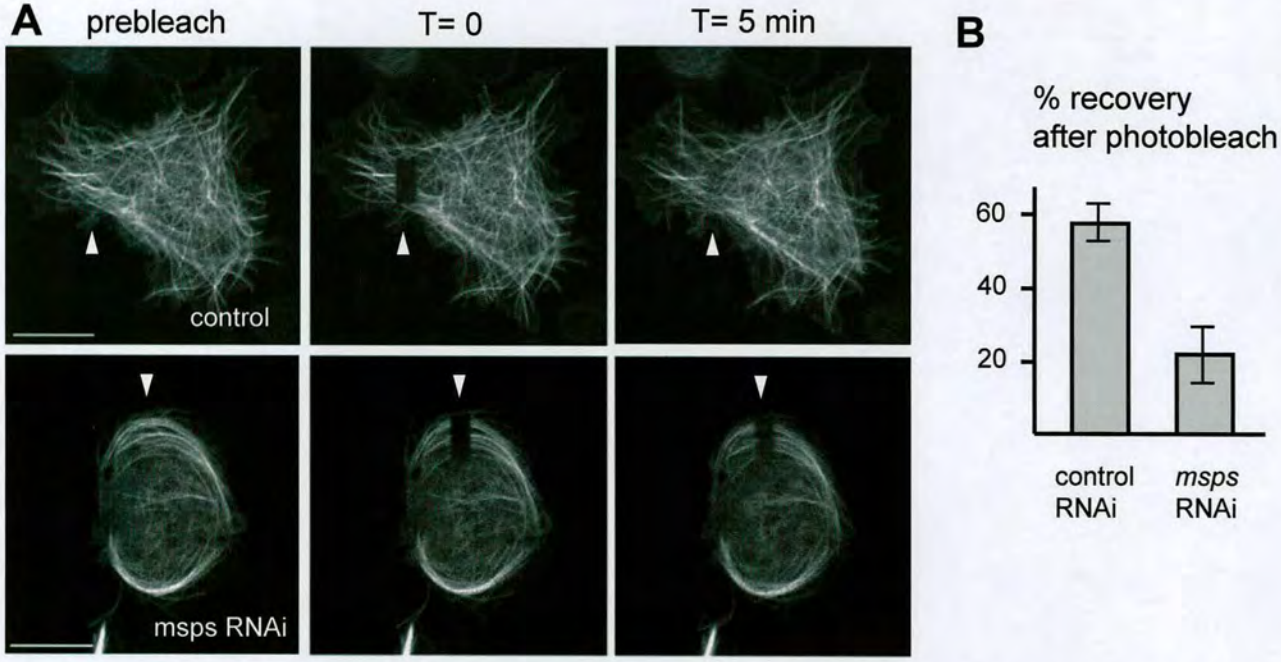

Figure 5.19. Msps depletion results in reduced microtubule dynamicity.
(A) Fluorescence recovery after photobleaching (FRAP) of tubulin-GFP. Small areas (arrowheads) of cells expressing tubulin-GFP were bleached and the recovery of fluorescence monitored for 5 minutes. Cells were treated with dsRNA for 120 hours before photobleach. Fluorescence recovered much slower in Msps depleted cells than in control cells. (B) Percentages of the fluorescence recovery 5 minutes after photobleaching. Lines indicate standard deviations. Decreased turnover of tubulin dimers into microtubules were observed in Msps-depleted cells, indicating decreased microtubule dynamics.

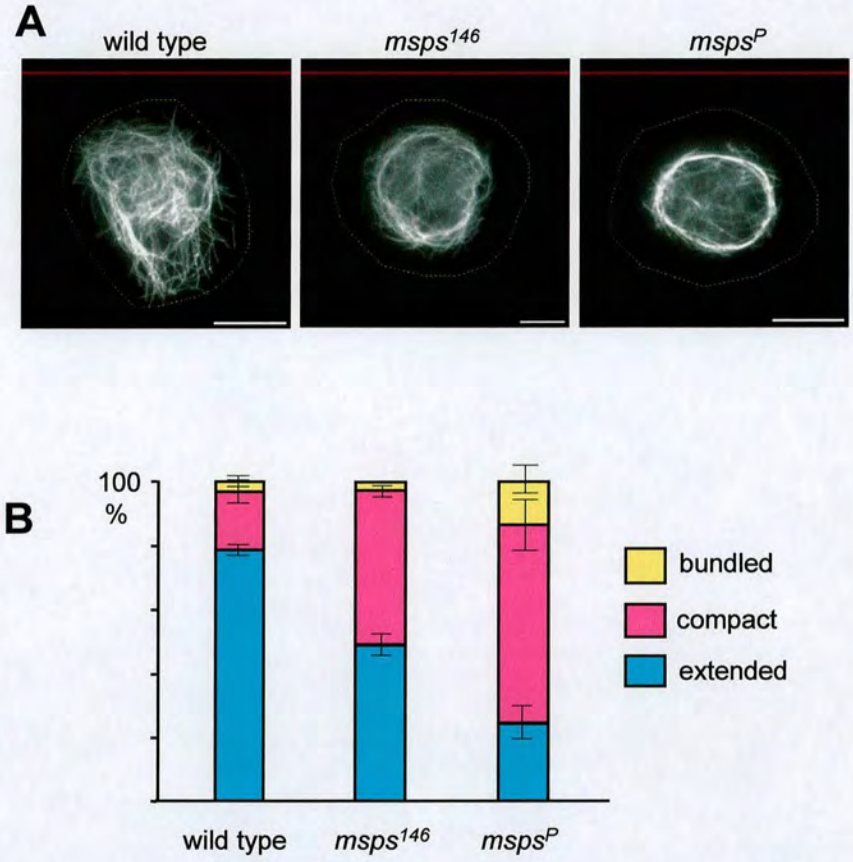

Figure 5.20. Abnormal interphase microtubule organisation in haemocytes from *msps* mutants

(A) Haemocytes were isolated from larvae of wild-type and *msps* mutants (allele 146 and P) and plated out on a concanavalin A coated surface. Most haemocytes from wild-type have 'extended' microtubule organisation (left), while those from *msps* mutants contain 'compact' (middle) or 'bundled' (right) microtubule organisation, as seen in Msps depleted S2 cells. (B) Quantitative analysis of interphase microtubule organisation in *msps* mutants. Both *msps* mutants show abnormal interphase microtubule organisation. Standard deviations are indicates as lines at the top of each bar. >100 cells were scored per genotype in 3 separate experiments

Chapter 6 Genetic interaction of a new meiotic spindle mutant, with *msps, d-tacc* and *ncd.*

6.1 Background

Female meiotic spindles in *Drosophila*, as in many other organisms, lack conventional centrosomes. Female meiotic spindle form in an "inside out" mechanism with the assembly of microtubules around the chromosomes, followed by sorting and bundling of the microtubules into a bipolar spindle (Theurkauf and Hawley, 1992). Whilst mechanisms specific to spindle formation in the absence of centrosome must exist, some mechanisms are conserved from centrosomal spindle formation. Msps and D-TACC, both identified as key players in mitotic spindle function, were subsequently found to have roles in meiotic spindle formation, and were the first proteins to be identified as localising to the accentrosomal poles in female meiosis (Cullen and Ohkura, 2001). The minus end motor, Ncd, is essential for the focussing of meiotic spindle poles (Matthies *et al.*, 1996) and has a role in recruiting Msps to the poles (Cullen and Ohkura, 2001) .

A screen was carried out in the lab to identify new molecules involved in meiotic spindle formation. Finding such molecules will aid in the understanding of acentrosomal spindle formation and may also uncover mechanisms conserved in mitosis.

Collections of mutants were screened cytologically for the presence of spindle defects in the oocytes (F Cullen). One such mutant, *triplet*^{GT28}, was found to form separate spindles around the chromosomes, instead of one unified bipolar spindle.
The mutation was mapped and identified as an uncharacterised gene encoding a conserved protein kinase, related to a kinase found in the Vaccina virus (Banham and Smith, 1992). Recently, another group reported that the *Drosophila* Triplet (Trip) kinase phosphorylates histone H2A (Aihara *et al*, 2004). The protein localises to the

chromosomes in mitosis and nuclear localisation was also demonstrated for the mammalian homologues (Nichols and Traktman, 2004). No spindle defects have been reported.

To understand more about the role of *trip* in spindle formation a double mutant was made between the $trip^{GT28}$ allele and the $d\text{-}tacc^{sella}$ allele. Preliminary results suggested that there was a genetic interaction between the two mutants (Fiona Cullen, personal communication). In this chapter, I describe the $trip^{GT28}$ phenotype and examine its genetic interactions with *d-tacc, msps* and *ncd*. Furthermore, the role of Trip in mitosis was explored through depletion of the protein from *Drosophila* S2 cells.

6.2 Genetic interactions between *triplet* and previously identified meiotic spindle mutants

6.2.1 Creation of double mutants

Genetic interactions between genes can be investigated by the creation of double mutants. The combined effect of the two mutants on the phenotype can reveal information about the relationship between the two proteins. Interactions, both direct and indirect, have been identified between Msps, D-TACC and Ncd proteins. To investigate if the newly identified gene, *trip*, also interacts with this network, double mutants of the three proteins with the $trip^{GT28}$ allele were made.

All four genes are located on the third chromosome, facilitating the creation of double mutants by recombination. A double mutant between $trip^{GT28}$ and $d\text{-}tacc^{stella}$ was made previously (Fiona Cullen). The recombination strategy for the creation of the *msps* and *trip* double mutant is shown in figure 6.1. The female sterile allele $msps^{208}$ was recombined with a chromosome carrying the $trip^{GT28}$ allele and a number of

multiple marker alleles. Double mutants were identified by selecting chromosomes carrying only the *ebony (e)* marker (figure 6.1 A) as this would indicate that crossing over had occurred in the desired location.

Of the $msps^{208}$ $triplet^{GT28}$ recombinants obtained 4 were viable but female sterile and 2 were lethal (figure 6.1.B). All the recombinants were female sterile over the original $triplet^{GT28}$ and $msps^{208}$ alleles, indicating that they all contained both alleles. The lethality of two of the recombinants must come from the presence of an unknown lethal mutation in one of the stocks. As the $msps^{208}$ stock is quite old, it may have picked up lethal mutations that are floating within the stock.

A double mutant between trp^{GT28} and ncd^{1} was created by a similar strategy (figure 6.2.A). Recombinants containing both alleles were selected by the transfer of the *claret* (*ca*) marker to the trp^{GT28} chromosome. All of the $triplet^{GT28}$ ncd^{1} recombinants are viable but female sterile (figure 6.2.B). The presence of the $triplet^{GT28}$ allele was confirmed by testing the fertility of heterozygotes created between the recombinants and the original $triplet^{GT28}$ chromosome. All recombinants containing the *claret* marker will also contain the ncd^{1} mutant as they are so closely linked.

All combinations of alleles are viable indicating that the alleles do not interact to produce synthetic lethality. The combination of alleles is not detrimental for viability or fertility. Cytological analysis is necessary to observe the combined effect of the mutations on spindle formation.

6.2.2 Cytological analysis indicates that *trip* genetically interacts with *msps* and *d-tacc* but not *ncd*.

In oocytes from $trip^{GT28}$ homozygotes, individual spindles formed around the chromosomes (figure 6.3.A). This phenotype has not been encountered in any previous meiotic spindle mutants. Viable mutant alleles of *d-tacc* and *msps* have been found to form distinct tripolar spindles and the null allele, ncd^{1}, results in unfocussed poles. By

examining the phenotype of the double mutants it will be possible to see the combined effect of two alleles. Such analysis may give insights into the roles of the two proteins, in relation to each other in spindle formation.

Oocytes from wild-type and mutant flies were obtained by dissecting the ovaries of fat females directly into 100% methanol in a watch glass. The ovaries were sonicated to remove the chorion and individual oocytes picked up and placed in fresh methanol. The oocytes were immunostained with antibodies against alpha-tubulin and the DNA counterstained with propidium iodide or Topro3, mounted and examined microscopically. Oocytes were examined in batches and at least 25 spindles examined for each genotype.

The *trip*^{GT28} phenotype had already been partially examined, however, in order to characterise the frequency of the *triplet* phenotype, I examined more spindles in the *triplet*^{GT28} mutant. In approximately 50% of cases, the oocytes contained more than one bipolar spindle (figure 6.3). The individual spindles appear to have no other defects and are focused correctly. The remaining 50% of spindles were single and bipolar. More than one spindle was never seen in wild-type oocytes.

Combinations of *msps*^{208} or *d-tacc*^{stella} with *trip*^{GT28} resulted in the same phenotype as the single *trip*^{GT28} phenotype. Again approximately 50% of the spindles had more than one spindle with the remaining oocytes containing single spindles. A third of spindles in the oocytes of single *msps*^{208} and *d-tacc*^{stella} mutants are tripolar in shape; however, this phenotype was never seen in the double mutants.

The single *ncd*^{1} allele results in most spindles having unfocused poles, and the combination of *trip*^{GT28} and *ncd*^{1} results in a mixture of the two phenotypes (figure 6.4). The most common phenotype was the presence of multiple spindles with unfocused poles (45%) (figure 6.4.C). Many of the single bipolar spindles had unfocused poles (30%) displaying the *ncd*^{1} phenotype (figure 6.4.A). In this double mutant, the *triplet* and *ncd* phenotype are additive as can both be seen. There is no enhancement or suppression of either phenotype.

To concluded, in the *trip*^{GT28} *msps*^{208}/*d-tacc*^{stella} double mutants, only the *triplet* phenotype is visible whilst the *msps/d-tacc* phenotype is never found. This interaction indicates that *msps* and *d-tacc* genes are epistatic to the *triplet* gene. The presence of the *msps/d-tacc* phenotype is influenced by the presence of the *trip*^{GT28} allele. On the other hand, the function of *triplet* and *ncd* does not appear to be linked; the presence of one phenotype does not affect the other.

6.3 Analysis of Triplet function in S2 cells

To investigate the potential role of Trip protein in mitotic cells, I chose to deplete the protein from *Drosophila* S2 cells. The *trip*^{GT28} allele that has been isolated is not essential for mitosis as the flies are viable. The allele has been sequenced, revealing that the coding sequence contains a premature stop codon, deleting the C-terminal region of the protein (F. Cullen, personal communication). A small amount of protein, corresponding to the N-terminal region containing the kinase domain is still present. Complete removal of the protein may reveal that the protein is needed for the mitotic divisions.

RNAi was carried out as previously described. dsRNA corresponding to the N-terminal coding region of the trip gene was made. After 5 days of treatment with *trp* or control dsRNA, samples of cells were taken for western blotting and immunofluorescence.

Western blotting revealed that the protein was successfully depleted from the cells (figure 6.5). Control and triplet depleted cells were spread on con A coverslips, fixed and stained with an antibody against alpha-tubulin. No obvious spindle defects were observed in the Trip depleted cells. Mitotic index was also calculated by staining with a mitotic marker, phospho-histone H3 (PH3), and counting the percentage of mitotic cells in the population. There was a slight increase in mitotic index from around 2.6% to 4.6% (figure 6.5.B).

Triplet does not appear to have an essential role in *Drosophila* S2 cells. No gross defects in spindle shape were seen. It is possible that subtle defects were missed, as even control cells have a high background of spindle defects in these cells. Such subtle defects could result in the slight increase in mitotic index.

A

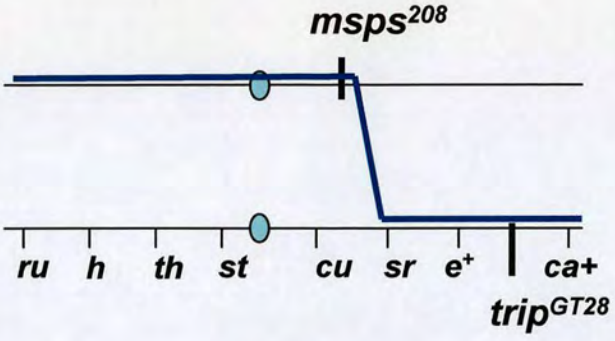

Select recombinants
msps^{208} *sr* *e*$^{+}$ *trip*^{GT28} *ca*$^{+}$

B

Genetic analysis of recombinants of *trip*^{GT28} and *msps*^{208}

No of recombinants	homozygote	Heterozygous with *trp*^{GT28}	Heterozygous with *msps*^{208}
4 *trp*^{GT28} *msps*^{208}	Viable female sterile	Viable female sterile	Viable female sterile
2 *trp*^{GT28} *msps*^{208}	Lethal	Viable female sterile	Viable female sterile

Figure 6.1. Creation of *trpGT28* and *msps208* double mutants by recombination.

(A) A chromosome containing the *msps*^{208} allele was recombined with a chromosome carrying *trip*^{GT28} and several visual markers. Recombinants were selected by the combination of markers described. (B) The table outlines the recombinants obtained and the outcome of viability and sterility tests. The presence of both *msps*^{208} and *trip*^{GT28} on the recombined chromosomes was confirmed by creating heterozygotes between the original stocks of *trip*^{GT28} and *msps*^{208} and the recombinants, and testing female sterility.

A

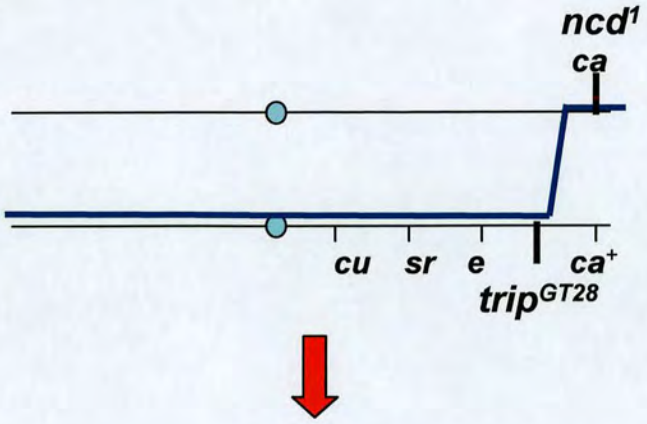

B

Genetic analysis of recombinants of *trip*^{GT28} and *ncd*^{1}

No of recombinants	homozygotes	Heterozygous with *trip*^{GT28}	*ncd/ca* marker present
8 *trip*^{GT28} *ncd*^{1}	Viable, female sterile	Viable, female sterile	yes

Figure 6.2. Creation of *trip*^{GT28} and *ncd*^{1} double mutants by recombination.

(A) A chromosome containing the *ncd*^{1} allele was recombined with a chromosome carrying *trip*^{GT28} and several visual markers. Recombinants were selected by the combination of markers described. The table outlines the recombinants obtained and the outcome of viability and sterility tests. The presence of *trip*^{GT28} was confirmed by creating heterozygotes between the original *trip*^{GT28} and the recombinants and testing female sterility. The presence of *ncd*^{1} was confirmed by the presence of the *ca* marker.

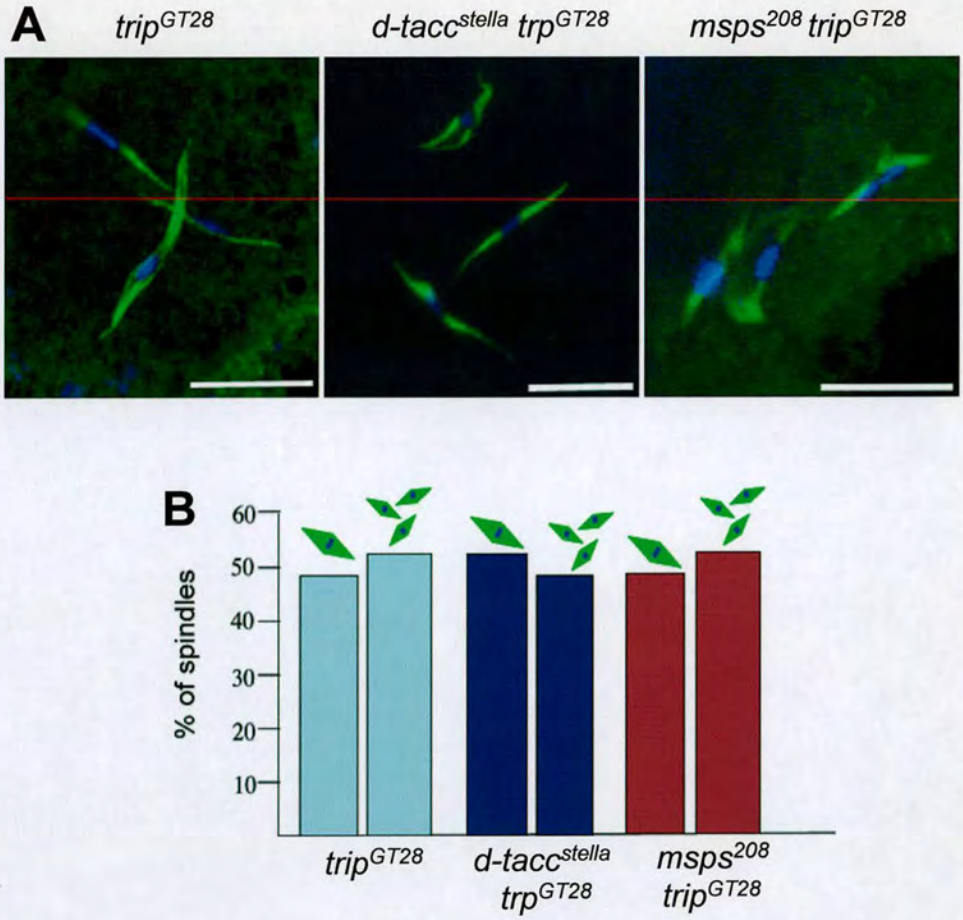

Figure 6.3. Individual spindles form around chromosomes in *trip*^{GT28}, *d-tacc*^{stella} *trip*^{GT28} and *msps*^{208} *trip*^{GT28} oocytes.

(A) Meiotic spindle phenotype in *trip*^{GT28}, *trip*^{GT28} *d-tacc*^{stella} and *trip*^{GT28} *msps*^{208} oocytes. Oocytes from mutant flies were stained for tubulin (green) and DNA (blue) to examine female meiotic spindles. The single and double mutant oocytes all had the phenotype of individual spindles forming around chromosomes. (B) The percentage of spindles with the *triplet* phenotype in the three mutants. At least 25 spindles were observed for each phenotype.

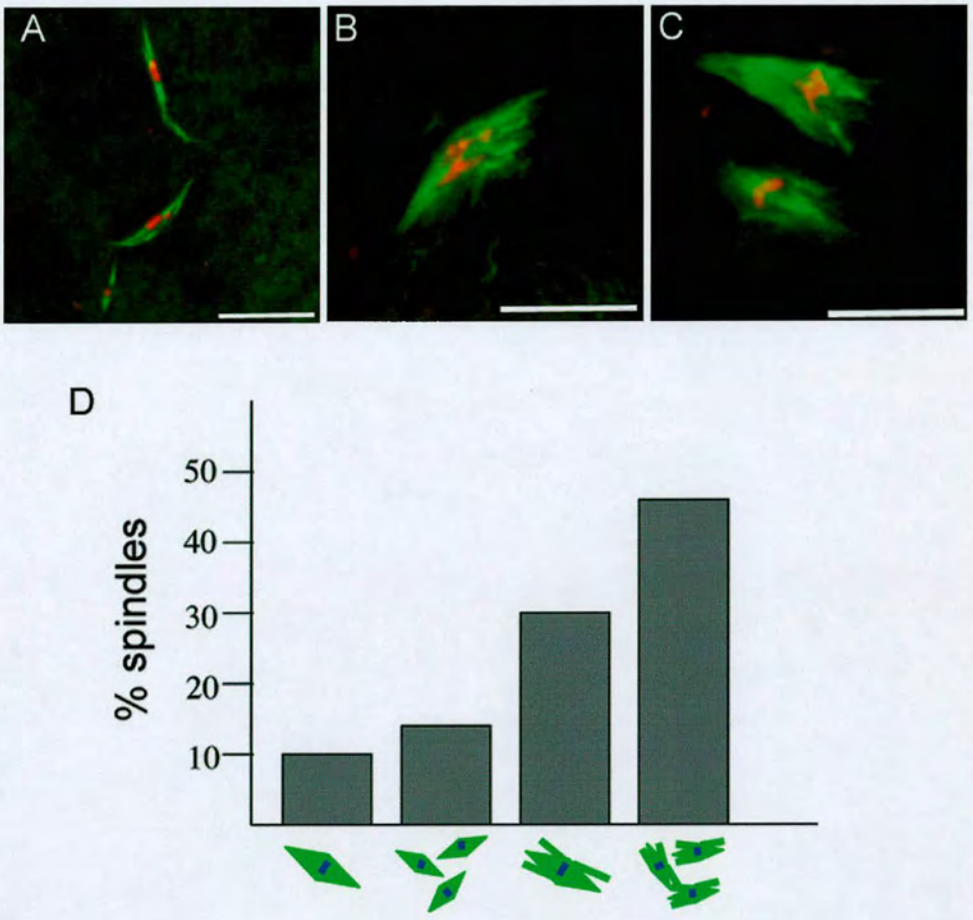

Figure 6.4. *trip*^{GT28} *ncd*^{1} oocytes display the *triplet* and *ncd* spindle phenotypes.

The top panel shows the spindle defects that were found in the double mutant: A) multiple bipolar spindles with focused poles, B) single bipolar spindles with unfocused poles and C) multiple spindles with unfocused poles. The graph (D) quantifies the spindle defects observed.

The scale bar is 10μm.

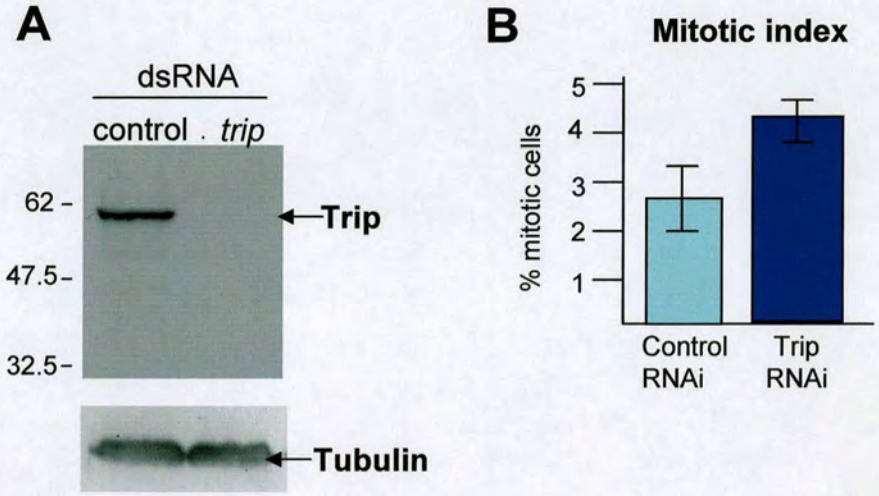

Figure 6.5. Trip depletion from S2 cells causes a slight increase in mitotic index

S2 cells were treated with dsRNA corresponding to the coding region of the *triplet* gene or a control sequence. (A) Western blot demonstrating Trip protein is depleted specifically in cells treated with *trip* dsRNA. Protein samples were prepared from cells 5 days after dsRNA treatment and western blotted with an anti-Trip antibody. The membrane was stripped of anti-Trip antibody and reprobed with anti-alpha-tubulin to check equal loading of protein. (B) Mitotic index increased in Trip depleted cells. The percentage of mitotic cells in the population were estimated. At least 600 cells were counted in three separate experiments. Standard deviation is shown.

Chapter 7 Discussion

7.1 Insights into Msps and D-TACC function provided by screening and analysis of new alleles

7.1.1 Alleles isolated in the screen

Studies of *msps* alleles have been vital in identifying functions of Msps protein in mitosis and female meiosis (Cullen and Ohkura, 2001; Cullen *et al.*, 1999). Similarly, mutant alleles of *d-tacc* and *ncd* proved to be crucial in revealing the interactions between the three proteins in spindle assembly (Gergely *et al.*, 2000; Lee *et al.*, 2001; Cullen and Ohkura, 2001). In this study, I aimed to isolate new alleles of *msps*, *d-tacc* and *ncd*, with the intention of revealing more information about the functions, localisation and interactions of these proteins.

All of the *msps* alleles, previously identified, result in a reduced level of wild-type protein, rather than expressing wild-type levels of dysfunctional protein. The strategy used in this study involved the use of a random mutagen, EMS, which has been shown to predominantly cause point mutations or small deletions (Ashburner, 1989). It was hoped that by screening for mutants with small DNA aberrations, alleles would be isolated with small changes in protein sequence that would disrupt specific functions of the protein. The domains of Msps protein responsible for localisation, protein interactions and function had not been identified, and by uncovering new mutants, characterisation of domain structure would be possible. In addition, new mutants may reveal novel functions for the proteins.

The screen identified 8 *msps* and one *d-tacc* allele. New alleles of *msps* were obtained at a high rate (1 mutant per 526 chromosomes screened) whilst obtaining *d-tacc* alleles proved more difficult (1 mutant per 2805 chromosomes screened). No *ncd* alleles were obtained. Size of the gene may be a factor in the success of obtaining new *msps*

alleles. *msps* is a large gene with a coding sequence covering over 6kb, providing a larger target for mutation, than the smaller *d-tacc* (3.7kb) and *ncd* (3.5 kb) coding sequences.

Sequencing revealed that point mutations or small deletions had occurred in the new alleles. All of the DNA mutations were predicted to produce truncated proteins, due to premature stop codons. Of the 8 alleles predicted to produce truncated proteins, $msps^{S10}$, $msps^{51}$ and $d\text{-}tacc^{S3}$ were found to produce the expected mutant proteins. No mutation in the coding sequence of $msps^{E}$ was found. However, I presume that a mutation must have occurred in an unsequenced coding region, as no Msps protein was detected in the mutant.

The screen isolated the first *msps* null allele, $msps^{D}$. Although the allele potentially produces a 20 amino acid protein, such a short peptide is unlikely to have any function. This allele reveals that a total lack of Msps protein results in lethality at the 2nd instar stage. The null allele is lethal earlier than $msps^{P}$, which retains a small amount of wild-type Msps protein.

Obtaining alleles producing mutant proteins with single amino acid substitutions proved elusive. Alleles producing truncated protein were the most common type of mutation. It is unsurprising that removal of large regions of an essential protein will seriously impair protein function and result in lethality or female sterility. Furthermore, truncation also affected the amount of protein present in a number of cases. As the mutagenesis was random, single amino acid substitutions are likely to have occurred, but these failed to affect protein function sufficiently to cause lethality or female sterility. This data indicates that it is easier to produce a stop codon and subsequent truncation, than it is to randomly mutate an amino acid and succeed in disrupting protein function.

With further screening, alleles may be isolated with single amino acid substitutions affecting protein function. If screening were to be repeated, I could isolate more alleles and establish if they contained mutant protein. If protein were detected, further characterisation and sequencing could be carried out.

The truncation mutants obtained were characterised, and proved useful in examining some aspects of domain structure, in relation to localisation and protein

interaction. Conclusions drawn from these studies are described in the following sections.

7.1.2 Mutant protein stability

Deletion of large C-terminal regions of Msps or D-TACC protein affects the level of the mutant protein in the fly. Mutant Msps proteins that are truncated before the 5th TOG domain (Msps^{C} and Msps^{1358}) were not detectable by western blotting, suggesting the protein was present at a very low level. Msps^{51} protein, missing half of the final TOG domain and the whole of the C-terminal region, is detected by western blotting but still at a lower level than wild-type Msps protein. D-TACC^{S3} protein level was also low. Clearly, truncation of these proteins affects stability.

Interestingly, it was possible to express MspsN protein, containing the first 4 TOG domains, in S2 cells at a detectable level. The discrepancy may be explained by a higher level of MspsN protein expression, due to transfection of more than one plasmid per cell. In this case, even if protein stability is affected, protein may still be detected due to the increases expression of protein in the cell.

7.1.3 The C-terminus of Msps is involved in D-TACC interaction

D-TACC is responsible for recruiting Msps to the centrosomes in mitosis and acentrosomal poles in female meiosis. An interaction between Msps and D-TACC has been previously demonstrated by co-immunoprecipition and pull down assays (Cullen and Ohkura, 2001; Lee *et al.*, 2001). The region of Msps responsible for centrosome localisation and D-TACC binding has not been identified. The availability of alleles expressing truncated proteins, gave the opportunity to examine the regions of Msps protein important for localisation and protein interaction.

In this study, immunoprecipitation experiments indicated that the C-terminal region of Msps is important for D-TACC binding. The small C-terminal deletion, present in the $Msps^{S10}$ mutant protein, does not affect binding, but removal of the entire C-terminal domain, in the $Msps^{51}$ mutant protein, abolishes binding. Furthermore, it has been demonstrated in our lab that a bacterially expressed GST fusion protein of the C-terminal of Msps, will bind to bacterially expressed MBP-D-TACC, in an *in vitro* binding assay (A Davidson, personal communication). The location of the D-TACC binding region of Msps appears to be conserved between *Drosophila* and *C. elegans*. In the Zyg-9 protein, TAC-1 interaction is mediated by the C-terminal domain (Bellanger and Gonczy, 2003). Further dissection within this area identified three separate regions able to bind to TAC-1 *in vitro*. Interestingly, the C-terminal region of Zyg-9 has no sequence homology with Msps, yet its role in binding TACC proteins appears to be conserved.

In addition to failing to interact with D-TACC, the $Msps^{51}$ protein also fails to localise to the centrosomes in mitosis. As D-TACC is important in recruiting Msps to the centrosome, it is unsurprising, that a mutant protein that fails to interact with D-TACC will be unable to localise to the poles.

I can not be certain that the C-terminal region is sufficient for Msps centrosome localisation from the studies of these mutant proteins. As $Msps^{51}$ is a truncated protein, the structure of the remaining protein may have been disrupted by removal of the C-terminal domain. If this is the case, the protein may still contain a centrosome localisation domain, but its function is lost due to protein misfolding. Whilst I can not rule out this possibility completely, evidence from other systems indicates that the centrosome localising region, in this family of proteins, lies in the C-terminal region (Graf *et al.*, 2000; Popov *et al.*, 2001). Expression of the Msps C-terminal region in cells and examining localisation, would determine if this region is sufficient for centrosome localisation.

7.1.4 Microtubule binding

The microtubule localisation domain in the Dis1/TOG family has not been well defined. In the budding and fission yeast proteins, relatively small regions in the C-terminal domain have been identified as microtubule binding sites (Usui *et al.*, 2003; Wang and Huffaker, 1997; Nakaseko *et al.*, 1996). In higher eukaryotes, a more complex picture of microtubule binding has arisen. In *Xenopus*, the C-terminal region of XMAP215 was found to localise to microtubules, but with a very punctate staining pattern (Popov *et al.*, 2001). The N-terminal region also localised to microtubules but only weakly. For correct wild-type localisation, the full length of protein was required. Conversely, in *Dictyostelium*, the C-terminal region was sufficient for localisation (Graf *et al.*, 2000).

In this study, I demonstrated that $Msps^{51}$ mutant protein does not localise along microtubules in mitotic cells of the larval neuroblasts. Similarly, an N-terminal fragment of a similar size to $Msps^{51}$ (Msps-N) does not show microtubule localisation when expressed in S2 cells (figure 5.15). This indicates that the N-terminal domain is not sufficient to localise Msps to microtubules. $Msps^{51}$ appears to have some affinity for microtubules in an *in vitro* microtubule binding assay, but this affinity is not sufficient for localisation in the cell. An N-terminal fragment of human TOG protein was shown to strongly bind to microtubules *in vitro*, suggesting such affinity is conserved (Charrasse *et al.*, 1998). The fact that both the N- and C-terminus have been implicated in microtubule binding signifies a complex association with microtubules that may involve various domains of the proteins.

In a microtubule spin down assay using embryo extracts, the majority of Msps protein was found to co-pellet with microtubules (Cullen *et al.*, 1999). In this study, the affinity of Msps for microtubules in larval extract was reduced compared to embryo extract. This difference could be due to the presence of different cell types in the two different tissues. Whilst embryos are predominantly full of rapidly dividing cells, larvae will contain more differentiated, interphase cells. Msps protein may have a

higher affinity for microtubules in mitotic cells than interphase cells, due to some kind of cell cycle or tissue specific regulation.

Protein activity is often regulated in a cell cycle dependent fashion by phosphorylation. XMAP215 is known to be hyperphosphorylated during mitosis and meiosis, suggesting that it is regulated during cell division (Gard and Kirschner, 1987). *In vitro* experiments indicated that the protein can be phosphorylated by CDK1, a regulator of mitotic progression, and that this phosphorylation alters XMAP215 function in regard to microtubule regulation (Vasquez *et al.*, 1999). It has not been demonstrated that this regulation occurs *in vivo*, so the true significance is not known.

7.1.5 Mitotic spindle function

Msps has been proposed to stabilise the spindle poles in both mitosis and female meiosis but the mechanism of this stabilisation has not been determined. As demonstrated in this study, following Msps mutation or depletion from S2 cells, multipolar spindles form. The mitotic spindle defects observed in the $msps^{51}$ mutant are very similar to those that result from near complete depletion of protein in the $msps^{P}$ mutant (Cullen *et al.*, 1999) and from Msps depletion from S2 cells. This result suggests that the $Msps^{51}$ protein is not carrying out any mitotic function, perhaps due to its failure to localise correctly. On the other hand, $msps^{51}$ homozygous larvae survive to a later stage of development than homozygotes of the null allele $msps^{D}$, suggesting that $Msps^{51}$ protein has some remaining function.

A possible explanation for such a phenotype could be the failure of the minus ends of microtubules to associate correctly with the centrosomes. Evidence from a study of budding yeast Stu2 described microtubules detaching from the SPB, when Stu2 localisation to the SPB was inhibited (Usui *et al.*, 2003). The spindle phenotype in *msps* mutant flies and Msps depleted culture cells could result from microtubules detaching from the centrosome. Live imaging of spindle formation in Msps depleted cells may

help to understand how these abnormal spindles form giving insight into the activity of Msps in maintaining spindle bipolarity.

7.1.6 Meiotic spindle function

The importance of Msps and D-TACC in maintaining spindle bipolarity in female meiosis was uncovered through the analysis a *msps* mutant allele (Cullen and Ohkura, 2001). The viable, female sterile allele, $msps^{208}$, contains wild-type Msps protein at approximately 10% of the level of wild-type flies. A third of the female meiotic spindles in this mutant are tripolar. Msps polar localisation is dependent upon the presence of D-TACC and a similar number of tripolar spindles were found in $d\text{-}tacc^{stella}$ oocytes.

As demonstrated in this study, $Msps^{S10}$ mutant protein retained spindle and pole localisation in female meiosis. However, tripolar spindles, at a lower level than in $msps^{208}$ oocytes, were seen in $msps^{S10}$ mutant oocytes. In the majority of cases, $Msps^{S10}$ protein functions sufficiently to produce a bipolar spindle. However, some loss of function must have occurred, resulting in the low level of spindle abnormalities. As localisation does not seem to be effected, there must be another change in protein activity.

The loss of function in the $Msps^{S10}$ protein has not been determined but there are a number of possibilities that could be investigated. Although many of the meiosis I arrested spindles in $msps^{S10}$ oocytes are bipolar, I do not know if they function correctly and progress to meiosis II. Furthermore, it is not known if they have a failure in pronuclear migration or the first mitotic divisions. Analysis of meiotic progression and the early stages of embryonic development may reveal more about function of Msps in these processes.

Unexpectedly, $d\text{-}tacc^{S3}$ does not produce a tripolar phenotype. The $d\text{-}tacc^{S3}$ allele is missing the C-terminal region, that has been shown to be sufficient for centrosome localisation and to recruit Msps to the centrosomes in mitosis (Lee *et al.*, 2001). It

would, therefore, be expected to fail to recruit Msps to the poles and result in a tripolar phenotype similar to *d-tacc*^{stella} and *msps*^{208}. However, the region of D-TACC responsible for acentrosomal poles localisation in female meiosis has not been determined, so it is possible that D-TACC^{S3} localises to the poles and recruits Msps. Due to absence of an antibody that would recognise D-TACC^{S3} in oocytes, I was unable to show if D-TACC^{S3} protein could localise to the poles by immunostaining. It is also important to establish if Msps can localise to the poles in this mutant.

7.1.7 Summary of screening and mutant analysis

Information about the domains of Msps can be deduced from studies of the new alleles. Mutant proteins (Msps^{51} and MspsN) specify a role for the C-terminal region in D-TACC binding and centrosome localisation. The N-terminal domain is implicated in microtubule binding but is not sufficient for normal microtubule localisation in the cell. Further characterisation of some of the alleles remains to be carried out. Further analysis of the *msps*^{S10} and *d-tacc*^{S3} female sterile mutants may give more insight into the functions of the two proteins. In addition, the phenotype of *msps*^{146} needs to be examined more closely, and the change in mutant protein sequence determined to understand the loss of function that has occurred in this protein.

Dissection of Dis1/TOG protein (e.g. N-terminal, mid and C-terminal regions) had already been carried out in a number of studies in other organisms (Nakaseko *et al.*, 1996; Popov *et al.*, 2001; Graf *et al.*, 2000), so I chose an alternative approach to investigate Msps domain structure and function. Random mutagenesis was used to try to isolate alleles with single amino acid substitutions or small deletions in order in investigate protein function in the fly. As many of the proteins produced by the new alleles have large truncations, leading to the loss of multiple functions, it has proved difficult to attribute specific functions to domains of the protein.

7.2 Msps function in interphase microtubule regulation

7.2.1 Msps has a role in interphase microtubule organisation

The Dis1/TOG family of MAPs are known regulators of microtubule dynamics and organisation but the majority of studies have focussed on functions in mitosis (Cassimeris and Morabito, 2004; Gergely *et al.*, 2003; Usui *et al.*, 2003; Nakaseko *et al.*, 2001; Severin *et al.*, 2001; Cullen and Ohkura, 2001; Cullen *et al.*, 1999; Matthews *et al.*, 1998), with interphase microtubule regulation featuring less prominently (Hestermann and Graf, 2004; Whittington *et al.*, 2001; Holmfeldt *et al.*, 2004; Hestermann and Graf, 2004). In this study, I used *Drosophila* culture cells to reveal the role of Msps in interphase microtubule regulation.

Msps protein localises to microtubules with particular concentrations at the plus ends, so is perfectly localised to influence microtubule organisation. Such a role was confirmed, as in Msps depleted cells, microtubules are unable to extend to the periphery of the cell and stable bundles of microtubules form. The importance of the protein for microtubule organisation in flies was confirmed by the presence of interphase microtubule defects in haemocytes, obtained from *msps* mutant larvae. In addition, a recent report described defects in microtubule organisation in *msps* mutant oocytes (Moon and Hazelrigg, 2004). Evidently, Msps is essential for interphase microtubule organisation, in addition to its previously described role in microtubule regulation in mitotic and meiotic cells (Cullen and Ohkura, 2001; Cullen *et al.*, 1999).

Roles in interphase microtubule regulation for Dis1/TOG family members in plants, *Dictyostelium* and yeast have been described (Whittington *et al.*, 2001; Kosco *et al.*, 2001; Radcliffe *et al.*, 1998; Graf *et al.*, 2003). Depletion of TOG from human cells was reported to give no interphase phenotype, although effects on microtubule dynamics were not measured (Gergely *et al.*, 2003; Holmfeldt *et al.*, 2004). The reason for the discrepancies between results for TOG and Msps proteins are not known. Perhaps there has been a divergence in function, the human protein not playing a major role in interphase microtubule regulation. Alternatively, microtubule dynamics can vary

between cell types (Shelden and Wadsworth, 1993) so it is possible that Msps microtubule regulation is of particular importance in S2 cells and in fly haemocytes but in the human cells used in the TOG studies, the protein plays a less significant role. It would be interesting to know if changes in microtubule dynamics did occur in TOG depleted cells, despite the lack of obvious changes in microtubule organisation.

7.2.2 A role for the Msps N-terminal domain in interphase function

In vitro microtubule regulating activities, for fragments of XMAP215 protein, have been described. Interestingly, an N-terminal fragment of XMAP215 has been reported to have both stabilising and destabilising activity *in vitro* (Popov *et al.*, 2001, Shiraz-Hisu., 2003). An N-terminal fragment (1-560aa) can suppress catastrophe in Xenopus egg extracts (Popov *et al.*, 2001). In fact, the fragment can fully rescue the loss of function caused by XMAP215 depletion. In experiments using GMPPCPP stabilised microtubules, the same N-terminal fragment had the ability to promote microtubule destabilisation (Shirasu-Hiza *et al.*, 2003).

Expression of the N-terminal domain of Msps (1-1133aa) partially rescues the interphase phenotype caused by Msps depletion, signifying that the domain contains an activity that is involved in Msps interphase function. This activity is disrupted by a point mutation in a conserved residue in the first TOG domain. The N-terminal region has some affinity for microtubules (this study and Charrasse *et al.*, 1998), explaining how the fragment, whilst not localising correctly, could act on microtubules when overexpressed. This data suggests that the N-terminal region can play an active role in interphase microtubule organisation, but for correct localisation to occur, the C-terminus is required.

The specific effect of MspsN on microtubule regulation is unknown. A smaller N-terminal fragment of XMAP215 is reported to fully rescue XMAP215 depletion. It would be interesting to examine if expression of a similar sized fragment of Msps fully rescues the Msps depletion.

7.2.3 Msps acts independently from the Kin I destabilising proteins in interphase microtubule regulation

In *Xenopus* egg extracts, XMAP215 antagonises the activity of the catastrophe promoter XKCM1 (Tournebize *et al.*, 2000), a member of the KinI family of destabilising proteins (Desai *et al.*, 1999). KinI homologues are conserved and roles in the regulation of microtubules in dividing and interphase have been confirmed in other organisms (Holmfeldt *et al.*, 2004; Kline-Smith and Walczak, 2002; Rogers *et al.*, 2004).

Msps regulation of interphase microtubule dynamics is not through the activity of the destabilising KinI proteins. In *Drosophila,* 3 kinesins closely related to *Xenopus* XKCM1 have been identified (Rogers *et al.*, 2004). Co-depletion of the KinI homologues with Msps, does not suppress the interphase microtubule defects, indicating that the abnormalities are not simply caused by overactivation of the KinI proteins. Intriguingly, co-depletion of Msps and Klp10A results in a stronger interphase phenotype, with microtubules becoming more compact and bundled. Rather than repressing the effect of Msps depletion, absence of Klp10A appears to be enhancing the effect. It is difficult to speculate on the reason behind this enhancement. Further experiments in live cells may reveal if there are alterations in microtubule dynamics, following Klp10A depletion, that may contribute to microtubule stability and bundling.

7.2.4 Msps acts independently of D-TACC in interphase

Depletion of Msps protein by RNAi in S2 cells results in a decrease in the level of D-TACC protein. Similar to results in *C. elegans,* the absence of Msps affects the stability of D-TACC protein (Bellanger and Gonczy, 2003; Le Bot *et al.*, 2003; Srayko *et al.*, 2003). On the other hand, D-TACC depletion did not affect the level of Msps protein when the reciprocal experiment was carried out. Furthermore, D-TACC does not influence Msps localisation to interphase microtubules and no interphase microtubule

phenotype is seen when D-TACC is depleted. From this evidence, D-TACC does not appear to play an obvious role with Msps in interphase microtubule regulation in S2 cells. Consistent with this idea, in the fly, Moon and Hazelrigg (2004) found no defects in cytoplasmic microtubule organisation in *d-tacc*^{stella} mutant oocytes, but clear changes in microtubule organisation in *msps* mutant oocytes. In conclusion, the data in this study and the study by Moon and Hazelrigg (2004) demonstrate that Msps function in interphase is independent of D-TACC.

7.2.5 Msps acts as an anti-pause factor in *Drosophila* cells

Analysis of microtubule dynamics revealed that, without Msps, there was a dramatic increase in the amount of time spent in a paused state, with very little time spent growing or shrinking. Anti-pausing activity has not been reported for members of the Dis1/TOG family, except for budding yeast Stu2, depletion of which moderately increased pausing of cytoplasmic microtubules (Kosco *et al.*, 2001). With such dynamics, the growth of microtubules will be very limited, explaining the failure of microtubules to extend out to the cell cortex. It is not known whether the microtubule bundling phenotype is a secondary consequence of the changes in microtubule dynamics, or whether Msps acts directly as an anti-bundling factor, in addition to its role in regulating microtubule dynamics.

One of the most mysterious functions of the Dis1/TOG family, that needs to be resolved, is the role of the proteins in regulating microtubule dynamics. *In vitro* experiments with XMAP215 established a role for the protein in the stabilisation of microtubules, through the promotion of growth and suppression of catastrophe (Charrasse *et al.*, 1998; Kinoshita *et al.*, 2002; Tournebize *et al.*, 2000; Gard and Kirschner, 1987; Vasquez *et al.*, 1994). Surprisingly, it was recently discovered that XMAP215 can also destabilise microtubules under certain conditions (van Breugel *et al.*, 2003; Shirasu-Hiza *et al.*, 2003) Furthermore, seemingly contradictory evidence from budding yeast indicates that Stu2 can also act as both a microtubule stabiliser and

destabiliser (Kosco *et al.*, 2001; van Breugel *et al.*, 2003). These recent findings have brought into question the true nature of Dis1/TOG function in microtubule regulation.

Shirasu-Hiza *et al.* (2003) proposed that the two opposing activities of stabilisation and destabilisation could be reconciled if the Dis1/TOG proteins functioned as anti-pause factors. The evidence from this study indicates that, in *Drosophila* cells, Msps acts as an anti-pause factor, promoting transitions from pause to growth and inhibiting transitions from growth to pause, supporting the hypothesis proposed by Shirasu *et al.* (2003). However, I did not find that Msps significantly promoted the transition from pause to shrinkage, as would be predicted if Msps was also acting as a destabiliser of the paused state. Brief pauses, not detected by our imaging system, could be the cause of the reduced depolymerisation rate found in Msps depleted cells. Such transitions would not be counted in our transition frequency data and could explain why an increase in shrinkage events was not detected. It is also possible that due to the partial depletion of the protein, the full effects of Msps are not apparent. In cells that are well depleted of Msps, microtubule stability is increased, as revealed by exposure to the depolymerising drug colchicine. The mechanism by which the microtubules are stabilised against colchicine is not clear, however, I speculate that a reduction in the number of catastrophes could result in this stabilisation.

The paused microtubule state has long been a mystery of microtubule dynamics *in vivo*. Pausing is much more frequent *in vivo* than *in vitro* (Shelden and Wadsworth, 1993; Tirnauer *et al.*, 1999; Rusan *et al.*, 2001; Walker *et al.*, 1988), and is often increased at the cortex (this study and (Komarova *et al.*, 2002)), suggesting that factors within the cell are involved in the promotion or suppression of the paused state. In the absence of Msps the paused state clearly predominates in the cell. Strikingly, partial depletion of Msps results in a more dramatic increase in pausing that near complete depletion of EB1, the only other protein shown to have a role as an anti-pause factor (Rogers *et al.*, 2002). Our data does not indicate if Msps protein directly destabilises the paused state by altering polymer conformation or whether it acts indirectly by preventing a pause factor from accessing the polymer. *In vitro* functional analysis of XMAP215 indicates that the protein has the intrinsic ability to promote the

polymerisation and depolymerisation of microtubules (Kinoshita *et al.*, 2002; Shirasu-Hiza *et al.*, 2003), supporting the former hypothesis. A factor that promotes pause in the cell has not been identified to date. Since microtubule pausing is so much higher in the cell than in pure tubulin solutions, it seems likely that such factors are still to be uncovered.

Much of the evidence for the role of the Dis1/TOG family in the regulation of microtubule dynamics has come from *in vitro* studies either with pure tubulin or in *Xenopus* egg extracts. Whilst these studies have been very informative, I felt that studying microtubules within an animal cell could help to resolve some of the conflicting data about these proteins that has recently come to light. We can clearly see that, at least in interphase, Msps acts as an anti-pause factor and consequentially is a major regulator of microtubule organisation in *Drosophila*. It is perhaps wrong to label the Dis1/TOG family as either stabilisers or destabilisers of microtubules, as at least in the case of Msps, promoter of microtubule dynamics appears to be more appropriate.

7.3 Characterisation of new meiotic spindle mutant, *triplet*

7.3.1 Role in spindle unification

The newly identified $trip^{GT28}$ allele produces a dramatic spindle phenotype in female meiosis, with the production of individual spindles around the chromosomes. To my knowledge such a phenotype has not been reported for any previous mutants. The individual spindles that form are well focused and appear to be functional, as they can progress to meiosis II (F. Cullen, personal communication).

Failure of spindle unification may result from defects in chromosome or spindle cohesion. The Trip protein was identified independently as a kinase with the ability to phosphorylate histone H2 when incorporated into chromatin (Aihara *et al.*, 2004). It is not known whether changes in histone phosphorylation produce the $trip^{GT28}$ spindle phenotype. Whilst this is a possibility, the spindle phenotype could be unrelated to the

histone phosphorylation, as kinases usually have many targets, and this may also be the case for the Trip kinase. Uncovering the phosphorylation targets of Trip will be vital in understanding the role of the kinase in spindle formation.

Depletion of Trip protein from S2 cells did not result in spindle abnormalities, suggesting that the protein is not essential for mitosis. Trip may have a function that is specific for spindle formation in female meiosis or it may have a non-essential role in mitosis. It would be interesting to inactivate the centrosomes, either by mutation or RNAi depletion of an essential component, in combination with Trip depletion, to examine if a mitotic function was revealed. The $trip^{GT28}$ allele produces a mutant protein in which the C-terminal region has been removed, but the kinase containing N-terminal region is still present and may retain some function. To determine if Trip is essential in the fly, a null allele of the gene will need to be isolated.

7.3.2 *trip* has an epistatic relationship with *msps* and *d-tacc*

To understand more about the role of *trip* in spindle assembly, double mutants between $trip^{GT28}$ and previously identified female meiotic spindle mutants were created. The interaction between $trip^{GT28}$ and ncd^{1} is purely additive. Both the individual spindles of the $trip^{GT28}$ mutation, and the unfocussed poles of the ncd^{1} mutation, can be seen in the double mutant, with no suppression or enhancement of either phenotype. On the other hand, the *trip* gene appears to have a more complex relationship with *msps* and *d-tacc*. The tripolar spindle phenotype witnessed in $msps^{208}$ and $d\text{-}tacc^{stella}$ mutant oocytes depends on some aspect of Trip protein function, as it was never found in $trip^{GT28}$ $msps^{208}/d\text{-}tacc^{stella}$ double mutants. This genetic interaction indicates that *d-tacc* and *msps* are epistatic to *trip,* as the genotype of the *trip* locus suppresses the phenotype of the *msps* and *d-tacc* alleles.

There are many possible interpretations of the genetic interaction between *msps/d-tacc* and *trip*. Msps/D-TACC may be acting downstream or upstream of Trip on spindle formation, or Msps/D-TACC, plus other proteins, may be activated by Trip

kinase activity. From the current data we can not determine how the two proteins functionally relate to produce this genetic interaction. The interaction between the three genes is intriguing, and through further understanding of Trip function, the nature of the relationship may be elucidated.

7.4 Summary and future directions

In this study, Msps was investigated by three approaches to understand more about its functions, and domains of the protein important for specific activities. Mutational analysis identified regions of the protein important for centrosomal localisation, D-TACC binding and microtubule affinity. The role of Msps in regulating microtubule plus end dynamics in interphase was uncovered by studies in *Drosophila* culture cells. Finally, a genetic interplay was discovered between *msps* and *d-tacc* and a novel meiotic spindle mutant, *trip*, through analysis of mutant alleles.

Many of the mutant alleles obtained in my screen produced truncations disrupting multiple protein functions. In the future, an alternative approach to domain analysis may be more successful in disrupting specific functional domains. For example, conserved residues may be specifically targeted by site-directed mutagenesis. Localisation and function could then be assayed by transfection into cells, transformation into flies or injection of recombinant protein into embryos.

The mechanism by which Msps maintains spindle pole integrity in both mitosis and meiosis has yet to be determined. Future experiments could focus on the role of Msps in maintaining spindle bipolarity. Live imaging of spindle formation, in cells depleted of Msps protein, may give insights into the mechanisms that may be involved.

Contrary to *in vitro* experiments in *Xenopus*, in *Drosophila cells*, Msps regulates interphase microtubule dynamics through the suppression of pausing. Future experiments could investigate the anti-pausing activity of Msps further, by examining regulation or interaction with other MAPs. Analysing the interplay between Msps and

other regulators of microtubule dynamics, such as EB (another pause suppressor), may result in a more comprehensive understanding of microtubule regulation in the cell.

Appendix I

The diagram below outlines the construction of a full length version of the *msps* gene with a single point mutation (E190K). This mutant was inserted into a transformation vector (pW8) and unsuccessful attempts were made to transform flies with the mutant gene construct

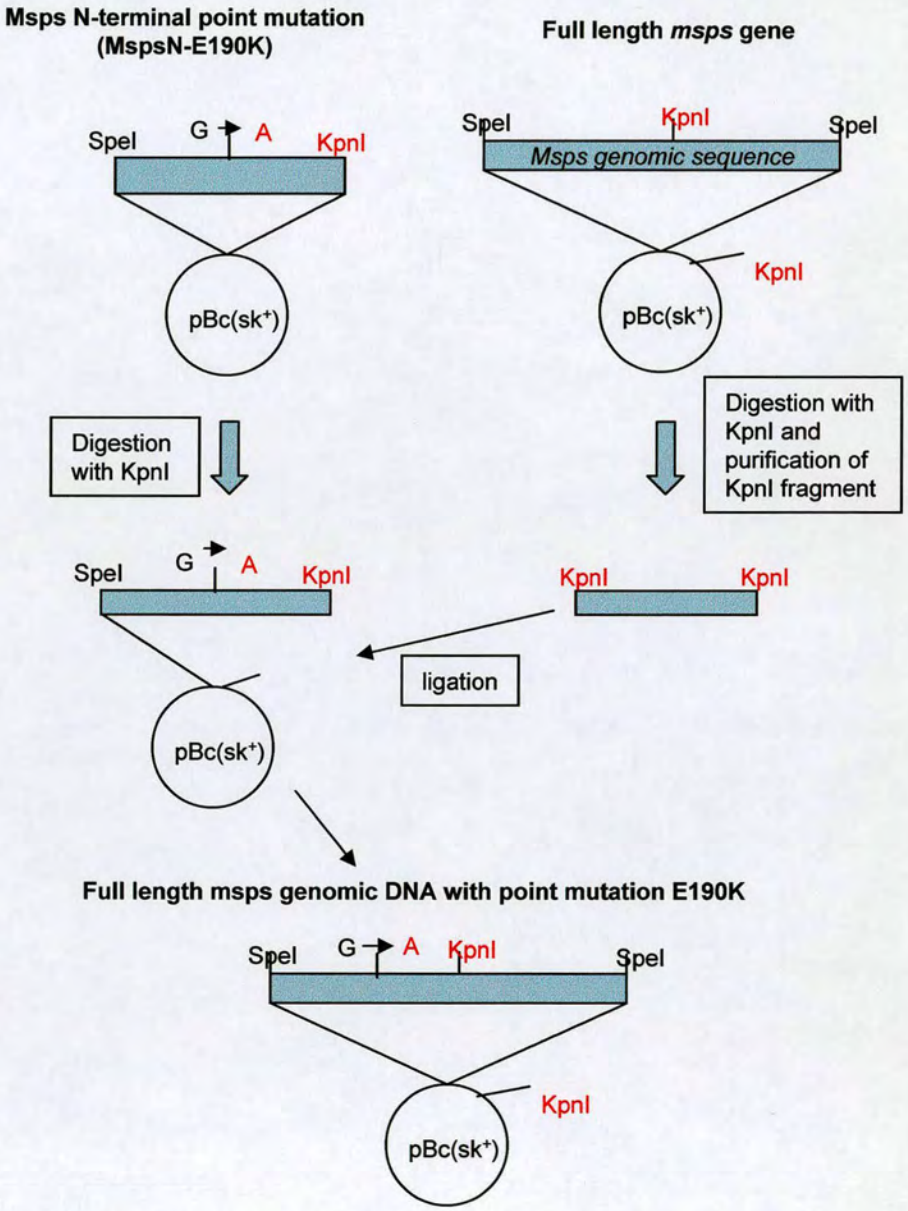

References

Ahmad,F.J., Yu,W., McNally,F.J., and Baas,P.W. (1999). An essential role for katanin in severing microtubules in the neuron. J. Cell Biol. *145*, 305-315.

Aihara,H., Nakagawa,T., Yasui,K., Ohta,T., Hirose,S., Dhomae,N., Takio,K., Kaneko,M., Takeshima,Y., Muramatsu,M., and Ito,T. (2004). Nucleosomal histone kinase-1 phosphorylates H2A Thr 119 during mitosis in the early Drosophila embryo. Genes Dev. *18*, 877-888.

Akhmanova,A., Hoogenraad,C.C., Drabek,K., Stepanova,T., Dortland,B., Verkerk,T., Vermeulen,W., Burgering,B.M., De Zeeuw,C.I., Grosveld,F., and Galjart,N. (2001). Clasps are CLIP-115 and -170 associating proteins involved in the regional regulation of microtubule dynamics in motile fibroblasts. Cell *104*, 923-935.

Allen,C. and Borisy,G.G. (1974). Structural polarity and directional growth of microtubules of Chlamydomonas flagella. J. Mol. Biol. *90*, 381-402.

Amos,L. and Klug,A. (1974). Arrangement of subunits in flagellar microtubules. J. Cell Sci. *14*, 523-549.

Andrade,M.A., Petosa,C., O'Donoghue,S.I., Muller,C.W., and Bork,P. (2001). Comparison of ARM and HEAT protein repeats. J. Mol. Biol. *309*, 1-18.

Arnal,I., Karsenti,E., and Hyman,A.A. (2000). Structural transitions at microtubule ends correlate with their dynamic properties in Xenopus egg extracts. J. Cell Biol. *149*, 767-774.

Arnaoutov,A. and Dasso,M. (2003). The Ran GTPase regulates kinetochore function. Dev. Cell *5*, 99-111.

Ashburner,M. (1989). Drosophila: A Laboratory Handbook. Cold Spring Harbor Laboratory Press, Cold Spring Harbor, NY, USA).

Banham,A.H. and Smith,G.L. (1992). Vaccinia virus gene B1R encodes a 34-kDa serine/threonine protein kinase that localizes in cytoplasmic factories and is packaged into virions. Virology *191*, 803-812.

Banks,J.D. and Heald,R. (2001). Chromosome movement: dynein-out at the kinetochore. Curr. Biol. *11*, R128-R131.

Bellanger,J.M. and Gonczy,P. (2003). TAC-1 and ZYG-9 form a complex that promotes microtubule assembly in C. elegans embryos. Curr. Biol. *13*, 1488-1498.

Belmont,L., Mitchison,T., and Deacon,H.W. (1996). Catastrophic revelations about Op18/stathmin. Trends Biochem. Sci. *21*, 197-198.

Belmont,L.D. and Mitchison,T.J. (1996). Identification of a protein that interacts with tubulin dimers and increases the catastrophe rate of microtubules. Cell *84*, 623-631.

Bornens,M. (2002). Centrosome composition and microtubule anchoring mechanisms. Curr. Opin. Cell Biol. *14*, 25-34.

Bouckson-Castaing,V., Moudjou,M., Ferguson,D.J., Mucklow,S., Belkaid,Y., Milon,G., and Crocker,P.R. (1996). Molecular characterisation of ninein, a new coiled-coil protein of the centrosome. J. Cell Sci. *109 (Pt 1)*, 179-190.

Brunner,D. and Nurse,P. (2000). CLIP170-like tip1p spatially organizes microtubular dynamics in fission yeast. Cell *102*, 695-704.

Bu,W. and Su,L.K. (2001). Regulation of microtubule assembly by human EB1 family proteins. Oncogene *20*, 3185-3192.

Caplow,M. and Fee,L. (2003). Concerning the chemical nature of tubulin subunits that cap and stabilize microtubules. Biochemistry *42*, 2122-2126.

Caplow,M., Ruhlen,R.L., and Shanks,J. (1994). The free energy for hydrolysis of a microtubule-bound nucleotide triphosphate is near zero: all of the free energy for hydrolysis is stored in the microtubule lattice. J. Cell Biol. *127*, 779-788.

Caplow,M. and Shanks,J. (1996). Evidence that a single monolayer tubulin-GTP cap is both necessary and sufficient to stabilize microtubules. Mol. Biol. Cell *7*, 663-675.

Carvalho,P., Tirnauer,J.S., and Pellman,D. (2003). Surfing on microtubule ends. Trends Cell Biol. *13*, 229-237.

Cassimeris,L. (1993). Regulation of microtubule dynamic instability. Cell Motil. Cytoskeleton *26*, 275-281.

Cassimeris,L. and Morabito,J. (2004). TOGp, the human homolog of XMAP215/Dis1, is required for centrosome integrity, spindle pole organization, and bipolar spindle assembly. Mol. Biol. Cell *15*, 1580-1590.

Charrasse,S., Schroeder,M., Gauthier-Rouviere,C., Ango,F., Cassimeris,L., Gard,D.L., and Larroque,C. (1998). The TOGp protein is a new human microtubule-associated protein homologous to the Xenopus XMAP215. J. Cell Sci. *111 (Pt 10)*, 1371-1383.

Chen,X.P., Yin,H., and Huffaker,T.C. (1998). The yeast spindle pole body component Spc72p interacts with Stu2p and is required for proper microtubule assembly. J. Cell Biol. *141*, 1169-1179.

Chretien,D., Fuller,S.D., and Karsenti,E. (1995). Structure of growing microtubule ends: two-dimensional sheets close into tubes at variable rates. J. Cell Biol. *129*, 1311-1328.

Cullen,C.F., Deak,P., Glover,D.M., and Ohkura,H. (1999). mini spindles: A gene encoding a conserved microtubule-associated protein required for the integrity of the mitotic spindle in Drosophila. J. Cell Biol. *146*, 1005-1018.

Cullen,C.F. and Ohkura,H. (2001). Msps protein is localized to acentrosomal poles to ensure bipolarity of Drosophila meiotic spindles. Nat. Cell Biol. *3*, 637-642.

David-Pfeuty,T., Erickson,H.P., and Pantaloni,D. (1977). Guanosinetriphosphatase activity of tubulin associated with microtubule assembly. Proc. Natl. Acad. Sci. U. S. A *74*, 5372-5376.

De Wulf,P., McAinsh,A.D., and Sorger,P.K. (2003). Hierarchical assembly of the budding yeast kinetochore from multiple subcomplexes. Genes Dev. *17*, 2902-2921.

DeLuca,J.G., Moree,B., Hickey,J.M., Kilmartin,J.V., and Salmon,E.D. (2002). hNuf2 inhibition blocks stable kinetochore-microtubule attachment and induces mitotic cell death in HeLa cells. J. Cell Biol. *159*, 549-555.

Desai,A. and Mitchison,T.J. (1997). Microtubule polymerization dynamics. Annu. Rev. Cell Dev. Biol. *13*, 83-117.

Desai,A., Verma,S., Mitchison,T.J., and Walczak,C.E. (1999c). Kin I kinesins are microtubule-destabilizing enzymes. Cell *96*, 69-78.

Desai,A., Verma,S., Mitchison,T.J., and Walczak,C.E. (1999b). Kin I kinesins are microtubule-destabilizing enzymes. Cell *96*, 69-78.

Desai,A., Verma,S., Mitchison,T.J., and Walczak,C.E. (1999a). Kin I kinesins are microtubule-destabilizing enzymes. Cell *96*, 69-78.

Drechsel,D.N. and Kirschner,M.W. (1994). The minimum GTP cap required to stabilize microtubules. Curr. Biol. *4*, 1053-1061.

Echard,A., Hickson,G.R., Foley,E., and O'Farrell,P.H. (2004). Terminal cytokinesis events uncovered after an RNAi screen. Curr. Biol. *14*, 1685-1693.

Ems-McClung,S.C., Zheng,Y., and Walczak,C.E. (2004). Importin alpha/beta and Ran-GTP regulate XCTK2 microtubule binding through a bipartite nuclear localization signal. Mol. Biol. Cell *15*, 46-57.

Endow,S.A., Henikoff,S., and Soler-Niedziela,L. (1990). Mediation of meiotic and early mitotic chromosome segregation in Drosophila by a protein related to kinesin. Nature *345*, 81-83.

Evans,L., Mitchison,T., and Kirschner,M. (1985). Influence of the centrosome on the structure of nucleated microtubules. J. Cell Biol. *100*, 1185-1191.

Fukata,M., Nakagawa,M., and Kaibuchi,K. (2003). Roles of Rho-family GTPases in cell polarisation and directional migration. Curr. Opin. Cell Biol. *15*, 590-597.

Fukata,M., Watanabe,T., Noritake,J., Nakagawa,M., Yamaga,M., Kuroda,S., Matsuura,Y., Iwamatsu,A., Perez,F., and Kaibuchi,K. (2002). Rac1 and Cdc42 capture microtubules through IQGAP1 and CLIP-170. Cell *109*, 873-885.

Garcia,M.A., Koonrugsa,N., and Toda,T. (2002). Spindle-kinetochore attachment requires the combined action of Kin I-like Klp5/6 and Alp14/Dis1-MAPs in fission yeast. EMBO J. *21*, 6015-6024.

Garcia,M.A., Vardy,L., Koonrugsa,N., and Toda,T. (2001). Fission yeast ch-TOG/XMAP215 homologue Alp14 connects mitotic spindles with the kinetochore and is a component of the Mad2-dependent spindle checkpoint. EMBO J. *20*, 3389-3401.

Gard,D.L. and Kirschner,M.W. (1987). A microtubule-associated protein from Xenopus eggs that specifically promotes assembly at the plus-end. J. Cell Biol. *105*, 2203-2215.

Gergely,F., Draviam,V.M., and Raff,J.W. (2003). The ch-TOG/XMAP215 protein is essential for spindle pole organization in human somatic cells. Genes Dev. *17*, 336-341.

Gergely,F., Karlsson,C., Still,I., Cowell,J., Kilmartin,J., and Raff,J.W. (2000a). The TACC domain identifies a family of centrosomal proteins that can interact with microtubules. Proc. Natl. Acad. Sci. U. S. A *97*, 14352-14357.

Gergely,F., Kidd,D., Jeffers,K., Wakefield,J.G., and Raff,J.W. (2000b). D-TACC: a novel centrosomal protein required for normal spindle function in the early Drosophila embryo. EMBO J. *19*, 241-252.

Giansanti,M.G., Bonaccorsi,S., Bucciarelli,E., and Gatti,M. (2001). Drosophila male meiosis as a model system for the study of cytokinesis in animal cells. Cell Struct. Funct. *26*, 609-617.

Glotzer,M. (2001). Animal cell cytokinesis. Annu. Rev. Cell Dev. Biol. *17*, 351-386.

Glotzer,M. (2004). Cleavage furrow positioning. J. Cell Biol. *164*, 347-351.

Glover,D.M. (1989). Mitosis in Drosophila. J. Cell Sci. *92 (Pt 2)*, 137-146.

Glover,D.M., Leibowitz,M.H., McLean,D.A., and Parry,H. (1995). Mutations in aurora prevent centrosome separation leading to the formation of monopolar spindles. Cell *81*, 95-105.

Goldstein,L.S. (2001). Molecular motors: from one motor many tails to one motor many tales. Trends Cell Biol. *11*, 477-482.

Gonzalez,C. and Glover D.M. (1993). Techniques for studying mitosis in *Drosophila*. In The Cell cycle: A Practical Approach., P.Fantes and R.Brooks, eds. IRL Press, Oxford, UK), pp. 163-168.

Goshima,G. and Vale,R.D. (2003). The roles of microtubule-based motor proteins in mitosis: comprehensive RNAi analysis in the Drosophila S2 cell line. J. Cell Biol. *162*, 1003-1016.

Graf,R., Daunderer,C., and Schliwa,M. (2000). Dictyostelium DdCP224 is a microtubule-associated protein and a permanent centrosomal resident involved in centrosome duplication. J. Cell Sci. *113 (Pt 10)*, 1747-1758.

Graf,R., Euteneuer,U., Ho,T.H., and Rehberg,M. (2003). Regulated expression of the centrosomal protein DdCP224 affects microtubule dynamics and reveals mechanisms for the control of supernumerary centrosome number. Mol. Biol. Cell *14*, 4067-4074.

Groves,M.R., Hanlon,N., Turowski,P., Hemmings,B.A., and Barford,D. (1999). The structure of the protein phosphatase 2A PR65/A subunit reveals the conformation of its 15 tandemly repeated HEAT motifs. Cell *96*, 99-110.

Gruss,O.J., Carazo-Salas,R.E., Schatz,C.A., Guarguaglini,G., Kast,J., Wilm,M., Le Bot,N., Vernos,I., Karsenti,E., and Mattaj,I.W. (2001). Ran induces spindle assembly by reversing the inhibitory effect of importin alpha on TPX2 activity. Cell *104*, 83-93.

Haren,L. and Merdes,A. (2002). Direct binding of NuMA to tubulin is mediated by a novel sequence motif in the tail domain that bundles and stabilizes microtubules. J. Cell Sci. *115*, 1815-1824.

Hatsumi,M. and Endow,S.A. (1992). Mutants of the microtubule motor protein, nonclaret disjunctional, affect spindle structure and chromosome movement in meiosis and mitosis. J. Cell Sci. *101 (Pt 3)*, 547-559.

Hayden,J.H., Bowser,S.S., and Rieder,C.L. (1990). Kinetochores capture astral microtubules during chromosome attachment to the mitotic spindle: direct visualization in live newt lung cells. J. Cell Biol. *111*, 1039-1045.

He,X., Rines,D.R., Espelin,C.W., and Sorger,P.K. (2001). Molecular analysis of kinetochore-microtubule attachment in budding yeast. Cell *106*, 195-206.

Heald,R. (2000). Motor function in the mitotic spindle. Cell *102*, 399-402.

Heald,R., Tournebize,R., Blank,T., Sandaltzopoulos,R., Becker,P., Hyman,A., and Karsenti,E. (1996). Self-organization of microtubules into bipolar spindles around artificial chromosomes in Xenopus egg extracts. Nature *382*, 420-425.

Hestermann,A. and Graf,R. (2004). The XMAP215-family protein DdCP224 is required for cortical interactions of microtubules. BMC. Cell Biol. *5*, 24.

Holmfeldt,P., Stenmark,S., and Gullberg,M. (2004). Differential functional interplay of TOGp/XMAP215 and the KinI kinesin MCAK during interphase and mitosis. EMBO J. *23*, 627-637.

Holy,T.E. and Leibler,S. (1994). Dynamic instability of microtubules as an efficient way to search in space. Proc. Natl. Acad. Sci. U. S. A *91*, 5682-5685.

Horio,T. and Hotani,H. (1986). Visualization of the dynamic instability of individual microtubules by dark-field microscopy. Nature *321*, 605-607.

Howe,M., McDonald,K.L., Albertson,D.G., and Meyer,B.J. (2001). HIM-10 is required for kinetochore structure and function on Caenorhabditis elegans holocentric chromosomes. J. Cell Biol. *153*, 1227-1238.

Howell,B., Larsson,N., Gullberg,M., and Cassimeris,L. (1999). Dissociation of the tubulin-sequestering and microtubule catastrophe-promoting activities of oncoprotein 18/stathmin. Mol. Biol. Cell *10*, 105-118.

Hunter,A.W., Caplow,M., Coy,D.L., Hancock,W.O., Diez,S., Wordeman,L., and Howard,J. (2003). The kinesin-related protein MCAK is a microtubule depolymerase that forms an ATP-hydrolyzing complex at microtubule ends. Mol. Cell *11*, 445-457.

Hyman,A.A., Chretien,D., Arnal,I., and Wade,R.H. (1995). Structural changes accompanying GTP hydrolysis in microtubules: information from a slowly hydrolyzable analogue guanylyl-(alpha,beta)-methylene-diphosphonate. J. Cell Biol. *128*, 117-125.

Janosi,I.M., Chretien,D., and Flyvbjerg,H. (1998). Modeling elastic properties of microtubule tips and walls. Eur. Biophys. J. *27*, 501-513.

Jourdain,L., Curmi,P., Sobel,A., Pantaloni,D., and Carlier,M.F. (1997). Stathmin: a tubulin-sequestering protein which forms a ternary T2S complex with two tubulin molecules. Biochemistry *36*, 10817-10821.

Kalab,P., Pu,R.T., and Dasso,M. (1999). The ran GTPase regulates mitotic spindle assembly. Curr. Biol. *9*, 481-484.

Khodjakov,A. and Rieder,C.L. (1999). The sudden recruitment of gamma-tubulin to the centrosome at the onset of mitosis and its dynamic exchange throughout the cell cycle, do not require microtubules. J. Cell Biol. *146*, 585-596.

Kinoshita,K., Arnal,I., Desai,A., Drechsel,D.N., and Hyman,A.A. (2001). Reconstitution of physiological microtubule dynamics using purified components. Science *294*, 1340-1343.

Kinoshita,K., Habermann,B., and Hyman,A.A. (2002). XMAP215: a key component of the dynamic microtubule cytoskeleton. Trends Cell Biol. *12*, 267-273.

Kirschner,M. and Mitchison,T. (1986). Beyond self-assembly: from microtubules to morphogenesis. Cell *45*, 329-342.

Kline-Smith,S.L., Khodjakov,A., Hergert,P., and Walczak,C.E. (2004). Depletion of centromeric MCAK leads to chromosome congression and segregation defects due to improper kinetochore attachments. Mol. Biol. Cell *15*, 1146-1159.

Kline-Smith,S.L. and Walczak,C.E. (2002). The microtubule-destabilizing kinesin XKCM1 regulates microtubule dynamic instability in cells. Mol. Biol. Cell *13*, 2718-2731.

Kobayashi,N. and Mundel,P. (1998). A role of microtubules during the formation of cell processes in neuronal and non-neuronal cells. Cell Tissue Res. *291*, 163-174.

Komarova,Y.A., Akhmanova,A.S., Kojima,S., Galjart,N., and Borisy,G.G. (2002a). Cytoplasmic linker proteins promote microtubule rescue in vivo. J. Cell Biol. *159*, 589-599.

Komarova,Y.A., Vorobjev,I.A., and Borisy,G.G. (2002b). Life cycle of MTs: persistent growth in the cell interior, asymmetric transition frequencies and effects of the cell boundary. J. Cell Sci. *115*, 3527-3539.

Kosco,K.A., Pearson,C.G., Maddox,P.S., Wang,P.J., Adams,I.R., Salmon,E.D., Bloom,K., and Huffaker,T.C. (2001). Control of microtubule dynamics by Stu2p is essential for spindle orientation and metaphase chromosome alignment in yeast. Mol. Biol. Cell *12*, 2870-2880.

Kwon,M. and Scholey,J.M. (2004). Spindle mechanics and dynamics during mitosis in Drosophila. Trends Cell Biol. *14*, 194-205.

Le Bot,N., Tsai,M.C., Andrews,R.K., and Ahringer,J. (2003). TAC-1, a regulator of microtubule length in the C. elegans embryo. Curr. Biol. *13*, 1499-1505.

Lee,M.J., Gergely,F., Jeffers,K., Peak-Chew,S.Y., and Raff,J.W. (2001). Msps/XMAP215 interacts with the centrosomal protein D-TACC to regulate microtubule behaviour. Nat. Cell Biol. *3*, 643-649.

Lemos,C.L., Sampaio,P., Maiato,H., Costa,M., Omel'yanchuk,L.V., Liberal,V., and Sunkel,C.E. (2000). Mast, a conserved microtubule-associated protein required for bipolar mitotic spindle organization. EMBO J. *19*, 3668-3682.

Li,H.Y. and Zheng,Y. (2004). Phosphorylation of RCC1 in mitosis is essential for producing a high RanGTP concentration on chromosomes and for spindle assembly in mammalian cells. Genes Dev. *18*, 512-527.

MacNeal,R.K. and Purich,D.L. (1978). Stoichiometry and role of GTP hydrolysis in bovine neurotubule assembly. J. Biol. Chem. *253*, 4683-4687.

Maiato,H., Fairley,E.A., Rieder,C.L., Swedlow,J.R., Sunkel,C.E., and Earnshaw,W.C. (2003). Human CLASP1 is an outer kinetochore component that regulates spindle microtubule dynamics. Cell *113*, 891-904.

Maiato,H., Sampaio,P., Lemos,C.L., Findlay,J., Carmena,M., Earnshaw,W.C., and Sunkel,C.E. (2002). MAST/Orbit has a role in microtubule-kinetochore attachment and is essential for chromosome alignment and maintenance of spindle bipolarity. J. Cell Biol. *157*, 749-760.

Mallik,R. and Gross,S.P. (2004). Molecular motors: strategies to get along. Curr. Biol. *14*, R971-R982.

Mandelkow,E.M., Mandelkow,E., and Milligan,R.A. (1991). Microtubule dynamics and microtubule caps: a time-resolved cryo-electron microscopy study. J. Cell Biol. *114*, 977-991.

Maney,T., Hunter,A.W., Wagenbach,M., and Wordeman,L. (1998). Mitotic centromere-associated kinesin is important for anaphase chromosome segregation. J. Cell Biol. *142*, 787-801.

Marklund,U., Larsson,N., Gradin,H.M., Brattsand,G., and Gullberg,M. (1996). Oncoprotein 18 is a phosphorylation-responsive regulator of microtubule dynamics. EMBO J. *15*, 5290-5298.

Matthews,L.R., Carter,P., Thierry-Mieg,D., and Kemphues,K. (1998). ZYG-9, a Caenorhabditis elegans protein required for microtubule organization and function, is a component of meiotic and mitotic spindle poles. J. Cell Biol. *141*, 1159-1168.

Matthies,H.J., McDonald,H.B., Goldstein,L.S., and Theurkauf,W.E. (1996). Anastral meiotic spindle morphogenesis: role of the non-claret disjunctional kinesin-like protein. J. Cell Biol. *134*, 455-464.

McCleland,M.L., Gardner,R.D., Kallio,M.J., Daum,J.R., Gorbsky,G.J., Burke,D.J., and Stukenberg,P.T. (2003). The highly conserved Ndc80 complex is required for

kinetochore assembly, chromosome congression, and spindle checkpoint activity. Genes Dev. *17*, 101-114.

McEwen,B.F., Chan,G.K., Zubrowski,B., Savoian,M.S., Sauer,M.T., and Yen,T.J. (2001). CENP-E is essential for reliable bioriented spindle attachment, but chromosome alignment can be achieved via redundant mechanisms in mammalian cells. Mol. Biol. Cell *12*, 2776-2789.

McNally,F.J., Okawa,K., Iwamatsu,A., and Vale,R.D. (1996). Katanin, the microtubule-severing ATPase, is concentrated at centrosomes. J. Cell Sci. *109 (Pt 3)*, 561-567.

McNally,F.J. and Thomas,S. (1998). Katanin is responsible for the M-phase microtubule-severing activity in Xenopus eggs. Mol. Biol. Cell *9*, 1847-1861.

Merdes,A., Heald,R., Samejima,K., Earnshaw,W.C., and Cleveland,D.W. (2000). Formation of spindle poles by dynein/dynactin-dependent transport of NuMA. J. Cell Biol. *149*, 851-862.

Mitchison,T. and Kirschner,M. (1984). Dynamic instability of microtubule growth. Nature *312*, 237-242.

Mogensen,M.M. (1999). Microtubule release and capture in epithelial cells. Biol. Cell *91*, 331-341.

Mogensen,M.M., Malik,A., Piel,M., Bouckson-Castaing,V., and Bornens,M. (2000). Microtubule minus-end anchorage at centrosomal and non-centrosomal sites: the role of ninein. J. Cell Sci. *113 (Pt 17)*, 3013-3023.

Mogensen,M.M. and Tucker,J.B. (1987). Evidence for microtubule nucleation at plasma membrane-associated sites in Drosophila. J. Cell Sci. *88 (Pt 1)*, 95-107.

Moon,W. and Hazelrigg,T. (2004). The Drosophila microtubule-associated protein mini spindles is required for cytoplasmic microtubules in oogenesis. Curr. Biol. *14*, 1957-1961.

Moore,W., Zhang,C., and Clarke,P.R. (2002). Targeting of RCC1 to chromosomes is required for proper mitotic spindle assembly in human cells. Curr. Biol. *12*, 1442-1447.

Moores,C.A., Yu,M., Guo,J., Beraud,C., Sakowicz,R., and Milligan,R.A. (2002). A mechanism for microtubule depolymerization by KinI kinesins. Mol. Cell *9*, 903-909.

Moritz,M., Braunfeld,M.B., Guenebaut,V., Heuser,J., and Agard,D.A. (2000). Structure of the gamma-tubulin ring complex: a template for microtubule nucleation. Nat. Cell Biol. *2*, 365-370.

Moritz,M., Braunfeld,M.B., Sedat,J.W., Alberts,B., and Agard,D.A. (1995). Microtubule nucleation by gamma-tubulin-containing rings in the centrosome. Nature *378*, 638-640.

Muller-Reichert,T., Chretien,D., Severin,F., and Hyman,A.A. (1998). Structural changes at microtubule ends accompanying GTP hydrolysis: information from a slowly hydrolyzable analogue of GTP, guanylyl (alpha,beta)methylenediphosphonate. Proc. Natl. Acad. Sci. U. S. A *95*, 3661-3666.

Nabeshima,K., Kurooka,H., Takeuchi,M., Kinoshita,K., Nakaseko,Y., and Yanagida,M. (1995). p93dis1, which is required for sister chromatid separation, is a novel microtubule and spindle pole body-associating protein phosphorylated at the Cdc2 target sites. Genes Dev. *9*, 1572-1585.

Nabeshima,K., Nakagawa,T., Straight,A.F., Murray,A., Chikashige,Y., Yamashita,Y.M., Hiraoka,Y., and Yanagida,M. (1998). Dynamics of centromeres during metaphase-anaphase transition in fission yeast: Dis1 is implicated in force balance in metaphase bipolar spindle. Mol. Biol. Cell *9*, 3211-3225.

Nachury,M.V., Maresca,T.J., Salmon,W.C., Waterman-Storer,C.M., Heald,R., and Weis,K. (2001). Importin beta is a mitotic target of the small GTPase Ran in spindle assembly. Cell *104*, 95-106.

Nakamura,M., Zhou,X.Z., and Lu,K.P. (2001). Critical role for the EB1 and APC interaction in the regulation of microtubule polymerization. Curr. Biol. *11*, 1062-1067.

Nakaseko,Y., Goshima,G., Morishita,J., and Yanagida,M. (2001). M phase-specific kinetochore proteins in fission yeast: microtubule-associating Dis1 and Mtc1 display rapid separation and segregation during anaphase. Curr. Biol. *11*, 537-549.

Nakaseko,Y., Nabeshima,K., Kinoshita,K., and Yanagida,M. (1996). Dissection of fission yeast microtubule associating protein p93Dis1: regions implicated in regulated localization and microtubule interaction. Genes Cells *1*, 633-644.

Neuwald,A.F. and Hirano,T. (2000). HEAT repeats associated with condensins, cohesins, and other complexes involved in chromosome-related functions. Genome Res. *10*, 1445-1452.

Nguyen,H.L., Gruber,D., and Bulinski,J.C. (1999). Microtubule-associated protein 4 (MAP4) regulates assembly, protomer-polymer partitioning and synthesis of tubulin in cultured cells. J. Cell Sci. *112 (Pt 12)*, 1813-1824.

Ogawa,T., Nitta,R., Okada,Y., and Hirokawa,N. (2004). A common mechanism for microtubule destabilizers-M type kinesins stabilize curling of the protofilament using the class-specific neck and loops. Cell *116*, 591-602.

Ohkura,H., Adachi,Y., Kinoshita,N., Niwa,O., Toda,T., and Yanagida,M. (1988). Cold-sensitive and caffeine-supersensitive mutants of the Schizosaccharomyces pombe dis genes implicated in sister chromatid separation during mitosis. EMBO J. *7*, 1465-1473.

Ohkura,H., Garcia,M.A., and Toda,T. (2001). Dis1/TOG universal microtubule adaptors - one MAP for all? J. Cell Sci. *114*, 3805-3812.

Ookata,K., Hisanaga,S., Bulinski,J.C., Murofushi,H., Aizawa,H., Itoh,T.J., Hotani,H., Okumura,E., Tachibana,K., and Kishimoto,T. (1995). Cyclin B interaction with microtubule-associated protein 4 (MAP4) targets p34cdc2 kinase to microtubules and is a potential regulator of M-phase microtubule dynamics. J. Cell Biol. *128*, 849-862.

Panda,D., Miller,H.P., and Wilson,L. (2002). Determination of the size and chemical nature of the stabilizing "cap" at microtubule ends using modulators of polymerization dynamics. Biochemistry *41*, 1609-1617.

Perez,F., Diamantopoulos,G.S., Stalder,R., and Kreis,T.E. (1999). CLIP-170 highlights growing microtubule ends in vivo. Cell *96*, 517-527.

Pierre,P., Scheel,J., Rickard,J.E., and Kreis,T.E. (1992). CLIP-170 links endocytic vesicles to microtubules. Cell *70*, 887-900.

Popov,A.V., Pozniakovsky,A., Arnal,I., Antony,C., Ashford,A.J., Kinoshita,K., Tournebize,R., Hyman,A.A., and Karsenti,E. (2001). XMAP215 regulates microtubule dynamics through two distinct domains. EMBO J. *20*, 397-410.

Putkey,F.R., Cramer,T., Morphew,M.K., Silk,A.D., Johnson,R.S., McIntosh,J.R., and Cleveland,D.W. (2002). Unstable kinetochore-microtubule capture and chromosomal instability following deletion of CENP-E. Dev. Cell *3*, 351-365.

Quintyne,N.J., Gill,S.R., Eckley,D.M., Crego,C.L., Compton,D.A., and Schroer,T.A. (1999). Dynactin is required for microtubule anchoring at centrosomes. J. Cell Biol. *147*, 321-334.

Quintyne,N.J. and Schroer,T.A. (2002). Distinct cell cycle-dependent roles for dynactin and dynein at centrosomes. J. Cell Biol. *159*, 245-254.

Radcliffe,P., Hirata,D., Childs,D., Vardy,L., and Toda,T. (1998). Identification of novel temperature-sensitive lethal alleles in essential beta-tubulin and nonessential alpha 2-tubulin genes as fission yeast polarity mutants. Mol. Biol. Cell *9*, 1757-1771.

Raemaekers,T., Ribbeck,K., Beaudouin,J., Annaert,W., Van Camp,M., Stockmans,I., Smets,N., Bouillon,R., Ellenberg,J., and Carmeliet,G. (2003). NuSAP, a novel microtubule-associated protein involved in mitotic spindle organization. J. Cell Biol. *162*, 1017-1029.

Rickard,J.E. and Kreis,T.E. (1990). Identification of a novel nucleotide-sensitive microtubule-binding protein in HeLa cells. J. Cell Biol. *110*, 1623-1633.

Rogers,G.C., Rogers,S.L., Schwimmer,T.A., Ems-McClung,S.C., Walczak,C.E., Vale,R.D., Scholey,J.M., and Sharp,D.J. (2004). Two mitotic kinesins cooperate to drive sister chromatid separation during anaphase. Nature *427*, 364-370.

Rogers,S.L., Rogers,G.C., Sharp,D.J., and Vale,R.D. (2002). Drosophila EB1 is important for proper assembly, dynamics, and positioning of the mitotic spindle. J. Cell Biol. *158*, 873-884.

Rogers,S.L., Wiedemann,U., Stuurman,N., and Vale,R.D. (2003). Molecular requirements for actin-based lamella formation in Drosophila S2 cells. J. Cell Biol. *162*, 1079-1088.

Rusan,N.M., Fagerstrom,C.J., Yvon,A.M., and Wadsworth,P. (2001). Cell cycle-dependent changes in microtubule dynamics in living cells expressing green fluorescent protein-alpha tubulin. Mol. Biol. Cell *12*, 971-980.

Sagolla,M.J., Uzawa,S., and Cande,W.Z. (2003). Individual microtubule dynamics contribute to the function of mitotic and cytoplasmic arrays in fission yeast. J. Cell Sci. *116*, 4891-4903.

Sambrook J, Fritsch EF, and Maniatis T (1989). Molecular Cloning: A Laboratory Manual. Cold Spring Harbor Laboratory Press, NY.

Sato,M., Vardy,L., Angel,G.M., Koonrugsa,N., and Toda,T. (2004). Interdependency of fission yeast Alp14/TOG and coiled coil protein Alp7 in microtubule localization and bipolar spindle formation. Mol. Biol. Cell *15*, 1609-1622.

Sawin,K.E., Lourenco,P.C., and Snaith,H.A. (2004). Microtubule nucleation at non-spindle pole body microtubule-organizing centers requires fission yeast centrosomin-related protein mod20p. Curr. Biol. *14*, 763-775.

Saxton,W.M. (2001). Microtubules, motors, and mRNA localization mechanisms: watching fluorescent messages move. Cell *107*, 707-710.

Saxton,W.M., Stemple,D.L., Leslie,R.J., Salmon,E.D., Zavortink,M., and McIntosh,J.R. (1984). Tubulin dynamics in cultured mammalian cells. J. Cell Biol. *99*, 2175-2186.

Schatz,C.A., Santarella,R., Hoenger,A., Karsenti,E., Mattaj,I.W., Gruss,O.J., and Carazo-Salas,R.E. (2003). Importin alpha-regulated nucleation of microtubules by TPX2. EMBO J. *22*, 2060-2070.

Severin,F., Habermann,B., Huffaker,T., and Hyman,T. (2001). Stu2 promotes mitotic spindle elongation in anaphase. J. Cell Biol. *153*, 435-442.

Sharp,D.J., Brown,H.M., Kwon,M., Rogers,G.C., Holland,G., and Scholey,J.M. (2000). Functional coordination of three mitotic motors in Drosophila embryos. Mol. Biol. Cell *11*, 241-253.

Sharp,D.J., McDonald,K.L., Brown,H.M., Matthies,H.J., Walczak,C., Vale,R.D., Mitchison,T.J., and Scholey,J.M. (1999). The bipolar kinesin, KLP61F, cross-links microtubules within interpolar microtubule bundles of Drosophila embryonic mitotic spindles. J. Cell Biol. *144*, 125-138.

Shelden,E. and Wadsworth,P. (1993). Observation and quantification of individual microtubule behavior in vivo: microtubule dynamics are cell-type specific. J. Cell Biol. *120*, 935-945.

Shiina,N., Gotoh,Y., and Nishida,E. (1995). Microtubule-severing activity in M phase. Trends Cell Biol. *5*, 283-286.

Shirasu-Hiza,M., Coughlin,P., and Mitchison,T. (2003). Identification of XMAP215 as a microtubule-destabilizing factor in Xenopus egg extract by biochemical purification. J. Cell Biol. *161*, 349-358.

Smith,D.E. and Fisher,P.A. (1984). Identification, developmental regulation, and response to heat shock of two antigenically related forms of a major nuclear envelope protein in Drosophila embryos: application of an improved method for affinity purification of antibodies using polypeptides immobilized on nitrocellulose blots. J. Cell Biol. *99*, 20-28.

Spiegelman,B.M., Penningroth,S.M., and Kirschner,M.W. (1977). Turnover of tubulin and the N site GTP in Chinese hamster ovary cells. Cell *12*, 587-600.

Srayko,M., Quintin,S., Schwager,A., and Hyman,A.A. (2003). Caenorhabditis elegans TAC-1 and ZYG-9 form a complex that is essential for long astral and spindle microtubules. Curr. Biol. *13*, 1506-1511.

Sunkel,C.E. and Glover,D.M. (1988). polo, a mitotic mutant of Drosophila displaying abnormal spindle poles. J. Cell Sci. *89 (Pt 1)*, 25-38.

Takei,Y., Teng,J., Harada,A., and Hirokawa,N. (2000). Defects in axonal elongation and neuronal migration in mice with disrupted tau and map1b genes. J. Cell Biol. *150*, 989-1000.

Theurkauf,W.E. and Hawley,R.S. (1992). Meiotic spindle assembly in Drosophila females: behavior of nonexchange chromosomes and the effects of mutations in the nod kinesin-like protein. J. Cell Biol. *116*, 1167-1180.

Tirnauer,J.S. and Bierer,B.E. (2000). EB1 proteins regulate microtubule dynamics, cell polarity, and chromosome stability. J. Cell Biol. *149*, 761-766.

Tirnauer,J.S., Canman,J.C., Salmon,E.D., and Mitchison,T.J. (2002a). EB1 targets to kinetochores with attached, polymerizing microtubules. Mol. Biol. Cell *13*, 4308-4316.

Tirnauer,J.S., Grego,S., Salmon,E.D., and Mitchison,T.J. (2002b). EB1-microtubule interactions in Xenopus egg extracts: role of EB1 in microtubule stabilization and mechanisms of targeting to microtubules. Mol. Biol. Cell *13*, 3614-3626.

Tirnauer,J.S., O'Toole,E., Berrueta,L., Bierer,B.E., and Pellman,D. (1999a). Yeast Bim1p promotes the G1-specific dynamics of microtubules. J. Cell Biol. *145*, 993-1007.

Tirnauer,J.S., O'Toole,E., Berrueta,L., Bierer,B.E., and Pellman,D. (1999b). Yeast Bim1p promotes the G1-specific dynamics of microtubules. J. Cell Biol. *145*, 993-1007.

Tournebize,R., Popov,A., Kinoshita,K., Ashford,A.J., Rybina,S., Pozniakovsky,A., Mayer,T.U., Walczak,C.E., Karsenti,E., and Hyman,A.A. (2000). Control of microtubule dynamics by the antagonistic activities of XMAP215 and XKCM1 in Xenopus egg extracts. Nat. Cell Biol. *2*, 13-19.

Tran,P.T., Joshi,P., and Salmon,E.D. (1997a). How tubulin subunits are lost from the shortening ends of microtubules. J. Struct. Biol. *118*, 107-118.

Tran,P.T., Walker,R.A., and Salmon,E.D. (1997b). A metastable intermediate state of microtubule dynamic instability that differs significantly between plus and minus ends. J. Cell Biol. *138*, 105-117.

Usui,T., Maekawa,H., Pereira,G., and Schiebel,E. (2003). The XMAP215 homologue Stu2 at yeast spindle pole bodies regulates microtubule dynamics and anchorage. EMBO J. *22*, 4779-4793.

Vaisberg,E.A., Koonce,M.P., and McIntosh,J.R. (1993). Cytoplasmic dynein plays a role in mammalian mitotic spindle formation. J. Cell Biol. *123*, 849-858.

Vale,R.D. (1987). Intracellular transport using microtubule-based motors. Annu. Rev. Cell Biol. *3*, 347-378.

Vale,R.D. (1991). Severing of stable microtubules by a mitotically activated protein in Xenopus egg extracts. Cell *64*, 827-839.

van Breugel,M., Drechsel,D., and Hyman,A. (2003). Stu2p, the budding yeast member of the conserved Dis1/XMAP215 family of microtubule-associated proteins is a plus end-binding microtubule destabilizer. J. Cell Biol. *161*, 359-369.

Vandecandelaere,A., Brune,M., Webb,M.R., Martin,S.R., and Bayley,P.M. (1999). Phosphate release during microtubule assembly: what stabilizes growing microtubules? Biochemistry *38*, 8179-8188.

Vasquez,R.J., Gard,D.L., and Cassimeris,L. (1994). XMAP from Xenopus eggs promotes rapid plus end assembly of microtubules and rapid microtubule polymer turnover. J. Cell Biol. *127*, 985-993.

Vasquez,R.J., Gard,D.L., and Cassimeris,L. (1999). Phosphorylation by CDK1 regulates XMAP215 function in vitro. Cell Motil. Cytoskeleton *43*, 310-321.

Walczak,C.E., Mitchison,T.J., and Desai,A. (1996). XKCM1: a Xenopus kinesin-related protein that regulates microtubule dynamics during mitotic spindle assembly. Cell *84*, 37-47.

Walker,R.A., Inoue,S., and Salmon,E.D. (1989). Asymmetric behavior of severed microtubule ends after ultraviolet-microbeam irradiation of individual microtubules in vitro. J. Cell Biol. *108*, 931-937.

Walker,R.A., O'Brien,E.T., Pryer,N.K., Soboeiro,M.F., Voter,W.A., Erickson,H.P., and Salmon,E.D. (1988). Dynamic instability of individual microtubules analyzed by video light microscopy: rate constants and transition frequencies. J. Cell Biol. *107*, 1437-1448.

Wang,P.J. and Huffaker,T.C. (1997). Stu2p: A microtubule-binding protein that is an essential component of the yeast spindle pole body. J. Cell Biol. *139*, 1271-1280.

Wang,X.M., Peloquin,J.G., Zhai,Y., Bulinski,J.C., and Borisy,G.G. (1996). Removal of MAP4 from microtubules in vivo produces no observable phenotype at the cellular level. J. Cell Biol. *132*, 345-357.

West,R.R., Malmstrom,T., Troxell,C.L., and McIntosh,J.R. (2001). Two related kinesins, klp5+ and klp6+, foster microtubule disassembly and are required for meiosis in fission yeast. Mol. Biol. Cell *12*, 3919-3932.

Westermann,S., Cheeseman,I.M., Anderson,S., Yates,J.R., III, Drubin,D.G., and Barnes,G. (2003). Architecture of the budding yeast kinetochore reveals a conserved molecular core. J. Cell Biol. *163*, 215-222.

Whittington,A.T., Vugrek,O., Wei,K.J., Hasenbein,N.G., Sugimoto,K., Rashbrooke,M.C., and Wasteneys,G.O. (2001). MOR1 is essential for organizing cortical microtubules in plants. Nature *411*, 610-613.

Wiese,C., Wilde,A., Moore,M.S., Adam,S.A., Merdes,A., and Zheng,Y. (2001). Role of importin-beta in coupling Ran to downstream targets in microtubule assembly. Science *291*, 653-656.

Wiese,C. and Zheng,Y. (2000). A new function for the gamma-tubulin ring complex as a microtubule minus-end cap. Nat. Cell Biol. *2*, 358-364.

Wigge,P.A. and Kilmartin,J.V. (2001). The Ndc80p complex from Saccharomyces cerevisiae contains conserved centromere components and has a function in chromosome segregation. J. Cell Biol. *152*, 349-360.

Wilde,A. and Zheng,Y. (1999). Stimulation of microtubule aster formation and spindle assembly by the small GTPase Ran. Science *284*, 1359-1362.

Wittmann,T., Bokoch,G.M., and Waterman-Storer,C.M. (2003). Regulation of leading edge microtubule and actin dynamics downstream of Rac1. J. Cell Biol. *161*, 845-851.

Wittmann,T., Bokoch,G.M., and Waterman-Storer,C.M. (2004). Regulation of microtubule destabilizing activity of Op18/stathmin downstream of Rac1. J. Biol. Chem. *279*, 6196-6203.

Wittmann,T., Hyman,A., and Desai,A. (2001). The spindle: a dynamic assembly of microtubules and motors. Nat. Cell Biol. *3*, E28-E34.

Zheng,Y., Wong,M.L., Alberts,B., and Mitchison,T. (1995). Nucleation of microtubule assembly by a gamma-tubulin-containing ring complex. Nature *378*, 578-583.